EXAMINATION OF ARRIVAL AND DEPARTURE TAXI TRAJECTORIES FOR EARTH-MARS CIRCULATING ORBITS

by

ANDREW JAMES KNOEDLER

B.S. AERO/ASTRO, MASSACHUSETTS INSTITUTE OF TECHNOLOGY
(1990)

SUBMITTED TO THE DEPARTMENT OF
AERONAUTICS AND ASTRONAUTICS
IN PARTIAL FULFILLMENT OF THE
REQUIREMENTS FOR THE DEGREE OF

MASTER OF SCIENCE

at the

MASSACHUSETTS INSTITUTE OF TECHNOLOGY
June, 1991

© Andrew James Knoedler, 1991. All rights reserved

The author hereby grants to MIT permission to reproduce and to distribute copies of this thesis document in whole or in part.

Signature of Author_____
Department of Aeronautics and Astronautics
February, 1991

Certified by_____
Walter M. Hollister
Professor, Aeronautics and Astronautics
Thesis Supervisor

Certified by_____
David Farless
Group Supervisor, Jet Propulsion Laboratory
Thesis Supervisor

Accepted by_____
Professor Harold Y. Wachman
Chairman, Department Graduate Committee
Department of Aeronautics and Astronautics

Aero
MASSACHUSETTS INSTITUTE OF TECHNOLOGY
JUN 12 1991
LIBRARIES

EXAMINATION OF ARRIVAL AND DEPARTURE TAXI TRAJECTORIES FOR EARTH-MARS CIRCULATING ORBITS

by

ANDREW JAMES KNOEDLER

Submitted to the Department of Aeronautics and Astronautics
February, 1991 in partial fulfillment of the
requirements for the Degree of Master of Science in
Aeronautics and Astronautics

ABSTRACT

In the last five years two new types of repeating, gravity-assist orbits between the Earth and Mars have been identified. These Cycler and VISIT orbits repeatedly pass by the Earth and Mars at set intervals. The circulating orbits can be used by large spacecraft, "CASTLEs in space", to provide comfortable crew accommodations for the long journeys between Earth and Mars. The two main studies previously performed on this subject left some details to be worked out.

The main detail to be considered was the transfer of personnel between the CASTLE in its circulating trajectory and local planetary spaceports. This study examines the trajectory of the personnel transfer vehicle, a "Taxi", between a spacecraft in a circulating orbit and a spaceport in orbit around a planet. Specific attention was paid to resolving the problems of plane changes, time delays, and phasing of the Taxi trajectory. A three-impulse trajectory was used to look at the transfers between the VISIT and Cycler circulating orbits and the spaceports in various orbits around both the Earth and Mars.

The results, which are shown in a series of graphs depicting total ΔV, transfer time, and initial transfer orbit orientation, show that minimum ΔV trajectories exist for each orbit of the spaceport. Plane changes are solved within the three-impulse transfer while the phasing and launch delays can be solved by adjusting the impulses in the trajectory. The work done in this study gives needed information for future studies comparing the feasibility of transportation system between Earth and Mars using circulating trajectories versus a system using direct trajectories.

Thesis Supervisor: Prof. Walter M. Hollister

Title: Professor of Aeronautics and Astronautics

ACKNOWLEDGEMENTS

This thesis would not have been possible without the generous support of many people, each making unique contributions. I would like to thank the people of the MIT Engineering Internship Program and the Jet Propulsion Laboratory EIP coordinator, Cheryl Hanson, for providing support in this special cooperative education program. I would like to thank Dave Farless, my JPL thesis supervisor, for his support, guidance, and advice through my thesis research and writing period. I would also like to thank all the JPL employees who gave their expertise, Paul Penzo, Dennis Byrnes, Laura Bass, and others. I am also indebted to Sam Wilson of TRW, Jim Knoedler, my father, of Rockwell International, and Prof. Walter Hollister, my MIT thesis supervisor, for their advice and technical critiques of my thesis. I would also like to thank Audra Garner for her proofreading help and constructive criticism. Finally, I would like to thank my parents, Jim and Britta, and my sisters, Alicia and Kristen, for their continued support and encouragement.

TABLE OF CONTENTS

LIST OF FIGURES

LIST OF TABLES

1. INTRODUCTION

In 1990 President George Bush outlined goals for the US Space Program; the first goal being a return to the Moon followed by the second goal of a manned mission to Mars. Returning to the Moon would help to mature the technology needed to go to Mars. The mission to Mars might then act as a forward base for further exploration of the solar system.

To many, the goals are admirable ones and the missions will challenge the scientists and engineers. One of the greater challenges is to overcome the problems associated with long-term human endurance in space. Preliminary studies have shown that a roundtrip to Mars with a stopover time of about a month will take approximately two years to complete (TRW, 1964, Niehoff, 1986, and Nock, 1987). Two years in the closed environment of a spacecraft will definitely tax the physiological and psychological limits of astronauts. To alleviate some of the stress, large CASTLEs (Cycling Astronautical Spaceships for Transplanetary Long-duration Excursions) have been envisioned that carry crews to and from Mars in relative comfort (Hollister, 1967 and Hoffman, 1986). The CASTLEs would be properly shielded against radiation and provide artificial gravity to ensure the health of the crew.

The CASTLE spacecraft would not be expendable but rather would be very durable ships capable of being used for tens of years. The key to the CASTLEs and the missions to Mars are the circulating or cyclical orbits which can be established between the Earth and Mars. The work done in 1986 by Friedlander, et al. has shown that two practical types of circulating orbits exist for the CASTLE to follow (Friedlander, 1986).

1.1 CIRCULATION ORBITS

Circulating orbits are an offshoot from planetary swingbys or gravity assisted orbits. Some of the early pioneers in the study of planetary swingbys include R. H. Battin and G. A. Crocco. Repeatable swingby orbits around the planets had been identified in the 1960s (Rall, 1971, Hollister 1968, 69, and Ross, 1963). New variations to these orbits have recently been found in which the CASTLE will be able to orbit between the Earth and Mars with lower propulsive requirements. The two types of circulating orbits that have been studied recently are VISIT (Versatile International Station for Interplanetary Transport) orbits and Up/Down Cycler orbits (Niehoff (a,b), 1985 and 1986 and Aldrin, 1985).

The VISIT types of circulating orbits which take advantage of the 2.14 year synodical period of Mars, were first proposed by Niehoff in 1985. The VISIT-1 orbit encounters the Earth every five years and Mars every 3.75 years. The VISIT-2 orbit encounters the Earth every three years and Mars every 7.5 years. The transfer time for Earth to Mars or Mars to Earth varies from 0.5 to 3.3 years. The retrograde shift of the encounter longitudes of the Earth and Mars requires minor velocity corrections about every 15 years for the VISIT class of orbits (Friedlander, 1986). See Figure 1 below.

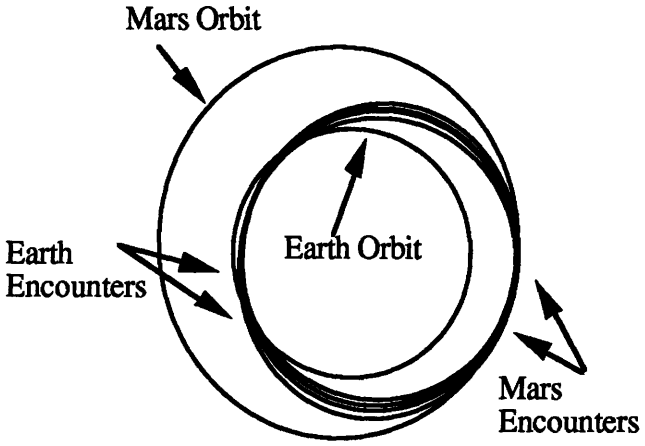

Figure 1 VISIT Orbit (Friedlander, et al., 1986)

The Up/Down Cycler orbits, first proposed by Dr. E. E. Aldrin, are orbits which are designed to exploit synodical precession of the line of apsides (Aldrin, 1985). The Cycler orbits have more frequent encounters with the Earth and Mars but at the price of additional ΔV requirements. Over a Cycler's 15 year cycle, three propulsive maneuvers have to be used to supplement the no-cost, gravity assist swingbys of the Earth (Byrnes, 1990). In a Mars mission scenario the two Cycler orbits have the same period but are oriented differently in order to preserve short outbound and inbound transfer times. Either way the Up Cycler (Earth-to-Mars) and the Down Cycler (Mars to Earth) transfers encounter the Earth or Mars every 2.14 years with a transfer time of 0.43 years (Friedlander, 1986). Figure 2 shows the trajectories of the CASTLE in the Up and Down Cycler Orbits. The drawing gives the heliocentric view of the Cycler orbits while the graph shows distance from the Sun versus time for the Up Cycler orbit. The tic marks and numbers on the drawing show the locations and order of the encounters. If the Mars encounters were

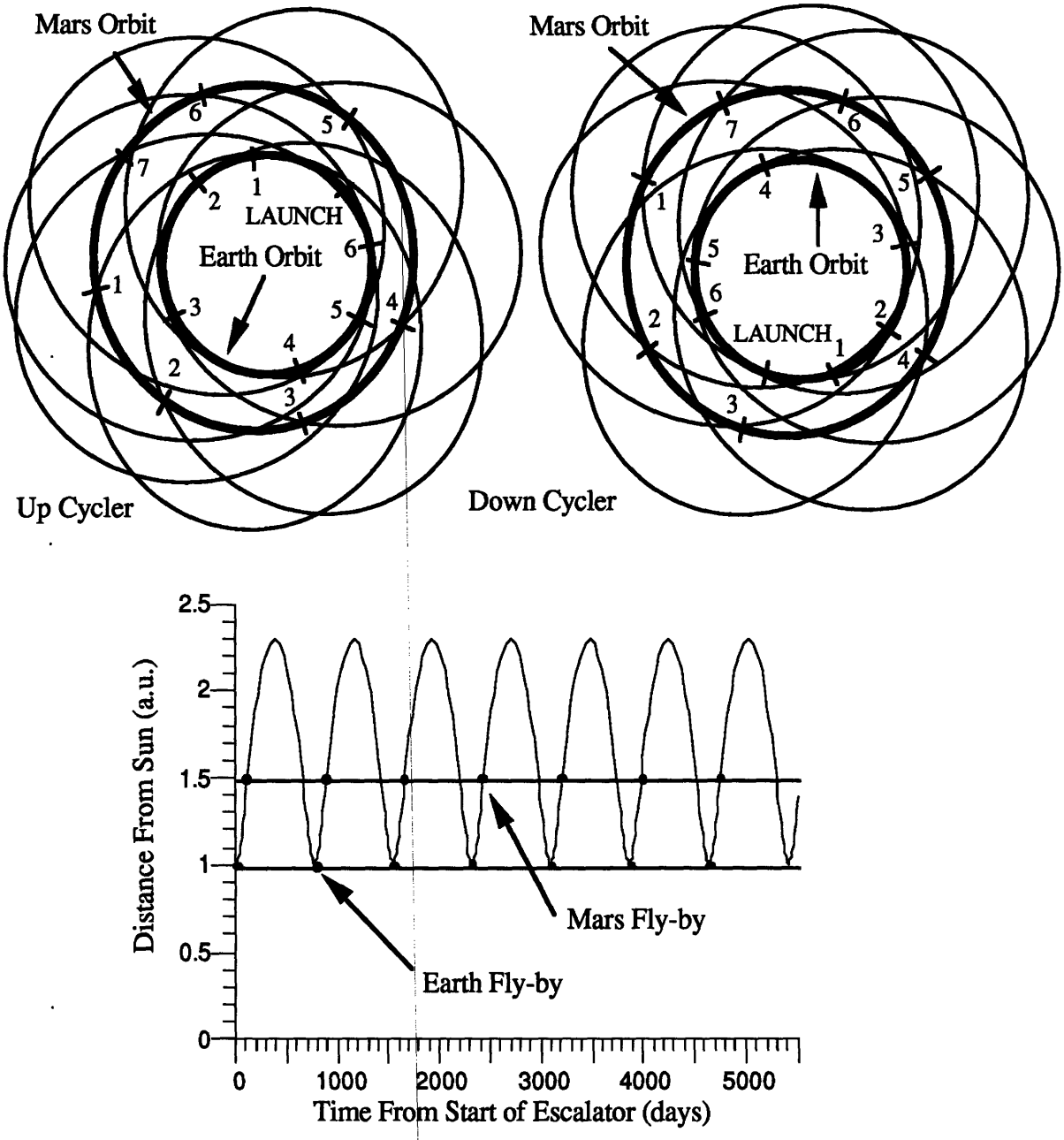

Figure 2 Up and Down Cycler Orbits (Friedlander, et al., 1986)

shifted to the descending leg of the repeating curve, the graph would represent the Down Cycler orbit. The combination of the two gives a clear indication of the timing of the Earth and Mars encounters.

The circulating VISIT and Cycler orbits are well defined for continuing service between the Earth and Mars. However, the trajectories to get on and off the circulating orbits have not been studied in great detail. The CASTLEs follow the circulating orbits but they are not

designed to stop at the planet; they just pass close to the planet. A smaller 'Taxi' vehicle transports crews from the CASTLE to the spaceport orbiting in the vicinity of the planet and vice versa. The Taxi trajectories need to be optimized for hyperbolic approaches and departures to account plane changes, time-phasing, and launch delays.

1.2 TAXI TRAJECTORIES

This thesis will focus primarily on the analysis of the Taxi trajectories with the goal to optimize the planetocentric maneuver strategies for arriving at and departing from the orbiting spaceports. The locations of the spaceports are important parameters to define. Suggested locations for the spaceport around the Earth include Low Earth Orbit (LEO), the Moon, an Earth-Moon Lagrangian point, the Earth-Sun Lagrangian point, and Earth-Moon cyclic orbits. Suggested locations for the Mars spaceport include a near-Phobos location, Sun-Mars L1 location, and highly elliptic orbits around Mars (Friedlander, 1986). See Figures 3 and 4 which follow.

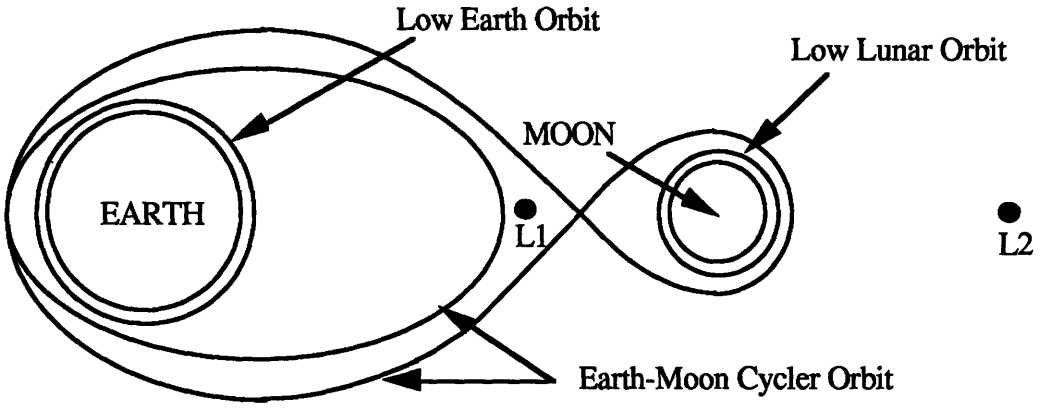

Figure 3 Possible Earth Spaceport Locations

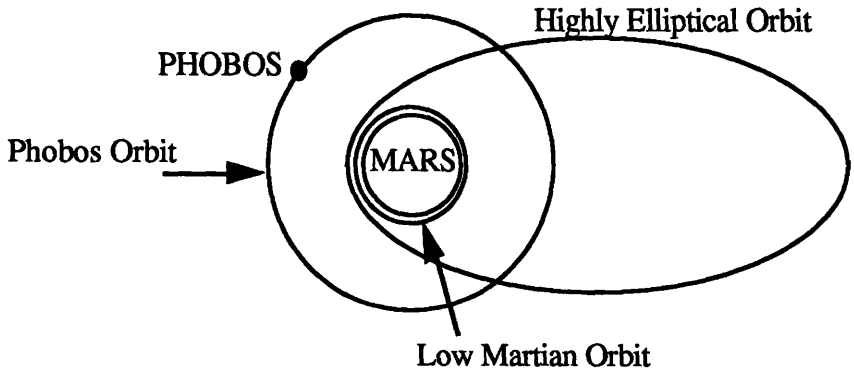

Figure 4 Possible Mars Spaceport Locations

This study will analyze the Taxi trajectories for the VISIT and Cycler orbits for spaceports located in LEO, the Earth-Moon L1 point, a low Mars orbit, and Phobos. The VISIT and Cycler orbits must first be reproduced to get initial conditions before the analysis to determine the Taxi trajectories can begin. A parametric study will be performed to get an insight into the general case: and the effects of plane changes, time-phasing, and launch delays will be included in order to find the optimum transfers. The input parameters will be varied over their limits, and the outputs will be examined and will be extrapolated to predict the behavior of other encounter orientations.

The final results will be in the form of a set of Taxi trajectories for each spaceport. The change in the total ΔV and transfer time of the trajectories for each encounter will be analyzed. For one spaceport location at both Earth and Mars, the time phasing problem will be examined in detail. Finally, the practical aspects of the Taxi trajectories will be discussed with respect to the trade-offs between the two types of circulating orbits.

2. ASSUMPTIONS AND METHODS

The stated problem of optimizing transfer between spaceports and vehicles in cycling orbits requires that a number of assumptions be made to confine the solutions to more practical possibilities. After the assumptions are stated, the operational constraints of the CASTLE and Taxi spacecraft will follow. Lastly, the details of the circulating and taxi orbits will be discussed along with the methods for optimizing the taxi trajectories.

As discussed and analyzed in the paper by Hoffman, et al. in 1986, a few assumptions have to be made for this study of circulating orbits between Earth and Mars; and these assumptions are summarized here for clarity. It is assumed that a permanently manned base on Mars does exist and is in regular operation along with an orbiting spaceport or space station in the vicinity of Mars to support hydrogen and oxygen mining on Phobos or the Martian polar caps. It is also assumed that a spaceport is orbiting in the Earth-Moon system to support Earth and Moon operations. Both spaceports will serve as staging points for the Taxi spacecraft.

Mining for propellant (hydrogen and oxygen) on Mars or Phobos and on the Moon is understood to be feasible and operational and will be the main source of hydrogen and oxygen to get the Taxi spacecraft to and from the CASTLE. However, the location of the propellant mining affects the location of the spaceports. In the near-Mars location the spaceport could be located in a low Mars orbit or in a highly elliptical Mars orbit, if the

mining occurs near the Martian poles. If, on the other hand, the mining operations are based on Phobos, then a spaceport in orbit near Phobos makes the most sense. In the Earth-Moon system, the spaceport could be located at the Earth-Moon L1 Lagrangian point or in a Earth-Moon cycler orbit, if oxygen is mined on the Moon. A low Earth orbit would make sense if no mining occurred on the Moon. For this study each location mentioned will serve as a possible staging point for the Taxi spacecraft on its journeys to and from the CASTLE.

The specific purpose of this thesis is to find the families of optimum trajectories for the Taxis which are traveling between the CASTLE and the designated spaceports. The question is 'What optimization criteria should be applied in design of the Taxi trajectories?', and the answer can be found in an examination of the purpose of the Taxi spacecraft. Its name says much. The main mission of the Taxi is not to provide comfort for the crew but to provide a quick, inexpensive way to get to the CASTLE. This provides one possible optimization criterion: Find the trajectory which gets the Taxi from the spaceport to the CASTLE (or vice versa) in the shortest amount of time. However, this minimum-time approach is very costly in ΔV. Therefore, a trade-off study between time and ΔV is a more appropriate approach to the problem of optimization. Limits on ΔV and transfer time will have to be imposed in order to get meaningful results.

Before the search for the Taxi trajectories can begin, the VISIT and Cycler orbits have to be generated to get the proper orbital elements during the approaches and departures around Earth and Mars. The procedure for producing the orbits uses software developed by the Jet Propulsion Laboratory's Mission Design section. A library of routines which aides astrodynamic calculations exists in the Mission Design section. The routines are written so that they can be integrated into other FORTRAN programs written on various computer systems at JPL. The library also includes routines that solve Lambert's problem and provide planetary ephemerides which are particularly useful for reproducing the circulating orbits.

The VISIT and Cycler orbits will then provide initial or final boundary conditions depending upon whether the Taxi is departing or arriving at the CASTLE. With the boundary conditions defined at both the CASTLE and the spaceport, transfer taxi trajectories can be generated between the two. The trajectories will then be subjected to optimization schemes to find the optimum transfer(s).

3. OPTIMIZATION SCHEMES

Initially, two different optimization schemes, primer vector and parameterization, were examined to determine which method works best under the present assumptions. Primer vector theory finds the optimal trajectory based upon the magnitude of the vector containing the three adjoint variables related to the velocity vector of the trajectory (Lawden, 1963 and Lion, 1967). Parameterization may be used for a variety of variable constraint problems such as totally unconstrained, linear constrained, and non-linear constrained. Each method has many different solutions.

3.1 PRIMER VECTOR THEORY

The primer vector method was introduced in the early 1960s as a useful mathematical tool to determine an optimal trajectory between two boundary points. The theory uses the equations of motion and the position and velocity vectors at each boundary in a rectangular Cartesian coordinate frame. The primer vector arises from the Lagrange multipliers used in minimizing parts of the equations of motion (Lion, 1967).

The present structure of the problem at hand, i.e. getting from the CASTLE to a spaceport, is not set up to handle a primer vector solution. Two boundary points do exist but they result from the patched conic solution of the circulating orbits in a spherical coordinate system. The boundary points could easily be changed into a rectangular Cartesian frame with just position and velocity components. The primer vector theory could then be applied to find an optimum trajectory. However, this technique does not aid in the visualization of the problem and its solution.

The problem can be better visualized by realizing that the end conditions vary when any of the initial conditions are changed. In the primer vector procedure, however, only the components of position and velocity can be changed. A change in one of the initial velocity components will change the trajectory, however, the effects of a change of, for example, 100 m/s in the y-component of the first boundary point is harder to visualize than the effects of a change in the parking orbit apoapse (a Keplerian orbital element). For this reason the primer vector theory was dropped in favor of parameterization.

3.2 PARAMETERIZATION

Parameterization, as its name implies, uses the various independent variables or parameters of a problem to optimize the trajectory for some dependent variable. The Taxi trajectory problem can be considered a non-linear constrained problem in which the starting and ending points are constrained within certain limits, and the behavior of the variables is non-linear. The parameters that will be used to optimize the Taxi trajectory come from the patched conic analysis of the path of the Taxi.

The CASTLE approaches and departs the Earth or Mars on a planetocentric hyperbolic path. Differences in the hyperbolic path for each fly-by makes each approach or departure of the Taxi a different situation.

Ideally, the trajectory taken by the Taxi should be optimized for the smallest amount of change in velocity (ΔV) in order to get from the spaceport to the CASTLE or vice versa for a given transfer time. The Taxi can make as few as two velocity changes (a burn or impulse) or as many as needed. However, fewer burns are desired for operational simplicity. Somewhere between two and many burns is a number that has the potential to give the smallest overall ΔV. Studies have been done that show a three-impulse technique for transferring between elliptical (or circular) orbits and a given non-coplanar V-infinity vector is better than one- or two-impulse transfer (Wilson,1967, Penzo, 1988). The advantage of the three-impulse transfer is that the additional impulse can be used to make any needed plane change thus making the total ΔV less (Penzo, 1988). More than three impulses does not significantly further reduce the total ΔV. The geometry of the three-impulse transfer is shown in Figure 5.

3.3 THREE-IMPULSE STRATEGY

The three-impulse strategy patches together a number of conic trajectories in order to get the desired trajectory. For a departure from a planetary circular or elliptical orbit to a given V-infinity vector, an initial burn is made to transfer into a larger intermediate elliptical orbit. Near the apoapse of the intermediate ellipse a second impulse is made to rotate the orbit into the plane of the V-infinity vector. Finally, a third impulse is made to transfer from the rotated intermediate ellipse to the orbit defined by the V-infinity vector.

The complexity of the optimization of the three-impulse trajectory is proportional to the number of parameters used in the procedure. Assuming that the burns cause a velocity

impulse at a point, constraining the positions of the points affects the optimization procedure. If all the impulses occur along the line of apsides and the flight path angles of the hyperbola and ellipse match at the last burn, then no optimization of variables occurs. This is not to say that an optimum trajectory could not occur in this situation, rather an optimization process was not used. When the impulses are not constrained and are

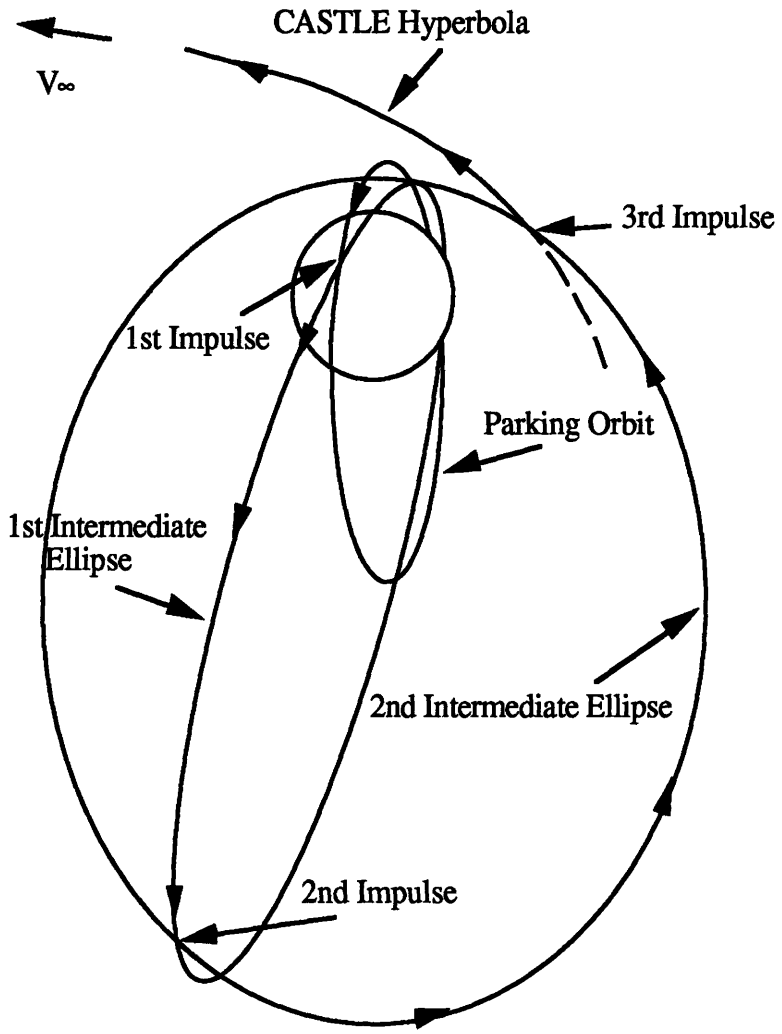

Figure 5 Three-Impulse Trajectory (Gerbracht, 1968)

positioned away from the line of apsides, the trajectory can be optimized. The transfer can be optimized with more variables by not constraining the flight path angles of the ellipse and hyperbola to exactly match at the third impulse and by allowing some of the plane change to be taken out at the first burn.

A number of programs were examined to determine their usefulness with respect to this problem. A program written by Paul Penzo and modified by Andrei Sergeyevsky both of

JPL, finds one-, two-, and three-impulse transfers, but only the two-impulse transfer is optimized. Sam Wilson from NASA/JSC has developed a quasi-optimum three-impulse trajectory program which minimizes total ΔV by optimizing the placement of the second impulse. The program also constrains the first and third impulses to be colinear while forcing the flight path angles to match at the third impulse. The third program considered was written in 1968 by R. Gerbracht from TRW. This program optimizes the three-impulse trajectory by minimizing ΔV over five variables (Gerbracht, 1968) and seems to be the best candidate for solving the problem. However, the geometry of the Taxi trajectories with respect to the planetary parking orbit and the V-infinity vector should be further analyzed before an attempt is made to find optimal transfers using the programs mentioned.

4. CASTLE APPROACH SCENARIOS

As was stated earlier, every arrival or departure opportunity is different because of the different fly-by hyperbolic trajectory of the CASTLE as viewed from the planet. The characteristics of the parking orbit also play a part in the design of the Taxi trajectory. VISIT and Cycler orbits produce different fly-bys so approaches/departures will be discussed in reference to various combinations of circulation orbit, planet, and spaceport position.

The approaches to the planet are the inbound legs of the hyperbolic fly-bys, and the departures are the outbound legs. The Taxi can rendezvous with the CASTLE hyperbola on either the outbound or inbound leg. The Taxi could rendezvous with the CASTLE on its inbound leg, but the mismatch of flight path angles would make the rendezvous expensive in ΔV. The Taxi could also fly a retrograde trajectory to meet the CASTLE on its inbound leg. However, the Taxi has to essentially stop and then speed up in the other direction just to catch the CASTLE. Rendezvousing with the CASTLE at its periapse or along its outbound leg is both easier because no retrograde orbit is used and more economical because the Taxi only has to speed up. The same reasoning is used to justify leaving the CASTLE on its inbound leg when rendezvousing with the spaceport. Whether the rendezvous is with the CASTLE or the spaceport, the three-impulse strategy is the same. Therefore, an approach can be considered the same as a departure except that the order of the burns is reversed.

4.1 LOW PLANETARY PARKING ORBITS

The following sections examine the relative orientations of low planetary parking orbits and the hyperbolic fly-by of the CASTLE. For the low planetary parking orbits, the Taxi can use two approaches to rendezvous with the CASTLE. The first is rendezvousing with the CASTLE at the periapse of the hyperbolic fly-by (see Figure 6). The second approach allows the Taxi to get on its own hyperbolic escape trajectory and then rendezvous with the CASTLE later. Figure 7 shows this option. This option requires a fourth impulse at the intersection of the hyperbolas.

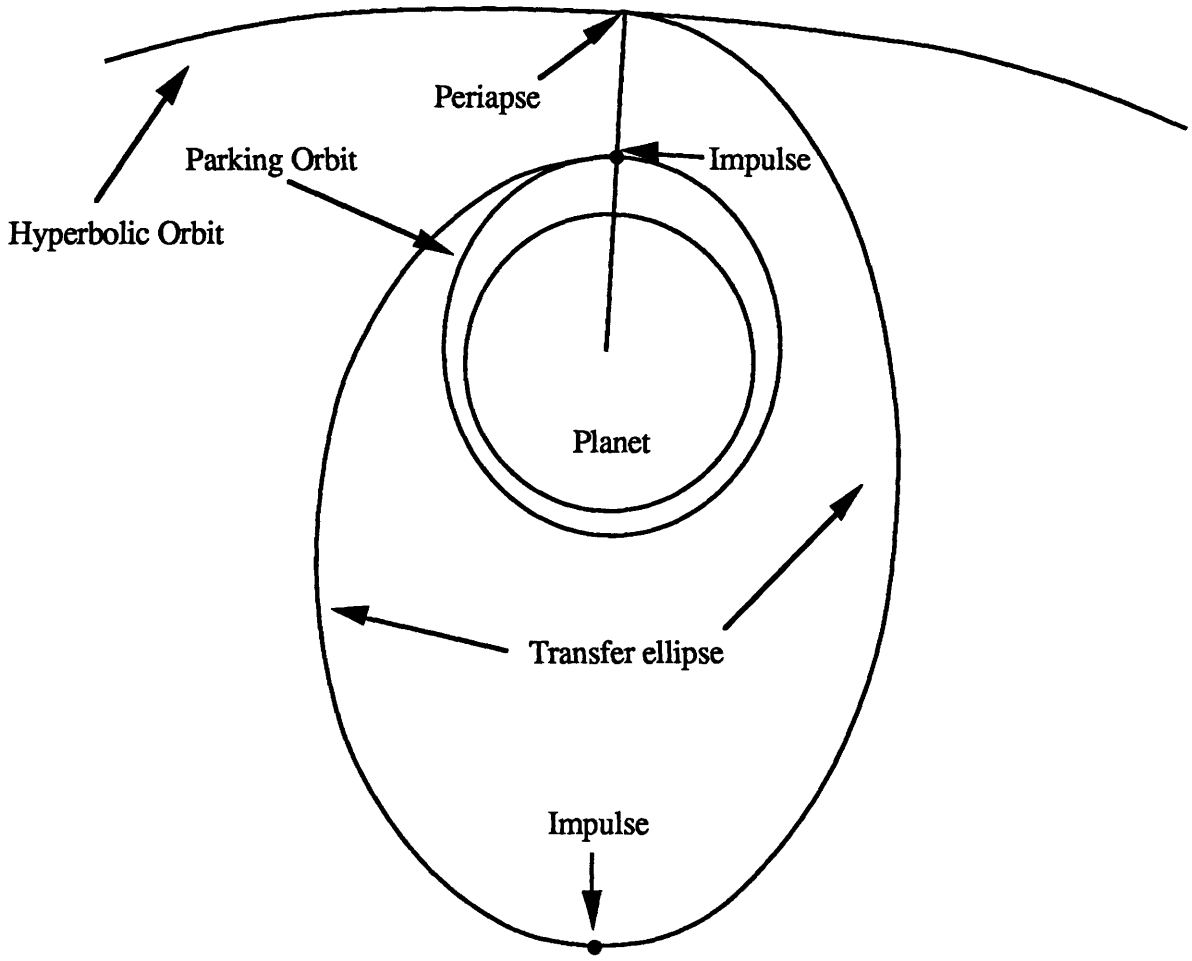

Figure 6 Two Dimensional Rendezvous at Periapse

Selecting a rendezvous option becomes a trade-off task. Rendezvousing at periapse has a higher ΔV than the hyperbolic intercept but, in most cases, an additional one to two days is cut off the transfer time by using this option.

4.1.1 Earth Fly-by of Cycler Orbits

The Cycler orbits come within 1.2 to 1.9 Earth radii which means the closest approach radius is between approximately 7650 km and 12,120 km. A Low Earth Orbit (LEO) is established at a tentative Space Station altitude of 370 km (Sharma, 1990, Henry, et al, 1989, and Sergeyevsky, 1989). The geometry between the V-infinity vector and the parking orbit allows the three-impulse trajectory to be implemented quite easily. The only tradeoff to be made is whether to meet the CASTLE at its perigee or to intercept the CASTLE later on an intersecting hyperbola.

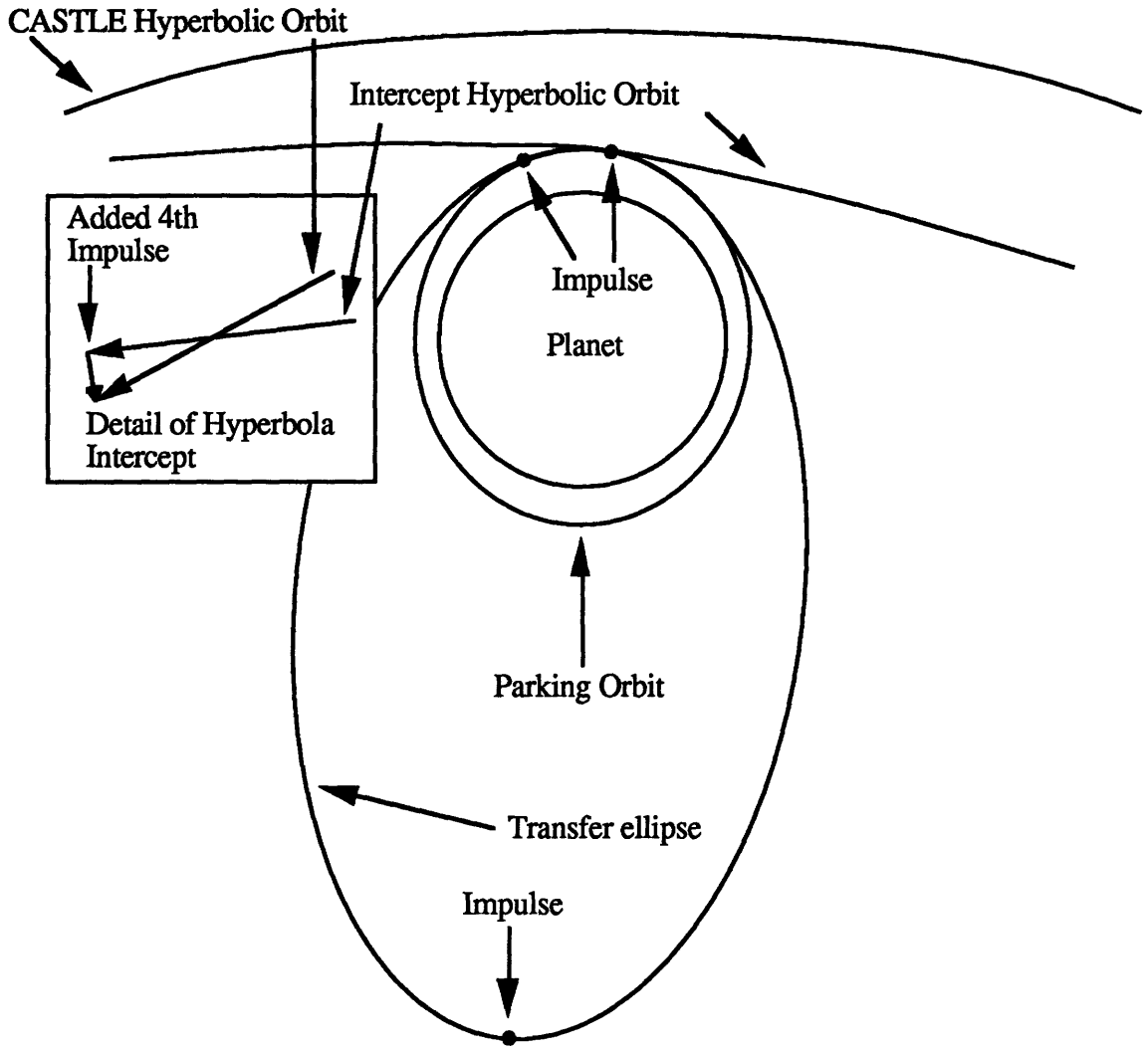

Figure 7 Two Dimensional Rendezvous at Intersection of Hyperbolas

4.1.2 Earth Fly-by of VISIT Orbit

The VISIT orbits come within 40 to 270 Earth radii which translates to approximately 255,000 km to 1,722,000 km. Assuming that the LEO is the same circular 370 km orbit a tradeoff again has to be made between ΔV and time. The closest approach radius is so large in some cases that transfer time using the three-impulse trajectory would be about the same for both the intercepting hyperbola option and the intercept at periapse option. This situation will be analyzed further when the actual transfer ΔVs and times are calculated.

4.1.3 Mars Fly-by of Cycler Orbits

For Mars, the Cycler orbits close within 1.3 to 29.1 Mars radii (4420 km to 99,000 km). A circular orbit around Mars was arbitrarily selected at an altitude of 200 km. The geometry between the parking orbit and the V-infinity vector is very similar to the orientation around the Earth. Therefore, the three-impulse trajectory can also be applied to this situation. Similar to the argument for Earth fly-bys, a tradeoff has to be made between meeting the CASTLE at its perigee or whether to intercept the CASTLE later on an intersecting hyperbola. Again the perigee intercept is expected to cost more ΔV but the hyperbola intercept requires a longer transfer time.

4.1.4 Mars Fly-by of VISIT Orbit

The CASTLE passes within 5100 km to 77,200 km (1.5 to 27.2 Mars radii) when it follows the VISIT circulating orbit. When the closest approach is greater, the time saved by rendezvousing directly with the CASTLE (rather than getting on the hyperbola that intersects the CASTLE's path at a great distance) becomes smaller. Even though the periapse of the CASTLE may pass at a large distance from Mars, that geometry does not prevent the three-impulse trajectory from being used.

4.2 PHOBOS ORBIT

A spaceport is located in the orbit of Phobos which has a semi-major axis of 9400 km and an inclination of 1°. The spaceport will be trailing Phobos far enough to avoid any adverse the gravitational perturbations.

4.2.1 Mars Fly-by of Cycler Orbits

The radius of closest approach for the Mars fly-by of the Cycler orbits vary from 4420 to 99,000 km. Since the altitude of Phobos is a medium altitude as compared to a low Mars orbit or a very high Mars orbit, the hyperbolic fly-by of the Cycler orbits may pass through the interior or the exterior of the orbit of Phobos. In either case, the three-impulse procedure works well because the geometry of the situation fits the normal profile used by the method. There are three intercept options to be considered. The Taxi can intercept or rendezvous with the CASTLE at nearly the same altitude, outside the Phobos orbit, or inside the Phobos orbit. In other words, the Taxi can rendezvous with the CASTLE at the periapse of its hyperbolic fly-by no matter what the periapse radius is in comparison with the radius of the spaceport's orbit. Alternately, the Taxi can get on an intercept hyperbola at the radius of Phobos' orbit allowing the Taxi to rendezvous with the CASTLE later. The third option is the Taxi can lower its periapse while doing a plane change at the second impulse to establish an intercept hyperbola with a periapse considerably lower than Phobos' orbit. See Figure 8 for the periapse and the low hyperbola rendezvous.

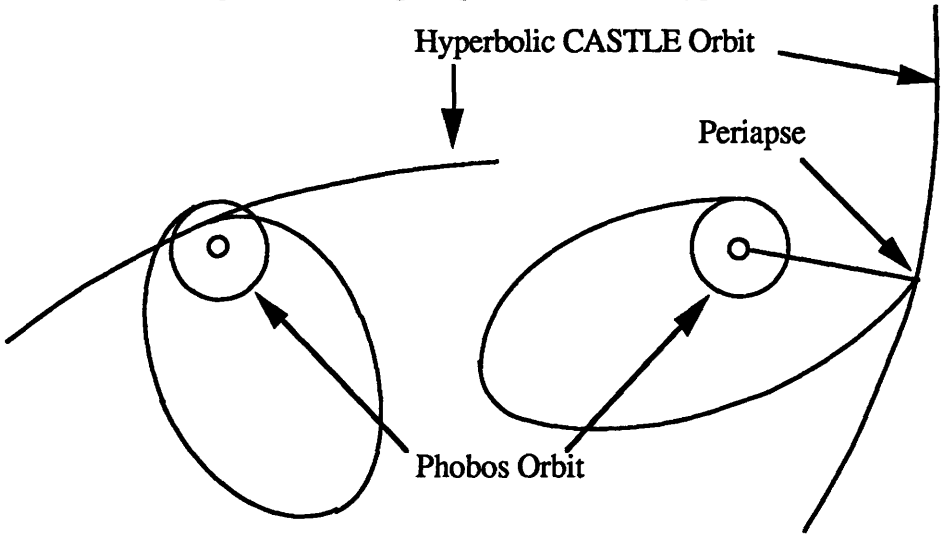

Low Hyperbolic Rendezvous Periapse Rendezvous

Figure 8 Two Rendezvous Options for the Taxi Around Mars

4.2.2 Mars Fly-by of VISIT Orbit

For this scenario it is assumed the CASTLE flies past Mars at distances of 5100 km to 77,200 km, and the spaceport is established in Phobos' orbit at 9400 km. Two of the VISIT encounters pass below the orbit of Phobos so three rendezvous options can be used in some of these encounters. A three-impulse Taxi trajectory variation should work well in

all the orientations of the parking orbit and the V-infinity vector of the CASTLE hyperbola. Another tradeoff between three options occurs here. The Taxi can try to meet the CASTLE at the periapse of the hyperbolic fly-by. The Taxi can get on an intercept hyperbola at the radius of Phobos' orbit. The third option is the Taxi can lower its periapse while doing a plane change at the second impulse and then get on an intercept hyperbola with a periapse considerably lower than Phobos' orbit.

4.3 L1 LAGRANGIAN POINT

The Lagrangian points have been mentioned previously as locations for spaceports but without much rationale. The Lagrangian points are a set of stable and unstable equilibrium points in the Earth-Moon system. They are not unique to the Earth-Moon system but are present in any two or more body system. The points arise from the equations of gravitational attraction between any two bodies. The positions of the points are shown in Figure 9.

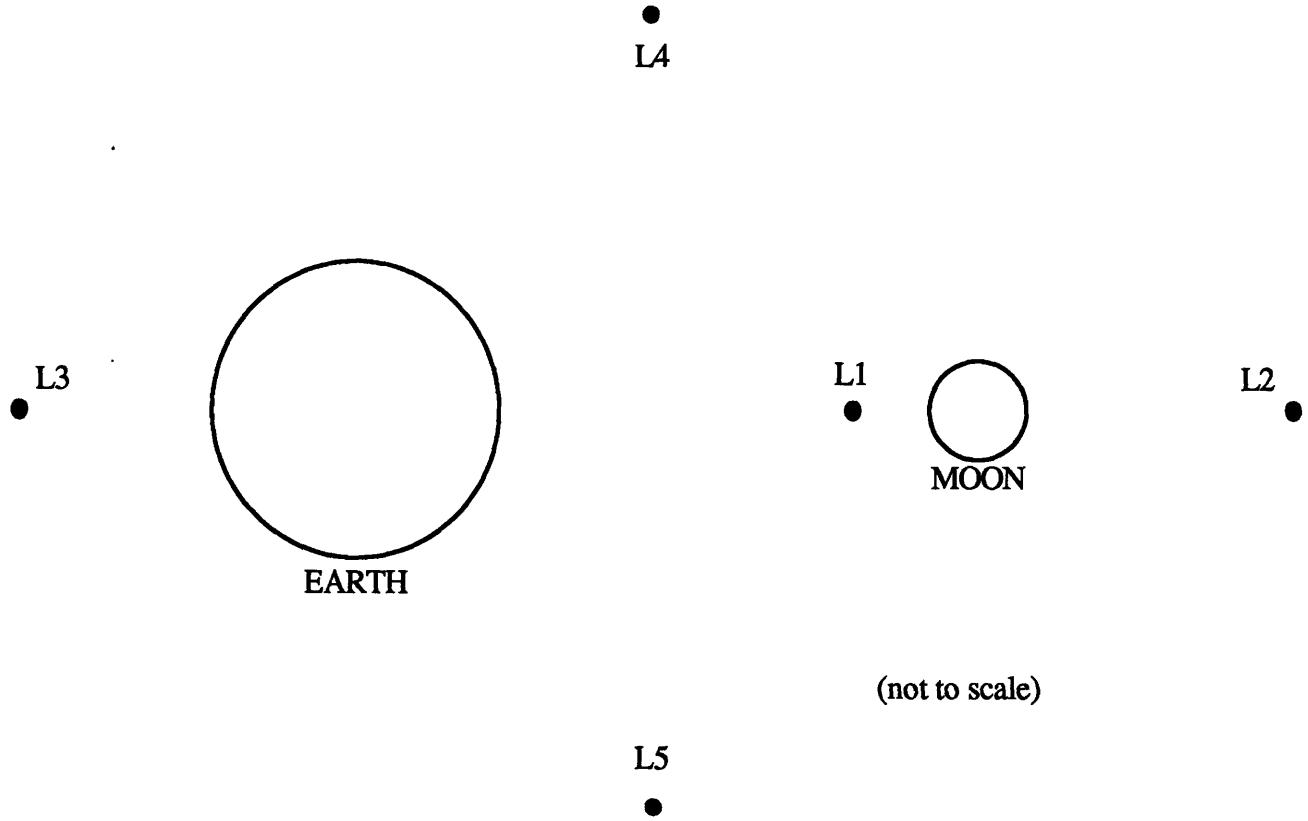

Figure 9 Lagrangian Point Positions in the Earth-Moon System

Points 4 and 5 are stable while points 1, 2, and 3 are unstable. In practical terms, an object placed at L4 or L5 will remain there in the absence of outside perturbations. At L1, L2, and L3 an object can remain at that point with a small expenditure of energy (Brykov,

1981). Section 6.4 will go further into detail about the practical aspects of a spaceport at L1.

The answer to the question "why would anyone want to put a spaceport at a Lagrangian point?" is not part of this analysis. Other studies have concerned themselves with the practical aspects of spaceport operations at Lagrangian points (Hoffman, et al., 1986). Another article in a recent Air and Space mentions using L2 as a spaceport location in conjunction with cycler orbits (Aldrin, 1990).

4.3.1 Earth Fly-by of Cycler Orbits

The previously described Cycler orbits would pass inside the orbits containing the Lagrangian points. Given that the L1 Lagrangian point is at a distance of 326,000 km from the Earth, the Taxi would follow a trajectory whose periapse would be well inside the L1 distance. A three-impulse trajectory is not practical here since all the plane change could be taken out in the first impulse because the Taxi is so far from the Earth. The plane change statement is based upon a spaceport being located at L1 with the capability of launching the Taxi in any direction. A two-impulse trajectory is an appropriate approach. However, most of encounters with the Earth will require trajectories that use non-apse burns because the relative orientations will not support pseudo-Hohmann trajectories. Figure 10 shows two of the possible encounter geometries for a spaceport located at L1.

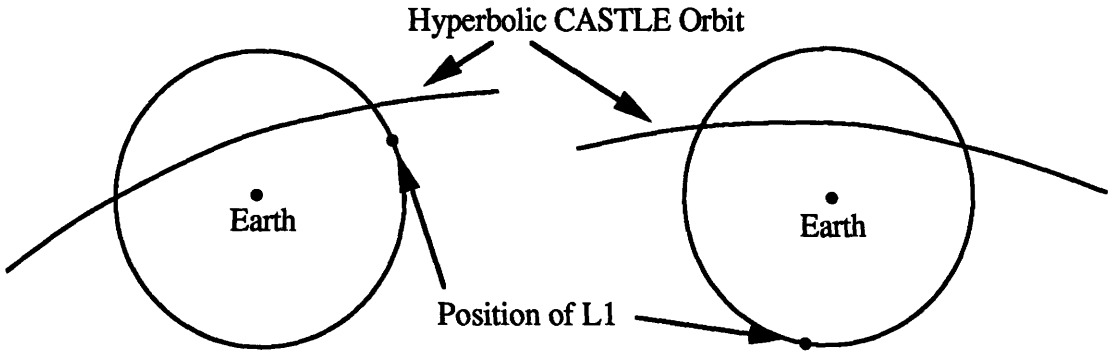

Figure 10 Various Positions of L1 with Respect to the CASTLE Hyperbola

Up to this point not much has been said about spaceport orbits with fixed phasing but a spaceport at L1 would have specified phasing. L1 sweeps out the same angle as the Moon does in its orbit, so the position of L1 can be predicted with planetary tables. The timing of the Taxi transfer becomes more critical than in the other transfers in which the parking orbits had unspecified phasing. The two-impulse Taxi trajectories and the phasing problem will be discussed further in Section 6.4.

4.3.2 Earth Fly-by of VISIT Orbit

The VISIT orbits pass the Earth at a radius of 250,000 to 1,722,000 km. In order to catch the CASTLE at its closest approach, a Taxi leaving L1 would have to follow a trajectory which would require the lowering of the perigee from the L1 altitude or raising apogee as the CASTLE approaches the distance dictated. In some cases a pseudo-Hohmann transfer might be feasible, but a two- or three-impulse trajectory with an intercepting hyperbola would be the general scenario (see Figure 11).

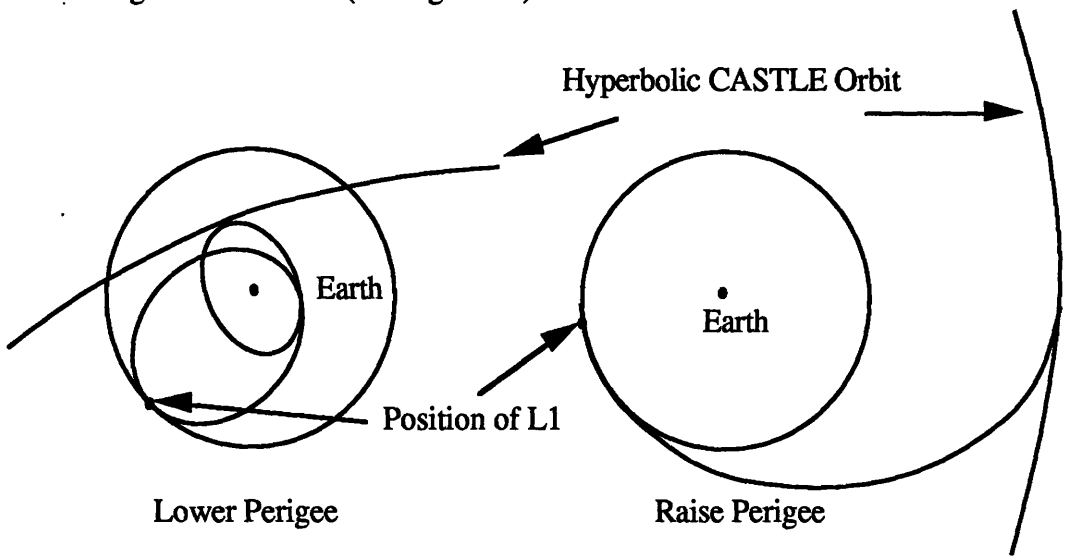

Figure 11 Possible Taxi Trajectories To and From L1

The majority of the cases presented in this section can be solved by a variation of the three-impulse transfer: meeting the CASTLE at its periapse or intercepting the CASTLE hyperbola with another hyperbola. When the phasing of the initial spaceport is known (L1 and Phobos parking orbits), the three-impulse transfer will be expanded to include an additional iteration step to ensure that the Taxi trajectory has the right conditions to rendezvous with the CASTLE. More will be said about this added step in Section 7.3.

The Cycler orbits both span 15 years and both start and end at the Earth which means the first planetary encounter will occur at Mars. For both the Up and Down Cycler orbits there are seven fly-bys of Mars and six of Earth. For the postulated VISIT orbit the time spanned is about 20 years, beginning and ending at Earth. The fly-bys are not as frequent as the Cycler orbits being five Mars fly-bys and three Earth fly-bys. The following tables contain the relevant information for all the encounters used in this study. The data was generated using a FORTRAN program using initial conditions from the paper by Hoffman,

et al. The declination and right ascension in the following tables are measured from the planet's equator and equinox of epoch.

Table 1 Up Cycler Orbit

Encounter	Planet	Date	Periapse radius (km)	V-infinity magnitude (km/sec)	Declination (incoming outgoing) (deg)	Right Ascension (incoming outgoing) (deg)
1	Mars	1 May 97	19541.41	10.73	-15.71 13.58	285.88 105.73
2	Earth	1 Jan 99	8505.39	5.92	14.83 16.74	160.21 43.26
3	Mars	28 May 99	98940.0	11.75	14.76 -14.72	246.91 67.06
4	Earth	8 Feb 01	7650.0	6.18	-8.35 33.70	197.85 101.80
5	Mars	6 Jul 01	4420.0	10.22	18.42 -17.63	305.06 130.40
6	Earth	16 Apr 03	7650.0	5.67	-31.01 18.38	253.43 175.36
7	Mars	12 Sep 03	4420.0	7.23	33.94 -34.60	356.41 193.30
8	Earth	7 Jul 05	7650.0	5.87	-19.44 -25.81	335.41 240.09
9	Mars	13 Dec 05	11560.0	6.05	-4.04 2.77	87.37 274.30
10	Earth	6 Sep 07	12000.0	5.87	16.99 -36.67	32.85 290.05
11	Mars	16 Feb 08	21812.20	7.47	-11.47 7.87	201.20 22.17
12	Earth	10 Oct 09	11986.78	5.89	32.99 -30.96	73.99 324.41
13	Mars	28 Mar 10	17163.92	8.66	-17.78 14.20	240.71 61.37

Table 2 Down Cycler Orbit

Encounter	Planet	Date	Periapse radius (km)	V-infinity magnitude (km/sec)	Declination (incoming outgoing) (deg)	Right Ascension (incoming outgoing) (deg)
1	Mars	20 Jan 97	18705.71	8.53	28.92 -32.40	71.63 251.24
2	Earth	9 Jul 97	11418.15	5.92	-18.50 -10.83	354.94 227.92
3	Mars	7 Mar 99	31960.0	7.37	25.05 -27.66	117.14 297.87
4	Earth	17 Aug 99	8930.0	5.98	-1.02 -25.78	21.23 272.22
5	Mars	15 May 01	17680.0	6.60	-37.86 39.60	222.13 45.27
6	Earth	8 Oct 01	7650.0	5.87	21.28 -16.31	53.31 346.13
7	Mars	7 Aug 03	4420.0	7.3	-71.11 71.82	315.42 166.23
8	Earth	2 Jan 04	8930.0	5.39	28.73 14.02	146.74 51.35
9	Mars	10 Oct 05	4420.0	9.96	-20.61 18.97	19.84 206.35
10	Earth	12 Mar 06	9840.26	5.45	-6.50 27.64	214.35 105.63
11	Mars	19 Nov 07	28560.0	11.59	18.53 -19.88	358.78 178.88
12	Earth	16 Apr 08	9567.0	5.96	-29.23 21.38	260.0 152.36
13	Mars	13 Dec 09	17149.82	10.55	16.62 -18.92	24.27 203.19

Table 3 VISIT Orbit

Encounter	Planet	Date	Periapse radius (km)	V-infinity magnitude (km/sec)	Declination (incoming outgoing) (deg)	Right Ascension (incoming outgoing) (deg)
1	Mars	5 Jan 98	8160.0	4.03	1.17 -1.08	1.73 135.30
2	Earth	21 Mar 01	43727.69	4.19	-41.52 80.64	195.47 37.67
3	Mars	28 Oct 01	5021.35	4.09	24.08 14.79	333.78 147.15
4	Mars	20 Jun 05	52266.74	4.08	-3.30 -.76	350.71 167.17
5	Earth	13 Apr 06	945164.26	4.42	-18.03 19.80	233.86 52.11
6	Mars	18 Apr 09	68000.0	3.79	-4.02 2.58	327.88 143.99
7	Earth	6 Apr 11	711784.8	4.23	-50.10 45.88	212.64 32.43
8	Mars	30 Dec 12	92480.0	3.84	-.28 1.19	341.06 159.51

5. THREE-IMPULSE PROGRAM

The foundation for the three-impulse trajectory program used to find the Taxi trajectories is the routine described in a 1968 TRW memo. The routine became the "Generalized Three-Impulse Processor (GTIP)" which served as a fast, stand alone module that could easily aid any planetary mission planning (Gerbracht (b), 1968). The actual working program or program listing could not be produced so the equations from the memo were used as a basis for the program used here. Gerbracht and Penzo's papers provide a complete discussion of the original routine. A brief explanation of the program used follows. A listing of the equations and a program listing can be found in the appendices.

The parking orbit is defined by its periapse, apoapse, latitude, and longitude with respect to some reference frame. The V-infinity vector is defined by its magnitude, latitude, and

longitude with respect to the same reference frame. Other initial conditions include the inclination and ascending node of the parking orbit and the apoapse of the intermediate ellipse. See Figure 12 for a description of the orientation of the initial conditions.

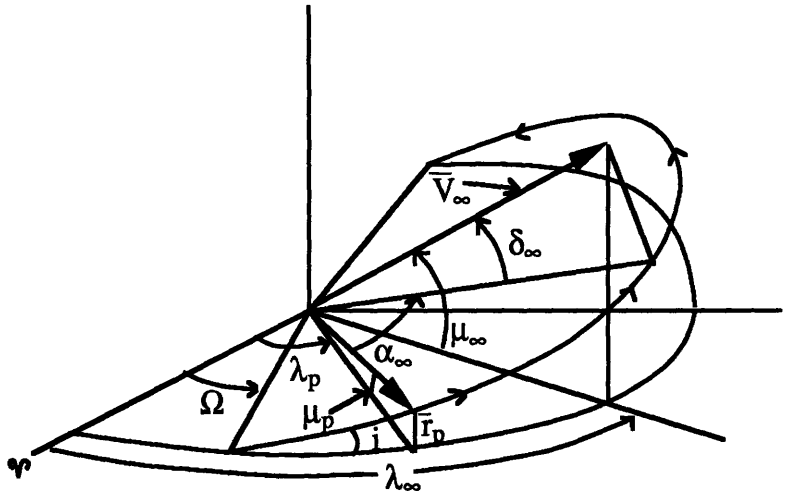

$\bar{r}_p$ = periapse of parking orbit
$\bar{V}_\infty$ = V-infinity vector
δ_∞ = realtive declination
α_∞ = angle between $\bar{r}_p$ and $\bar{V}_\infty$
Ω = ascending node
i = inclination
μ_∞ = declination of $\bar{V}_\infty$
λ_∞ = right ascension of $\bar{V}_\infty$
μ_p = latitude of $\bar{r}_p$
λ_p = argument of periapse

Figure 12 Initial Conditions (Gerbracht, 1968)

A transfer of coordinates from planetary latitude and longitude to relative coordinates between the parking orbit and the V-infinity vector is made before the optimization of the five variables is begun. The variables are: 1) $\theta 1$ - angle between the V-infinity vector and the first impulse, 2) $\Delta\beta$ - the change in flight path angle at the first impulse, 3) $\Delta A1$ - the plane change of the first impulse, 4) $\eta 2$ - the angle between the periapse of the intermediate ellipse and the second impulse, and 5) $\eta 3$ - the angle between the periapse of the intermediate ellipse and the third impulse. A "Golden ratio" algorithm is used to find the minimum of the function used to calculate ΔV (Wilson, 1990). First $\eta 3$ is optimized using the algorithm to find the minimum $\Delta V3$. Then the three variables $\theta 1$, $\eta 2$, $\Delta A1$ are optimized in a linear walk fashion, one variable at a time so that the change in total ΔV is

less than 1 m/sec. Each time one of the three variables above is optimized, $\eta 3$ is also optimized. Finally, $\Delta\beta$ is optimized in the outermost loop so that the change in total ΔV is less than 1 m/sec. Each time the outer loop is performed, the entire four variable optimization above has to be done. A more detailed explanation of the optimization process can be found in the reference by Gerbracht and Penzo (1968). Figures 13, 14, and 15 depict the details of the 1st, 2nd, and 3rd impulses.

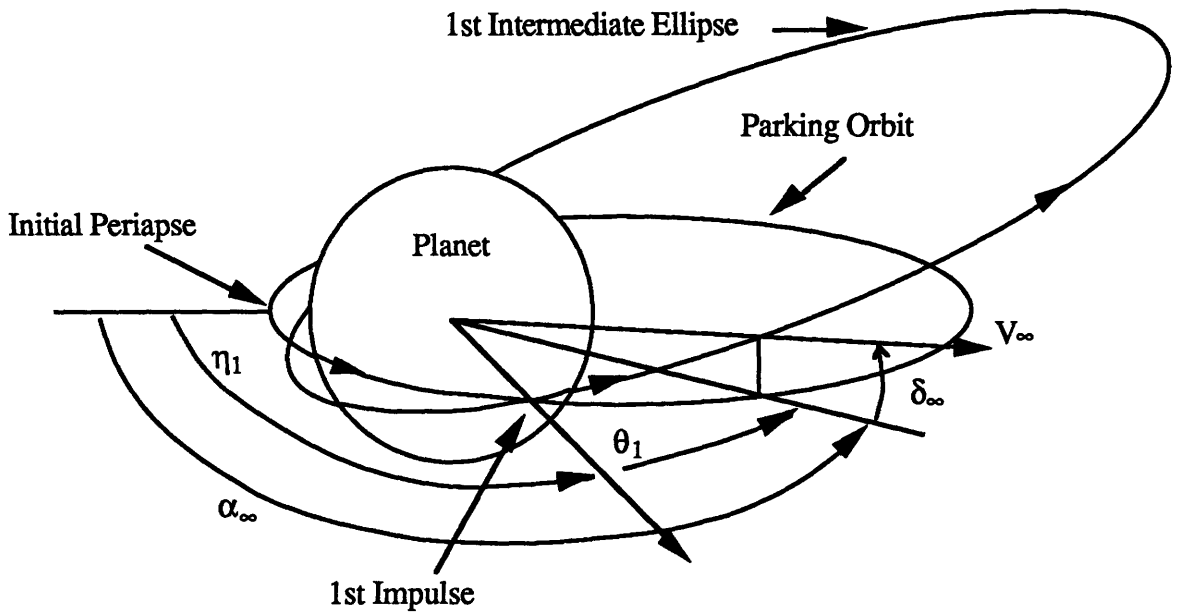

Figure 13 Detail of First Impulse (Gerbracht, 1968)

The Golden Ratio is related to the Golden Section, and both are roots of the Fibonacci quadratic equation. Its interesting applications and historical origins can be found in the references (Vajda, 1989, Battin, 1987, and Hoggatt, 1969). The algorithm's main advantage is the need to calculate only one value each iteration because the other value in the search is used from the previous iteration. However, the Golden Ratio minimization routine only works well when the function has one minimum, but it will not find the absolute minimum in a series of minimums (Wilson, 1990). The present situation was not guaranteed to have single minimums so a number of alternate test routines were run to verify the entire program. The function to be minimized was given a series of inputs over the range searched by the original program. The minimum value of the function found by the test was compared to the value found by the program. No major discrepancies were encountered during the verification process.

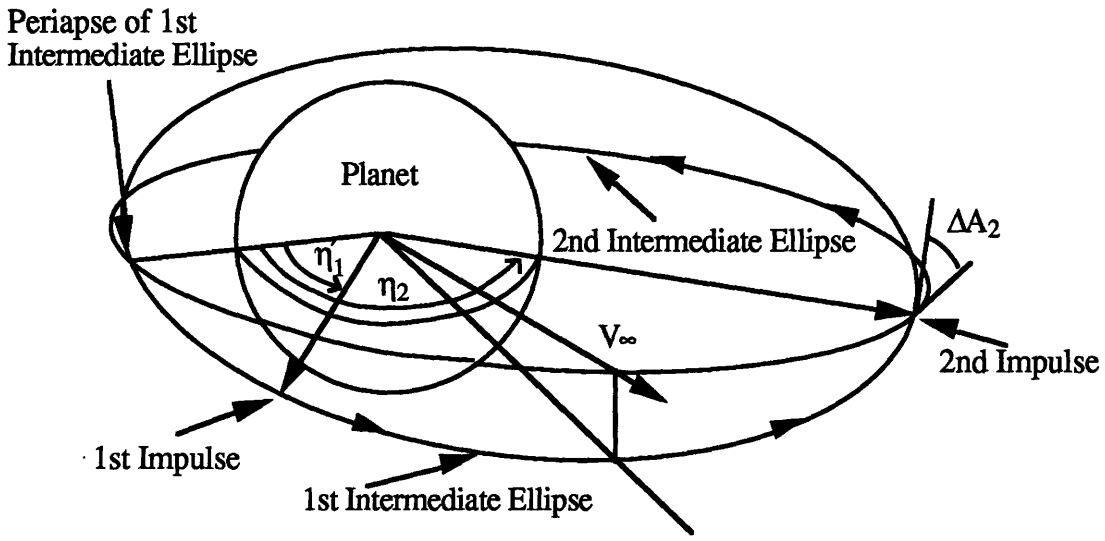

Figure 14 Detail of Second Impulse (Gerbracht, 1968)

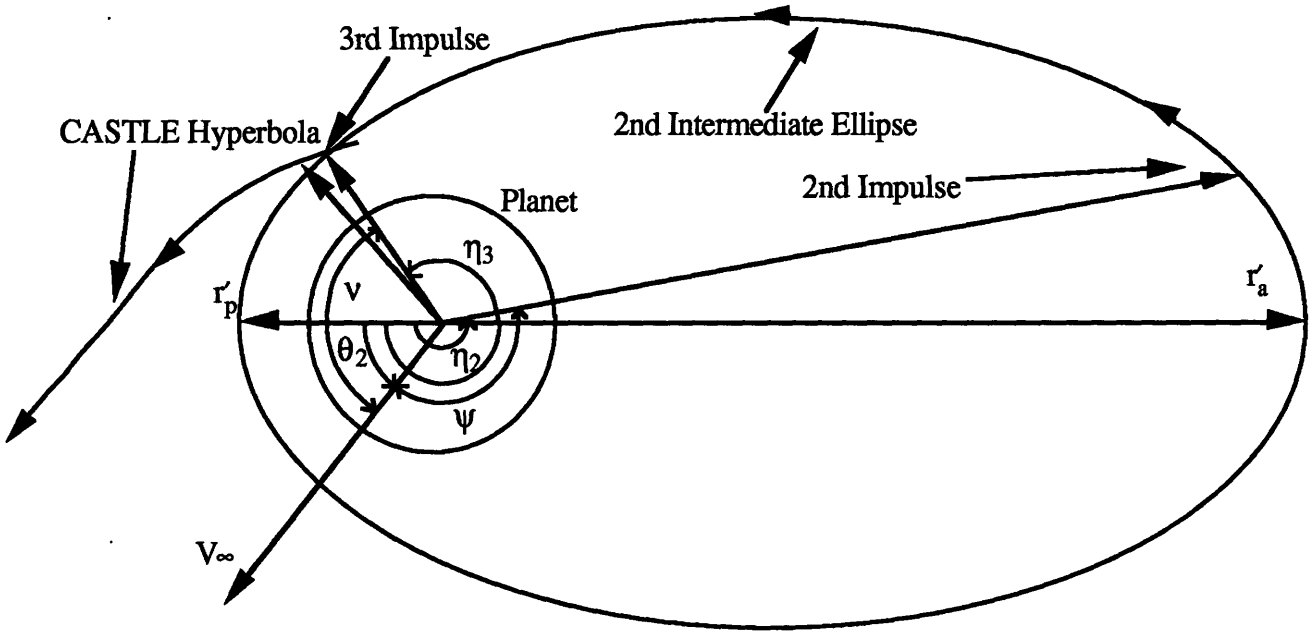

Figure 15 Detail of Third Impulse (Gerbracht, 1968)

6. APPLYING THE PROGRAM

The CASTLE passes by Earth or Mars at various altitudes which range from near surface (≈ 2000 km) to very high altitudes (≈ 700,000 km for Earth and ≈ 100,000 km for Mars). The transfer with the shortest transfer time will rendezvous with the CASTLE at its periapse (See Figure 6 in Section 4.1). However, if the periapse is quite high, the transfer time increases a great deal. In that case a separate hyperbolic escape trajectory can be used to intercept the CASTLE at some far distance like the sphere of influence where

perturbations would be smaller than if the intercept occurred close to the planet (see Figure 7). The program used both options in all encounters. Then the trade-offs between the two intercept options and between ΔV and transfer time can be examined.

The spaceport orbits to be discussed in this section are a low Earth orbit, a low Mars orbit, and a Phobos orbit. The scenarios with the spaceport located at L1 will be discussed later because the three-impulse program is not well suited to look at the behavior of the Taxi trajectory. The graphs presented in this section give a sense of the behavior of ΔV, time and $\theta 1$ vs the apoapse of the intermediate ellipse. Appendix A contains the graphs for all the encounters for all the circulating orbits. The comments made in this section refer to the graphs presented in the main text but are backed by the graphs in the appendix. The trade-off between transfer time and ΔV has to be determined from the data in the graphs. Also, the choice between a hyperbola rendezvous and a periapse rendezvous has to be made for each encounter based upon these graphs.

6.1 SPACEPORT IN LOW EARTH ORBIT

The placement of the spaceport in low Earth orbit is important because of the concerns with getting supplies from Earth's surface or the Moon. The consensus of researchers in the area of circulating orbits reason that the easiest orbit to get into is one launched from Cape Canaveral (Friedlander, 1990). Buzz Aldrin's recent article in Air and Space mentions the use of Space Station Freedom as a possible spaceport for staging from LEO (Aldrin,1990). The Low Earth Orbit used for this study was a potential Space Station circular orbit of 370 km inclined at 28.5°.

6.1.1 Cycler Orbits

The program was applied to the first fly-by of the Earth by the CASTLE in the Up Cycler orbit. The fly-by was characterized by a V-infinity vector with magnitude 5.92 km/sec, inclination 14.83°, right ascension 160.21° and a periapse radius of 8505.39 km.

The orbit of the spaceport was assumed not to be defined in time (i.e. it had unspecified phasing and its orbit did not regress because of the Earth's oblateness). Later the spaceport orbit will have a specified phasing to examine actual trajectories between the Taxi and the CASTLE. The main independent variable was the apoapse of the intermediate ellipse (ra') which was varied to achieve a spread of transfer times and total ΔV. Values from 50,000 to 300,000 km were input into the optimum three-impulse trajectory program. A graph of

ΔV vs ra' is shown in Figure 16. The program gives the optimum angular distance ($\theta 1$) between the longitude of the first impulse and the longitude of the V-infinity vector.

A comment should be made at this time about the presentation of data. When looking at interplanetary trajectories, the common method of graphical presentation are contour plots of C3 for launch and arrival dates in reference to some other parameters such as declination or right ascension of launch and arrival V-infinities. The key to the contour plots is that the V-infinity vector changes for each combination of launch and arrival dates. The vector is never one set value as it is here for each encounter. Therefore, the data can not be presented in a contoured format but will show a profile of a single V-infinity contour.

The graph depicting ΔV vs Apoapse in Figure 16 shows nothing unusual. The total ΔV decreases as the apoapse of the intermediate ellipse increases. This happens because the plane change at the second impulse becomes less costly as the distance from the Earth increases. The transfer time shown in Figure 17 on the following page has the opposite result. As the apoapse increases, the time for the entire transfer increases also.

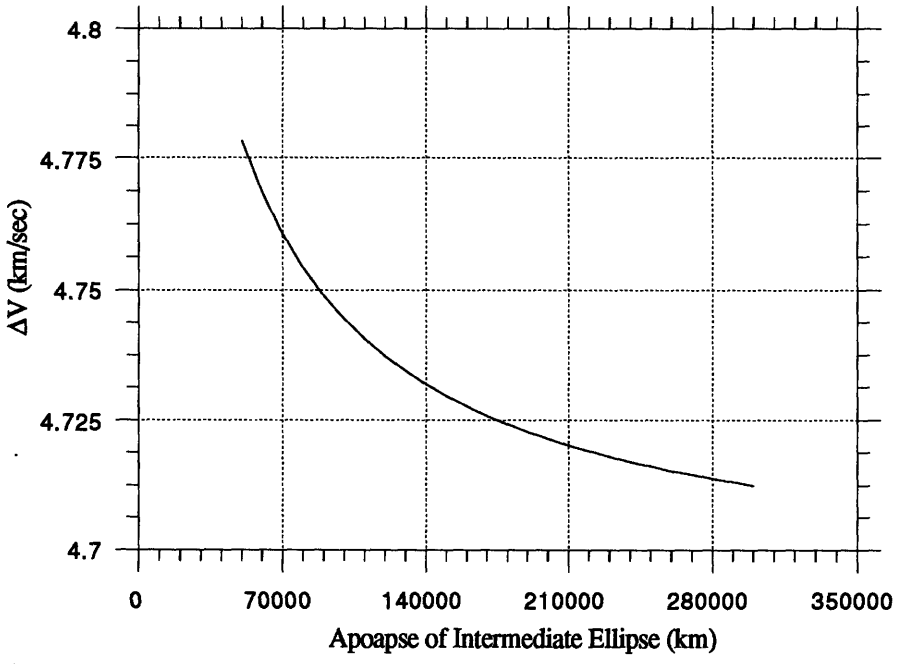

Figure 16 ΔV vs Apoapse for the First Earth Encounter - Up Cycler Orbit

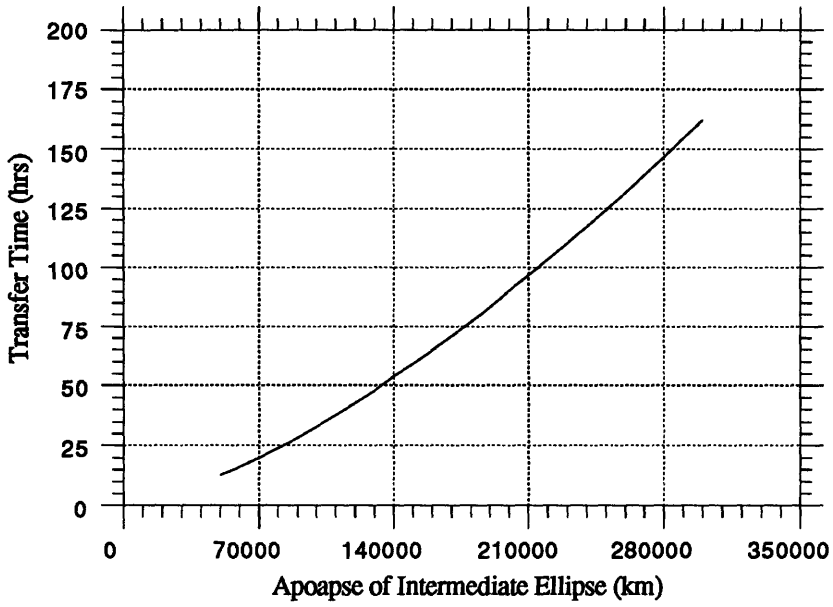

Figure 17 Transfer Time vs Apoapse for the First Earth Encounter - Up Cycler Orbit

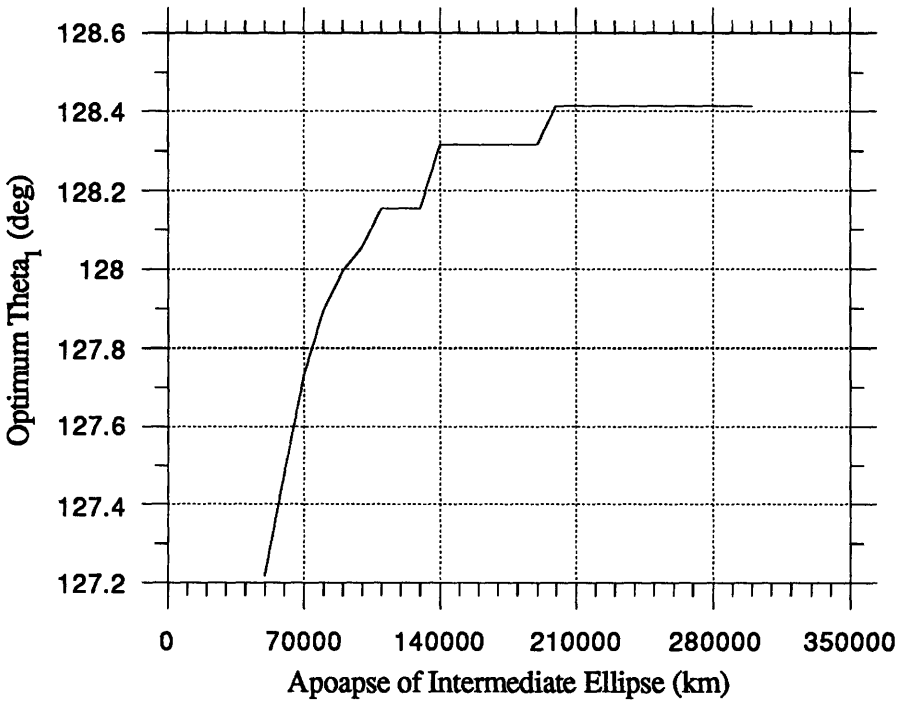

Figure 18 Optimum θ1 vs Apoapse for the First Earth Encounter - Up Cycler Orbit

If Figure 13 is recalled along with the explanation of the three-impulse optimization routine, θ1 is the angle between the first impulse and the projection of the V-infinity vector onto the

parking orbit plane. According to Figure 18, θ1 follows a smooth path upward as the apoapse increases but as the apoapse reaches its largest values, θ1 experiences some discontinuities. Although not confirmed, the discontinuities may arises from the numerical procedures in the optimization process (e.g. the tolerances on various comparisons).

Figure 19 combines all the Earth encounters for the Up Cycler Orbit. The behavior of the ΔV is identical to Figure 16. Two things should be noted here. The first is in the legend where the encounter numbers, E1, E2, etc., are followed by 'hyp'. That identifies the plot as depicting the intercept hyperbola option (see Figure 7). This option requires an additional rendezvous (fourth) impulse at the Earth's sphere of influence to rendezvous with the CASTLE. The second are the differences between the curves for the different encounters. The flatter curves represent encounters where the relative declination between the parking orbit inclination and the declination of the V-infinity vector are small. Smaller relative declinations mean a smaller plane change and thus a smaller second impulse.

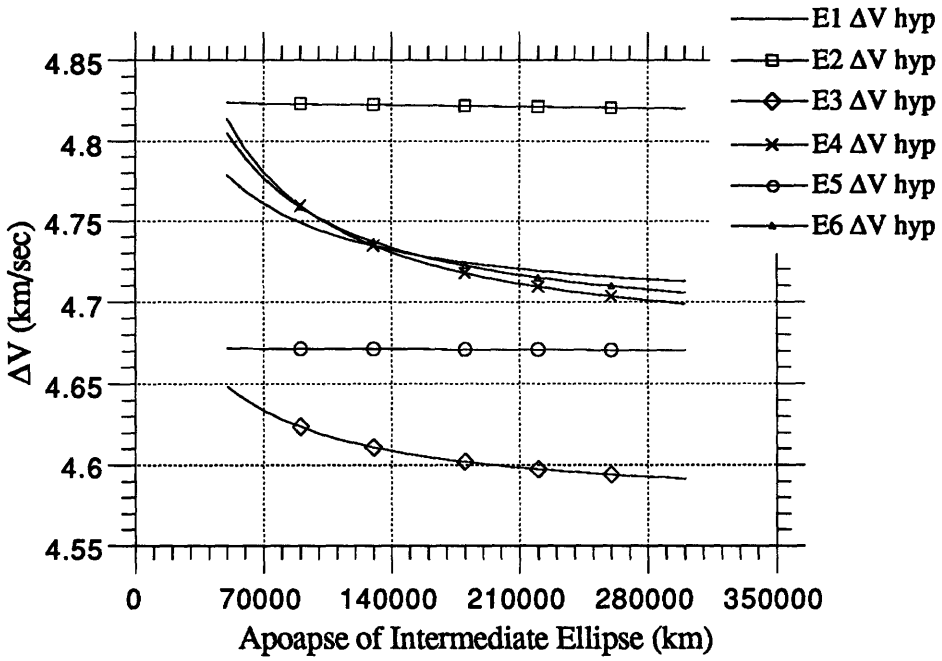

Figure 19 ΔV vs Apoapse for the All Earth Encounters - Up Cycler Orbit

Figure 20 depicts the Taxi transfer time for rendezvousing with the CASTLE versus the increasing length of the apoapse. This graph differs from the one in Appendix A because both the hyperbolic and the periapse rendezvous options are shown. In Appendix A, the transfer time is only the time up to the third impulse which does not include the additional

time it takes for the Taxi to travel along its hyperbola toward the rendezvous with the CASTLE. The additional time on the hyperbolic rendezvous case is a constant 41.48 hours for the first Earth encounter on the Down Cycler orbit and 41.04 hours for the second encounter. The difference in the time between the two encounters is a result of the different V-infinity vectors.

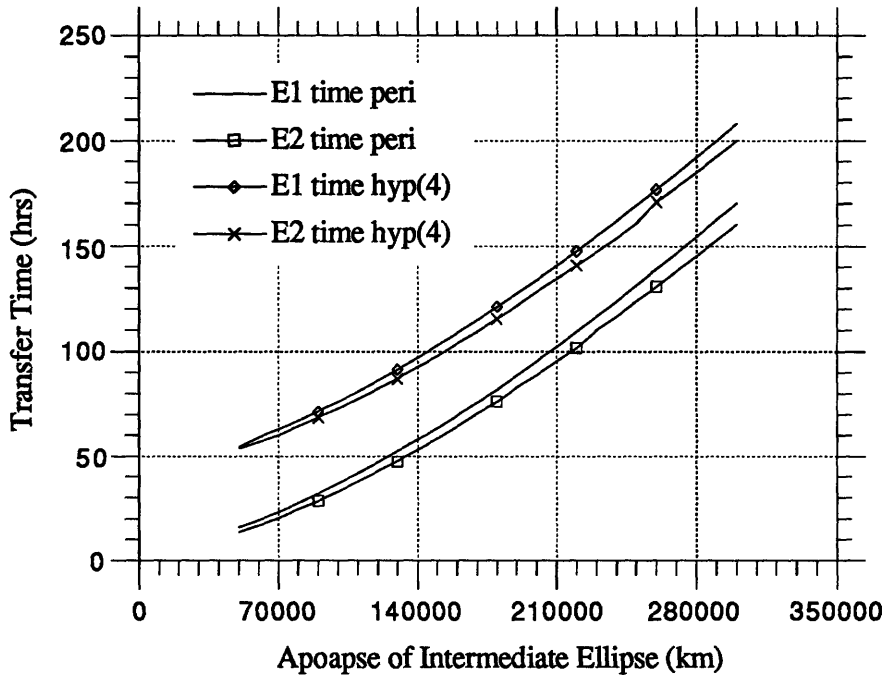

Figure 20 Transfer Time vs Apoapse for 1st and 2nd Earth Encounters - Down Cycler Orbit

6.1.2 VISIT Orbit

The program was applied next to the first Earth approach of the VISIT orbit. The fly-by was characterized by a V-infinity vector with magnitude 4.19 km/sec, inclination -41.52°, and right ascension 195.47°. The spaceport was in a circular 370 km Earth orbit inclined at 28.5°. Figure 21 shows ΔV vs Apoapse length for the first Earth encounter of the VISIT orbit.

The figure also includes Earth encounters from the Up and Down Cycler orbits for comparison. The ΔV is much lower for the VISIT orbit than the Cycler orbits because the magnitude of the V-infinity vector is on the average 1 km/sec slower (see Tables 1, 2, and 3). The VISIT curve is steeper because of its large initial relative declination.

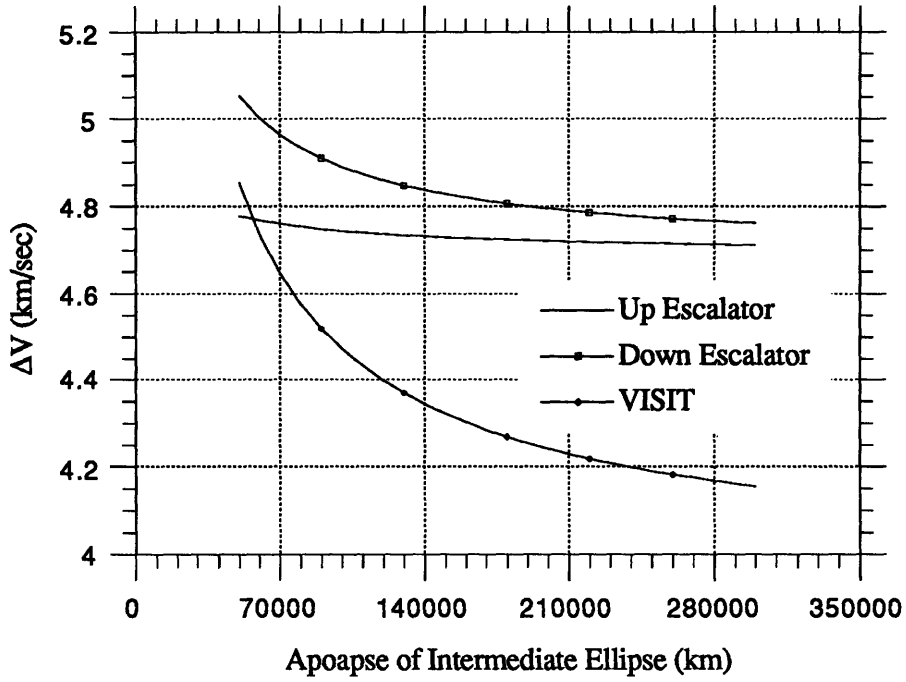

Figure 21 ΔV vs Apoapse for First Earth Encounter - All Circulation Orbits

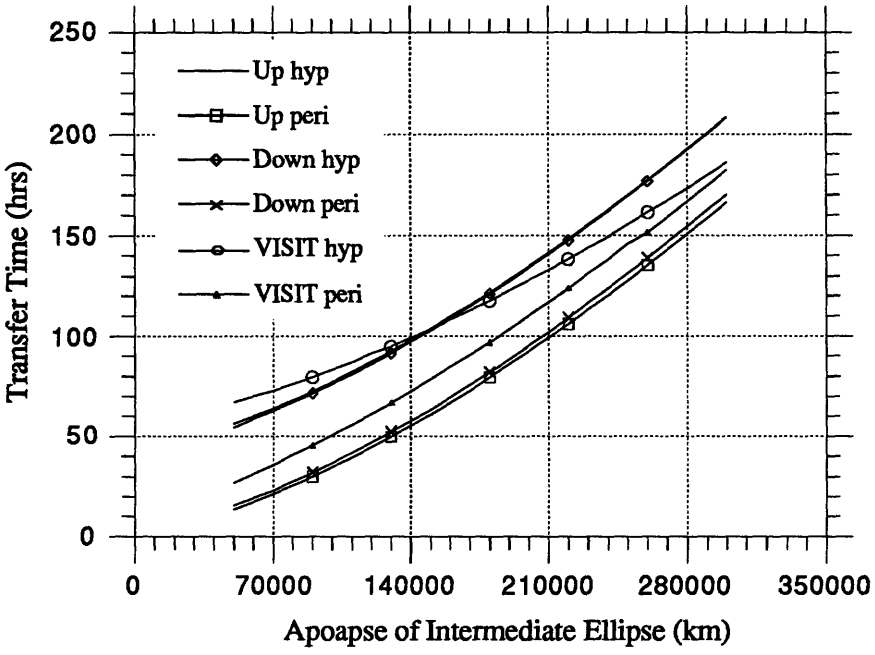

Figure 22 Transfer Time vs Apoapse for the Two Rendezvous Options

Figure 22 page is the corresponding transfer time versus apoapse graph for all three circulating orbits. The first Earth encounter is shown for the Down Cycler and the both the Cycler orbits are almost identical because the V-infinity vectors for the encounters are fairly similar. The time for the periapse rendezvous of the VISIT orbit is longer because of the higher periapse radius of the CASTLEs fly-by. Again the time for the hyperbolic rendezvous option is higher.

Figure 23 is a continuation of the circulation orbit comparison. The graph shows ΔV vs Apoapse for the second Earth encounters for the Up and Down Cycler orbits and the first Earth encounter for the VISIT orbit. Hyp is the hyperbolic intercept case and peri is the CASTLE hyperbola periapse rendezvous case. The added fourth impulse for the hyperbolic intercept case is on the order of 100 m/sec and increases with the radius of the CASTLEs closest approach. The ΔV for periapse rendezvous case also increases with the closest approach radius.

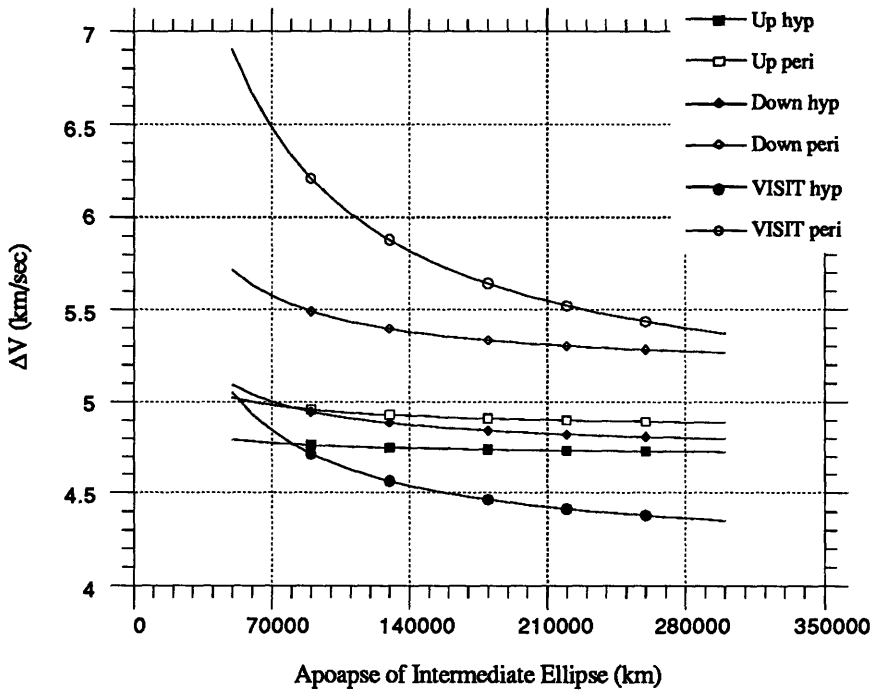

Figure 23 ΔV vs Apoapse for the Two Rendezvous Options - All Circulation Orbits

More than likely, two Taxis will rendezvous with the CASTLE at each encounter. A manned Taxi will transfer the crew and an unmanned Taxi will transport supplies. ΔV requirements need to be minimized for both Taxis but transfer time is more critical on the

manned Taxi. The shorter transfer time will expose the crew to less space radiation and less time in a zero-g environment. The unmanned Taxi does not have to worry about the radiation so it can take a longer time to rendezvous. This means that the manned Taxi will have to expend extra ΔV to use the periapse rendezvous to avoid the extra 40 hours of exposure the hyperbola intercept causes (24 hours for Mars encounters). The cargo Taxi can use the hyperbola intercept to take advantage of the lower ΔV values without having to worry about exposure time.

6.2 SPACEPORT IN LOW MARS ORBIT

The spaceport orbit around Mars was arbitrarily chosen to be at an altitude of 200 km with 0° inclination. A base on Mars would most likely be located at the equator to take advantage of the planetary rotation when launching from Mars to orbit. This section will follow a similar format as Section 6.1 when discussing the behavior of the different encounters at Mars.

6.2.1 Cycler Orbits

For a spaceport located in a low Mars orbit the curves for ΔV vs Apoapse are relatively flat as compared to the graphs for Earth (See Figure 24 on the following page). The figure shows all the encounters of Mars by the CASTLE on the Down Cycler orbit. The curves are flatter than those for Earth encounters because the parking orbit has 0° inclination so the relative declination varies less.

A comparison of the Up and Down Cycler orbits show that for Mars the Down Cycler orbit has lower ΔV values for many of the encounters. The figures in Appendix A substantiate this. The lower ΔV values make the Down Cycler orbit more economical than the Up Cycler orbit for return trips because the Taxi will not have the larger V-infinity magnitudes. See Tables 1 and 2 and consult the references by Friedlander and Hoffman for a detailed discussion of this topic.

Figure 25 shows the transfer times for four Mars encounters of the Up Cycler Orbit. The times, from the hyperbolic rendezvous option, all follow a similar curve but initial times vary from 25.1 hrs to 37.7 hrs.

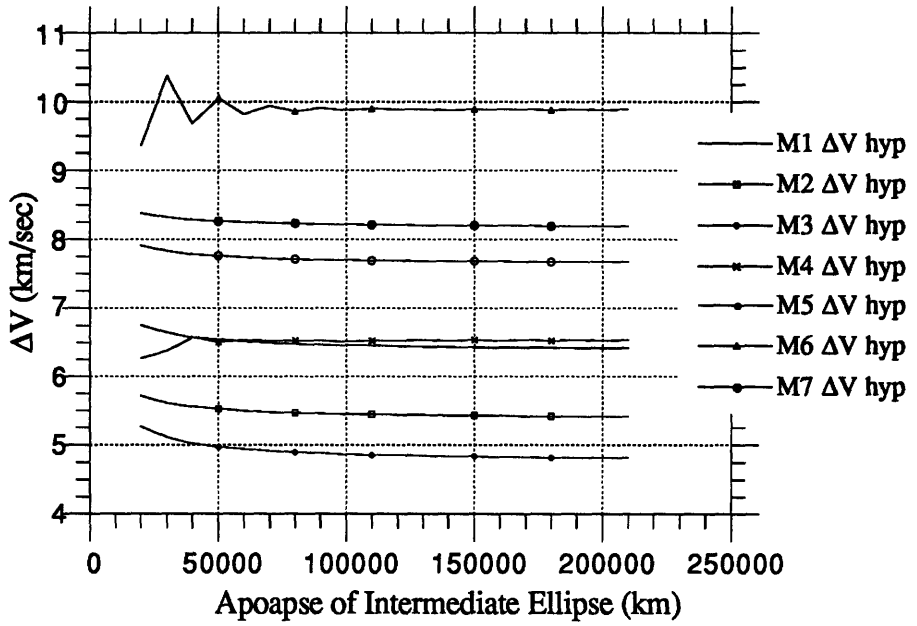

Figure 24 ΔV vs Apoapse for All Mars Encounters - Down Cycler Orbit

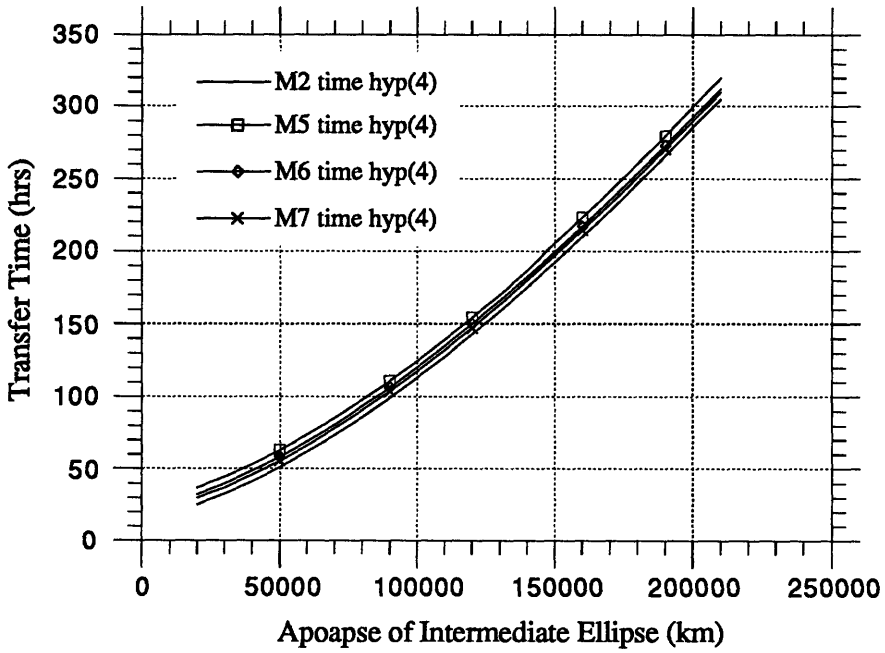

Figure 25 Transfer Time vs Apoapse for Some Mars Encounters - Up Cycler Orbit

6.2.2 VISIT Orbit

Figure 26 shows a comparison between the Up and Down Cycler orbits and the VISIT orbit for ΔV vs Apoapse length. The encounters were selected to show that , for the most part, the Up Cycler encounters have higher ΔV totals than either the Down Cycler or the VISIT encounters. The number following the Up, Down, or VISIT indicate the encounter number.

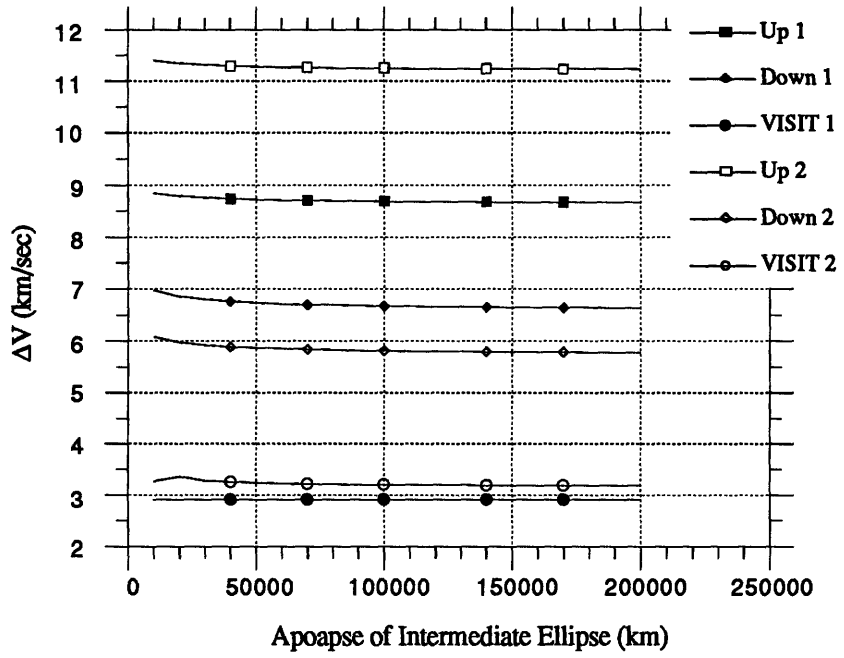

Figure 26 ΔV vs Apoapse for Two Mars Encounters - All Circulation Orbits

6.3 SPACEPORT NEAR PHOBOS

As mentioned before, the location of a spaceport near Phobos would support a fuel mining operation. The orbit of Phobos is inclined approximately 1° and has a semi-major axis of ≈9400 km. The spaceport would be located very near Phobos but not near enough to run into any gravitational attraction problems.

A third intercept option exists for the Taxi, besides the periapse intercept and the hyperbolic intercept, in which the three-impulse trajectory would be followed, except the second impulse would not only perform a plane change but also lower the periapse from ≈9400 km

to 3600 km. The lower periapse will lower the total ΔV because the speed at a 3600 km radius is much faster than at 9400 km. The gain in speed cuts the third impulse which moves the Taxi onto a hyperbolic escape path.

6.3.1 Cycler Orbits

For the encounter at Mars on the Cycler orbit with the spaceport near Phobos, the three-impulse program has produced optimum values of θ1 for a range of ra' from 20,000 km to 200,000 km. Appendix A contains the graphs of the Cycler orbits for ΔV, time, and optimum θ1 vs the apoapse of the intermediate ellipse. Figure 27 gives a sample of the transfer times for the Taxi trajectories seen in the Mars encounters of the Down Cycler orbit. The transfer times are for the first and second Mars encounters for a spaceport in Phobos' orbit and include the hyperbolic and low hyperbolic rendezvous options. The low hyperbolic rendezvous has a periapse below the radius of Phobos' orbit. The transfer times in this graph do not include the approximately 19 extra hours it takes the Taxi to go along its hyperbola to rendezvous with the CASTLE. The time comparison for the two rendezvous options reveals nothing concrete because in one encounter the transfer time for the normal hyperbolic option is longer than the low hyperbolic option while in the other encounter the opposite is true. The times all depend upon the initial orientations of the V-infinity vector.

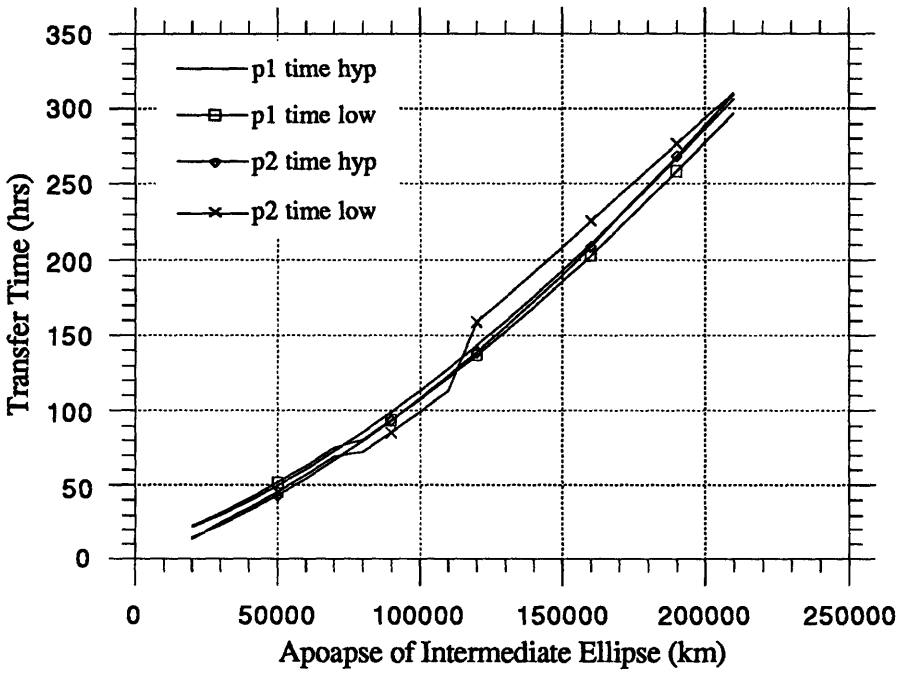

Figure 27 Transfer Time vs Apoapse for Two Mars Encounters - Up Cycler Orbits

6.3.2 VISIT Orbit

Figure 28 shows the Mars encounters of the VISIT orbit in relation to a spaceport located in the orbit of Phobos. Phobos' orbit is inclined slightly with respect to Mars' equator so the relative declination can vary a great deal to produce a large plane change angle as shown in the behavior of the second encounter

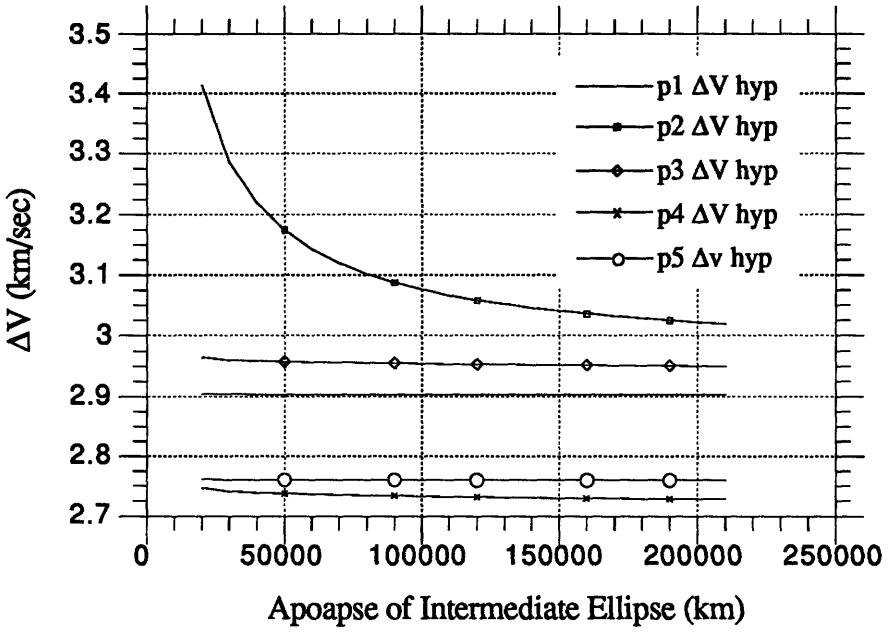

Figure 28 ΔV vs Apoapse for All Phobos Encounters - VISIT Orbit

Figure 29 depicts the comparison of the three circulating orbits for the second and third Mars encounters. Again the encounters by the CASTLE in the VISIT orbit have lower ΔV values due to the lower V-infinity magnitudes.

Figure 30, like Figure 29, shows all the circulating orbits. However, in this figure two of the three rendezvous options for Phobos are shown rather than the different encounters. The "hyp" represents a hyperbola rendezvous with the Taxi's hyperbola having a periapse equal to the radius of Phobos' orbit (≈ 9400 km). The "low" represents a different hyperbola rendezvous with the periapse of the hyperbola equal to a much lower 3600 km. The figure shows quite clearly that a low hyperbola rendezvous offers a lower total ΔV because of the lower ΔV needed at the third impulse.

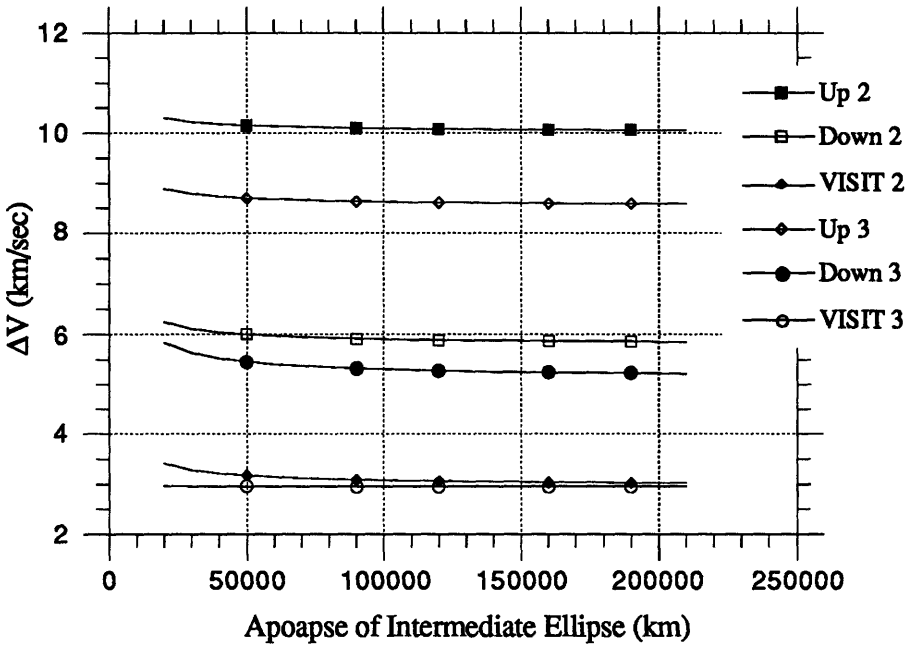

Figure 29 ΔV vs Apoapse for Two Phobos Encounters - All Circulation Orbits

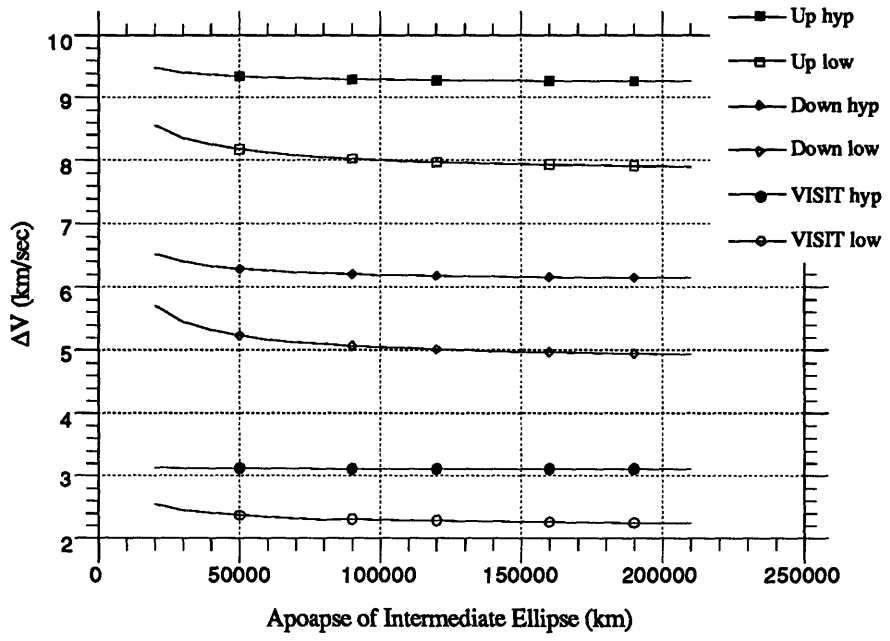

Figure 30 ΔV vs Apoapse for Two Rendezvous Options - All Circulation Orbits

6.4 SPACEPORT AT L1

The spaceport at L1 presents the most complex Taxi trajectories in this analysis. A literature search did not produce any papers that examined ways to launch from L1 to a specified V-infinity vector. However, trajectories to and from L1 to LEO and to the Moon are well documented (Eagle Engineering (a,b), 1988). The combination of elliptical orbits provides many solutions but common sense dictates that some trajectories have to be better than others.

A spaceport at L1 does not have the same velocity or period as an object in a circular orbit around the Earth at the same altitude. A spaceport at L1 would be travelling with the period of the Moon (≈27.5 days) and at velocity of approximately 1.02 km/sec. The spaceport would be travelling slower at L1 than if it was in a circular orbit at the same altitude relative to the Earth. If the Moon suddenly disappeared or if the spaceport was jolted out of its semi-stable position, the spaceport would enter an elliptic orbit with L1 at the apoapse. Conversely a spaceport located at L2 would be travelling with a velocity that is faster than if it was in a circular altitude. Then the spaceport would be in an elliptical orbit with the periapse located at the distance of L2 if the Moon disappeared.

Since the three-impulse method is not well suited for the spaceport located at a Lagrangian point, the behavior just mentioned might be exploited to aid in the Taxi trajectories from Lagrangian points. The Taxi would just have to nudge itself from the spaceport and would automatically enter an elliptical orbit because it does not have the stability the spaceport provided in order to stay at L1. Another condition to be exploited is the distance of L1 from the Earth. The distance, which is on the order of 300,000 km, allows an inexpensive plane change. The ΔV for a plane change is

$$\Delta V = 2\, V_c \sin \frac{\delta_\infty}{2}$$

where V_c is the circular velocity of L1 and δ_∞ is the plane change angle.

The maximum the ΔV could be is 2.04 km/sec with a $\delta_\infty = 180°$. In any type of trajectory the first impulse will be a plane change along with ΔV to alter the periapse of the elliptical orbit the Taxi entered when it left the spaceport.

A different approach is required for the L1 to CASTLE trajectories because the three-impulse program is not suited to the initial conditions. The large distance of L1 from the

Earth does not make L1 a low planetary parking orbit. A separate program was written to look at the various paths the Taxi could follow from L1 to the CASTLE hyperbola. The first trajectory is a simple point-to-point path from L1 to the periapse of the CASTLE hyperbola. See Figure 31.

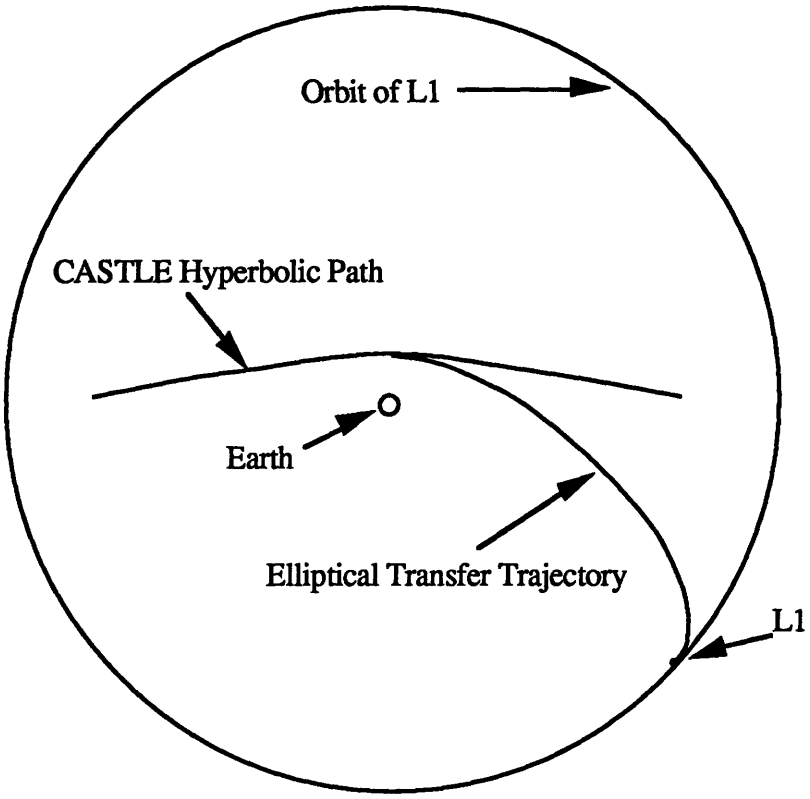

Figure 31 Two-Impulse Transfer from L1 to the CASTLE

To calculate the trajectory, a routine was written from the Improved Method of Gauss (Battin, 1987). Gauss' method takes two distances, a transfer angle, and a transfer time to produce a connecting trajectory. The transfer angle was varied from 0° - 360° and the time from 20 -200 hours. The orbits produced from this routine included some hyperbolas and high elliptic orbits which would be of questionable use for Taxi transfers. The routine was then modified to identify the possible two impulse transfers for each Earth Encounter. The relative position of L1 to the axis of the CASTLE hyperbola was calculated for the date of closest approach. Then a time increment was selected and L1 was moved backward from the time before closest approach. At each new position, the transfer angle was calculated along with another trajectory. The total time was limited to the period of the ellipse with a semi-major axis of the sum of the closest approach radius and the radius of L1. That number was longest time the Taxi had to make its rendezvous. For each Earth encounter 20 trajectories were calculated.

Figure 32 depicts the ΔV needed for a Taxi trajectory from L1 using the Improved Method of Gauss. The transfer angles were adjusted to make the graph readable (where appropriate negative angles and angles greater than 360° were used to eliminate discontinuities). For some of the encounters a minimum ΔV does exist, but in most cases the resulting trajectory is a rectilinear ellipse. After examining the data using Gauss' method, a low ΔV trajectory is a rare find.

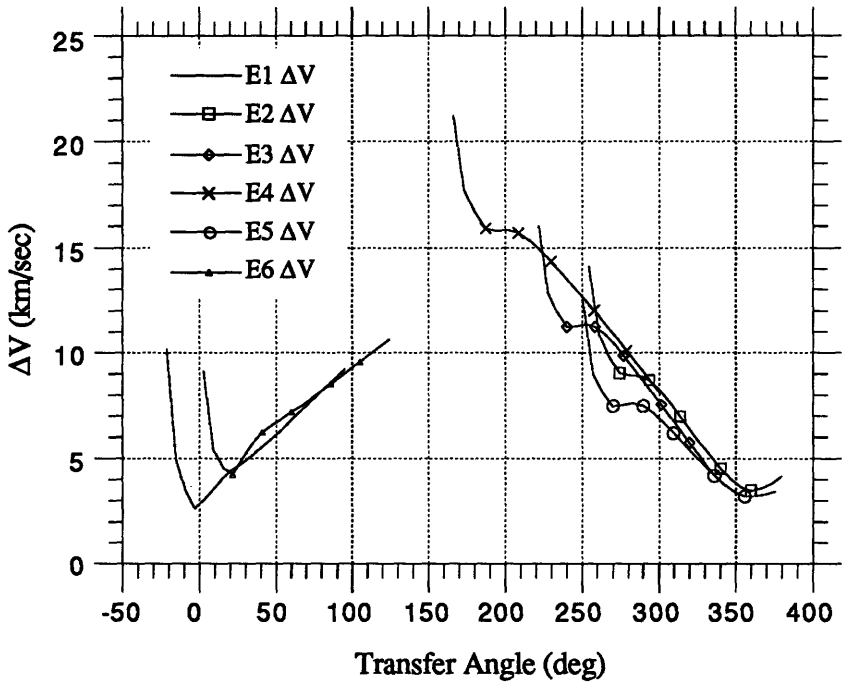

Figure 32 ΔV vs Transfer Angle for the L1 Encounters - Up Cycler Orbit

The second path type uses two ellipses to travel from L1 to the periapse of the CASTLE hyperbola. One ellipse is assumed to have a periapse that coincides with the periapse of the hyperbola. Figure 33 shows this trajectory type.

The second ellipse connects L1 and the first ellipse. The angular position of L1 at the Taxi launch to the axis of the hyperbola at Taxi arrival is the main variable. The relative positioning determines the difference in flight path angles between the two ellipses (Δbeta). The Δbeta in turn affects the second ΔV given by

$$\Delta V = \sqrt{V_{e1}^2 + V_{e2}^2 - 2\, V_{e1} V_{e2} \cos \Delta beta}$$

where V_{e1} and V_{e2} are the velocities on the 1st and 2nd ellipses respectively

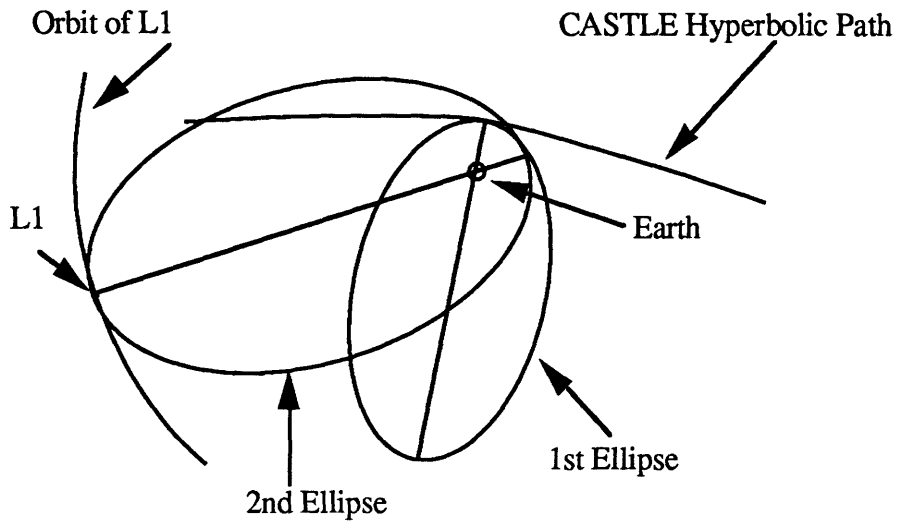

Figure 33 Two-Ellipse Transfer Between L1 and the CASTLE

The apoapse of the first ellipse also affects the total ΔV be changing the velocity at the periapse of the 2nd ellipse. To calculate the trajectory a patched-conic routine was used which varied the relative position angle between L1 and the axis of the hyperbola from 0° to 360°. Therefore, the total ΔV was made up of the plane change, ellipse to ellipse ΔV, and ellipse to hyperbola ΔV.

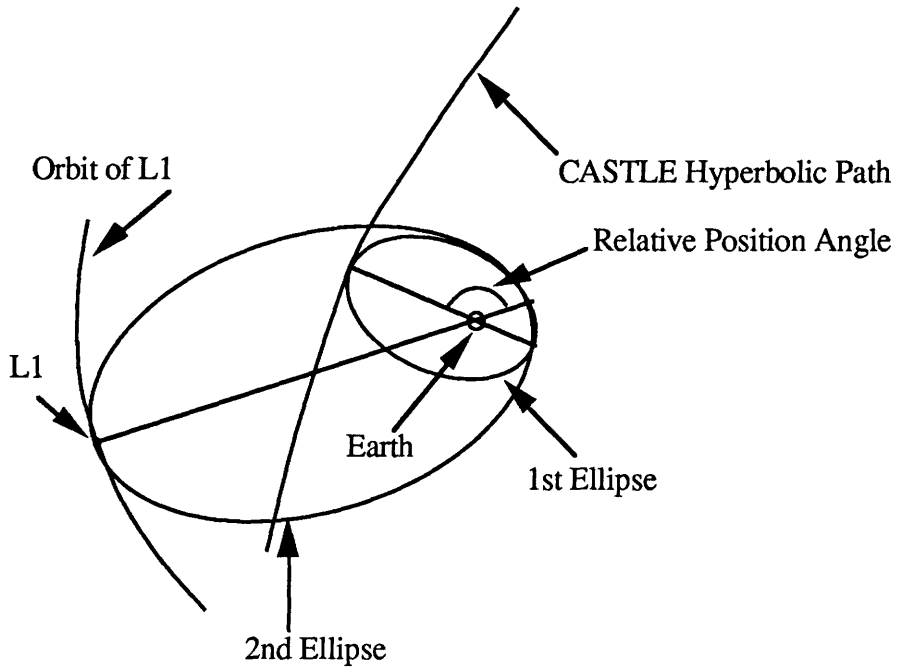

Figure 34 Second Option on Two-Ellipse Transfer

An addition was made to the routine to see if any savings could be made when the hyperbola was between the Earth and L1. Instead of the periapse of the ellipse coinciding with the periapse of the hyperbola, the apoapse would. See Figure 34.

This option was used only when the relative position angle is between 90° and 270°. When the position is outside that limit the hyperbola is not between the Earth and L1. Additionally, this option is not used when the periapse of the hyperbola is greater than the distance to L1.

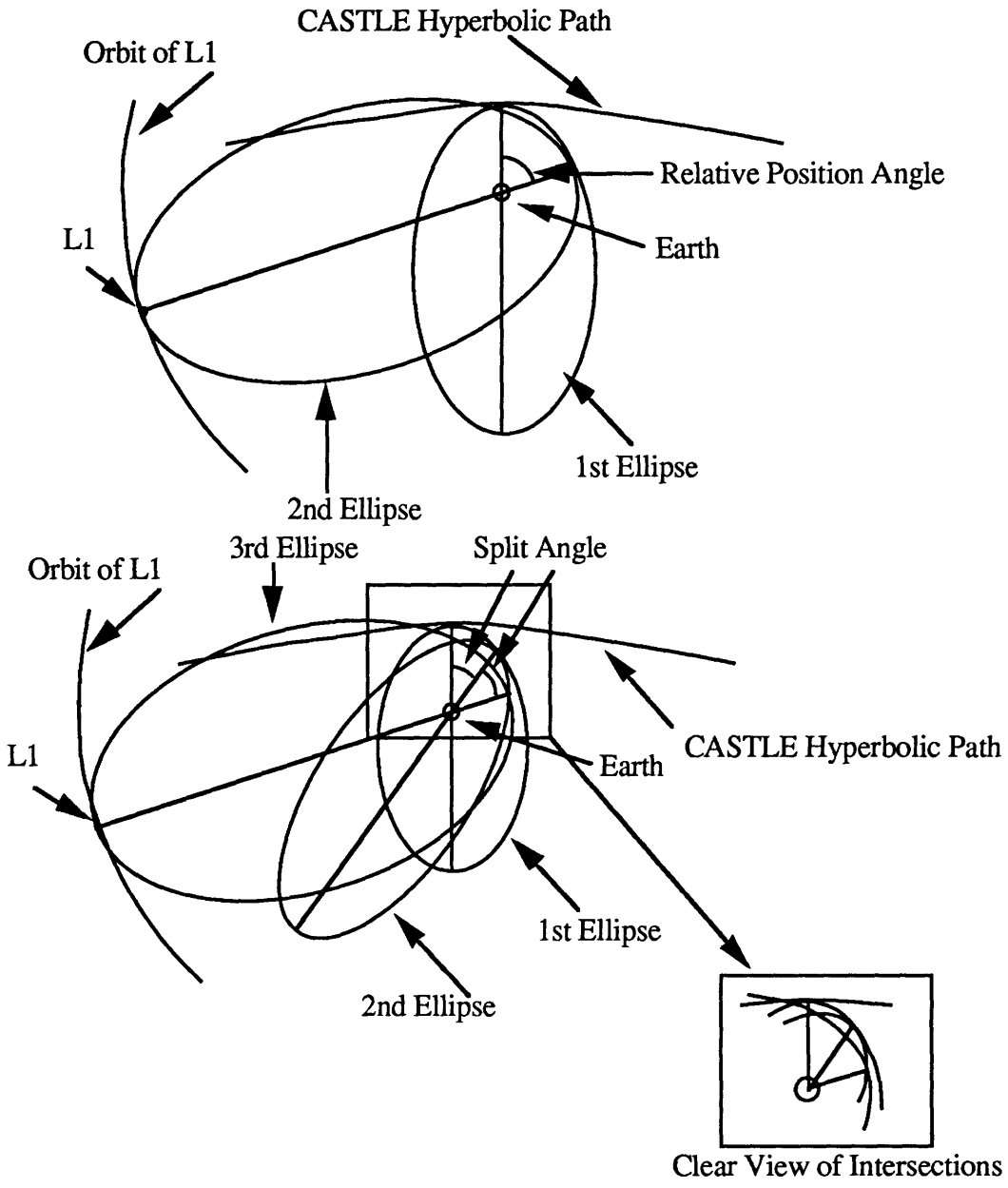

Figure 35 Difference Between Two and Three-Ellipse Transfer

The third path examined tried to exploit any savings found in making a three ellipse trajectory. The rationale behind trying this three ellipse approach is the hope that breaking up the large position angle into two smaller angles will reduce Δbeta, the change in flight path angles between the ellipses. The smaller Δbetas would in turn produce a smaller total ΔV than the original ΔV with only two ellipses. Figure 35 illustrates the two and three ellipse trajectory.

The three options were all integrated into one program. The program made no attempt to optimize the ΔV. The only optimization that could be made is have the relative position angle equal 180°. However, the position is fixed within the encounter. L1 has a position when the CASTLE arrives and a position when the Taxi leaves. The encounters of Earth by the different circulating orbits do not produce a relative angle of 180° every time. The departure position is the only thing that can be varied to achieve the proper position angle. Again a trade off must be made between transfer time on the Taxi and the ΔV needed to make the transfer.

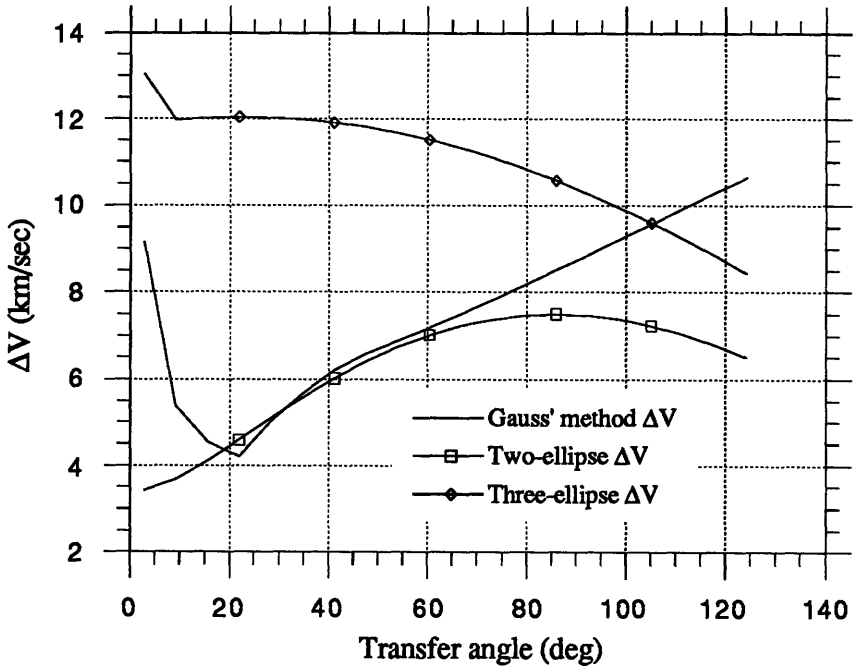

Figure 36 ΔV vs Transfer Angle Comparing Three Methods for 6th L1 Encounter - Up Cycler Orbit

The program was run first as a general case for all relative position angle. Then it was modified to look at each Earth encounter. Figure 36 uses the results of the program in a comparison of three of the methods used to calculate the ΔV for the Taxi trajectory between L1 and the CASTLE. At some angles the two-ellipse method produces a ΔV which is lower than Gauss' method, and even the three-ellipse method produces some ΔVs that are lower than the first method. The conclusion to be drawn here is that a number of methods have to be analyzed to find the minimum ΔV trajectory from L1.

6.5 COMPARISON TO PSEUDO-HOHMANN

This section will compare some of the results from the three-impulse program to Pseudo-Hohmann trajectories for the various cases already discussed.

The situation here is a transfer from an elliptical or circular parking orbit to a hyperbolic orbit. In reality, the transfer is not, in the strictest sense, a pure elliptical Hohmann transfer from one circular orbit to another. However, that does not take away the usefulness from the comparison of a pseudo-Hohmann orbit to another non-Hohmann transfer. In the analysis the transfer angle is assumed to be 180°, and the impulses are at the periapse of the parking orbit / periapse of the transfer ellipse and at the periapse of the hyperbola / apoapse of the ellipse. Figure 37 depicts the geometry. In some cases in which the hyperbola flies below the parking orbit the apoapse and the periapse of the transfer ellipse will switch pairings (see Figure 38).

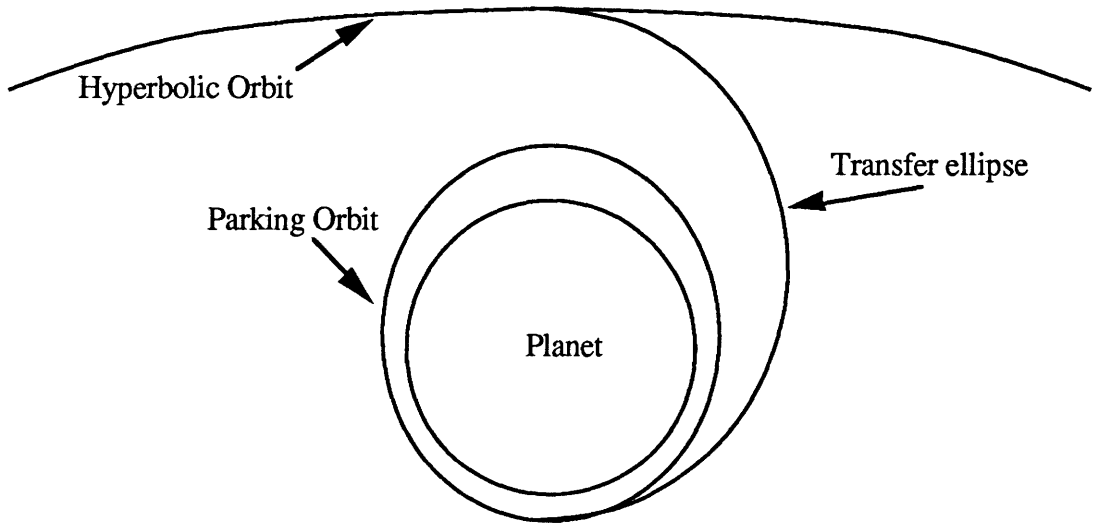

Figure 37 Pseudo-Hohmann Transfer

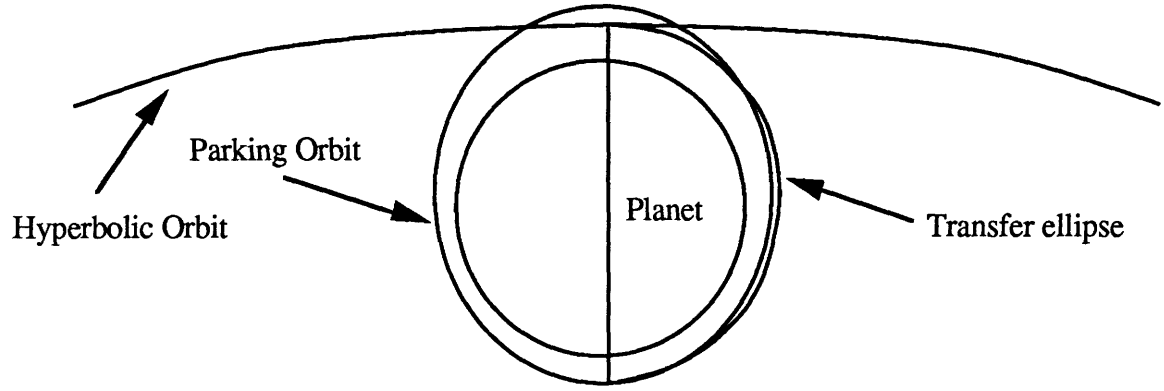

Figure 38 Transfer With Hyperbola Below Parking Orbit

The speed at the periapse of the parking orbit is

$$V_{ppo} = \sqrt{\mu\left(\frac{2}{r_{ppo}} - \frac{1}{a_{po}}\right)}$$

The speed at the periapse of the hyperbola is

$$V_{ph} = \sqrt{\frac{2\mu}{r_{ph}} + V_{\infty}^2}$$

The semi-major axis of the transfer ellipse is the sum of the two periapses.

$$a_e = r_{ppo} + r_{ph} \quad \text{and} \quad r_{pe} = r_{ppo} \quad r_{ae} = r_{ph}$$

The velocities at the periapse and apoapse of the transfer ellipse respectively are

$$V_{pe} = \sqrt{\mu\left(\frac{2}{r_{pe}} - \frac{1}{a_e}\right)} \text{ and } V_{ae} = \sqrt{\mu\left(\frac{2}{r_{ae}} - \frac{1}{a_e}\right)}$$

The total ΔV is the sum of the differences of the velocities at each impulse.

$$\text{Total } \Delta V = (V_{ppo} - V_{pe}) + (V_{ph} - V_{ae})$$

The equations above came from astrodynamic textbooks (Bate, et. al, 1971 and Roy, 1988).

Examining the scatter graphs in Figures 39 and 40 reveal that the Pseudo-Hohmann trajectories can not compete with the three-impulse trajectories. The advantage of reducing the plane change ΔV in the three-impulse trajectory can readily be seen in the following

figures. This section may be considered to be trivial but it is the verification of the choice of the three-impulse trajectory in this situation.

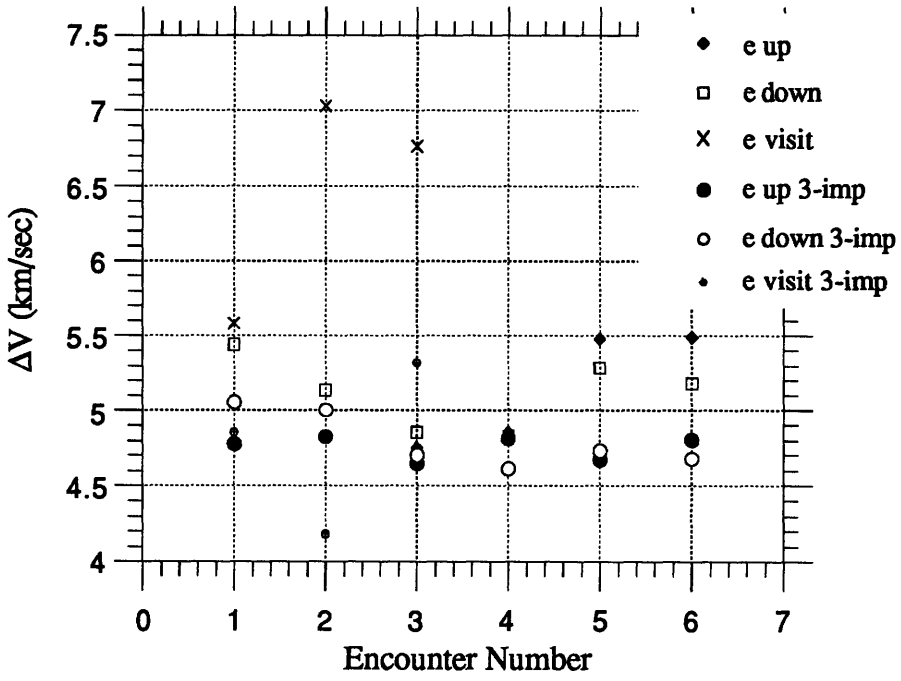

Figure 39 Pseudo-Hohmann Comparison to 3-Impulse for Earth Encounters

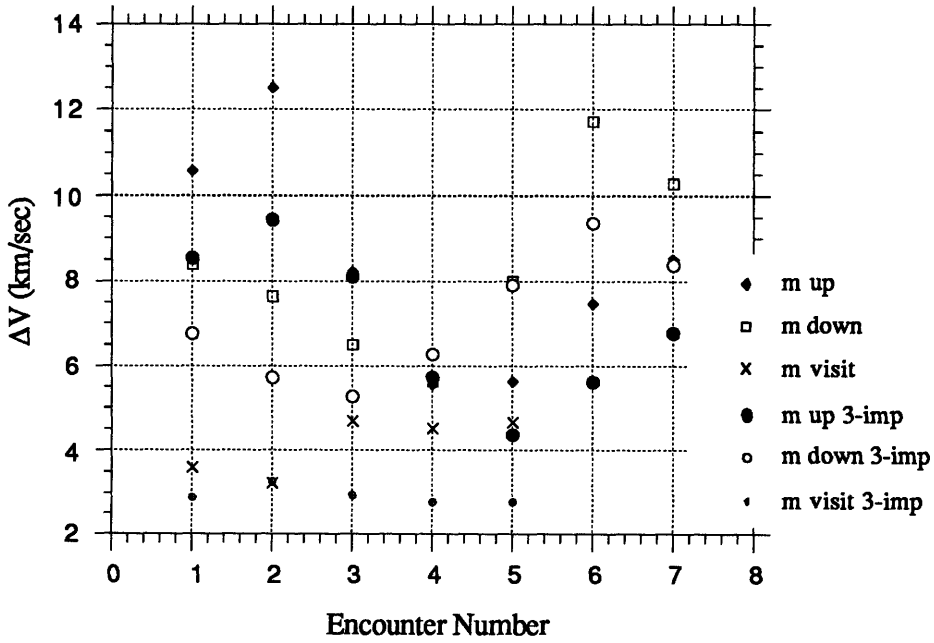

Figure 40 Pseudo-Hohmann Comparison to 3-Impulse for Mars Encounters

7. LAUNCH DELAYS AND TIME PHASING

In the Introduction a number of problems with the Taxi trajectories were mentioned as points for the analysis to address. The problem of plane changes has been successfully solved by the use of the three-impulse trajectory. Launch delays and time phasing are the other two serious problems that have to be addressed in order to achieve the initial goals of this thesis. Launch delays can be considered the penalty ΔV incurred when the Taxi leaves at a position other than the optimal position and the associated problems of catching the CASTLE on an outbound trip when the launch is delayed. The time phasing problem occurs because of the orbit of the spaceport which restricts the position the Taxi can launch from. The timing of the launch of the Taxi is critical for rendezvous because a late Taxi may not be able to rendezvous with the CASTLE. Launch windows have to be defined for each encounter to locate when the Taxi can leave or arrive at the spaceport.

7.1 LAUNCH DELAYS

Launch delays are both easy to define and visualize in this situation. However, different options exist to correct for the delays. Given the situation where the Taxi is going from a spaceport in low Earth orbit to the CASTLE. The Taxi has the option of rendezvousing with the CASTLE at the periapse of the hyperbolic fly-by or rendezvousing by getting on a hyperbola that will intercept the CASTLEs hyperbola at a specified point. If the rendezvous is with the periapse, then the transfer has to be very precise because one error will result in the Taxi missing the CASTLE as it passes its periapse at about 10 km/sec. If the rendezvous is carried out by using an intercepting hyperbola, mistakes can be corrected more easily.

The mistakes that are alluded to are the launch delays which include errors made at any of the impulses. In real operations the burn could be started or stopped early or late which made the position of the burn incorrect. Options for correcting for these mistakes are critical in order for the Taxi to rendezvous with the CASTLE. Mistakes such as complete mechanical failures which can be fixed in a set time can be accommodated for by allowing the spaceport to orbit once or more times around to allow the Taxi to launch later but at an optimum position. The opportunities to launch on every spaceport orbit will be addressed in Section 7.3.

The timing of the rendezvous is critical because the CASTLE encounters the Earth or Mars only once every couple of years. Options are needed to correct for launch delays in order

to complete the rendezvous. The options available to correct the delays will depend on the delays themselves. In this analysis of launch delays the burns will be considered to cause velocity impulses so the error can be either a burn that has not occurred in the proper position or one that has not occurred at the proper time. The time when the error was recognized will also contribute to the options. If the first or second burn is misplaced and the error is not discovered until just before the third burn is to be made, the only correction that can be made is at the third impulse. If the rendezvous had been set up for a periapse rendezvous then the only option available is to enter a short phasing orbit in order to get on a different hyperbola that would intercept the CASTLE many days later. If the rendezvous was a hyperbola intercept, the correction can be made in two parts. The first being an adjustment at the third burn to boost the hyperbola to achieve a new V-infinity vector (Wilson, 1990). The second correction can be made at the fourth impulse that Taxi makes to turn its hyperbola into the CASTLE hyperbola.

In a simple linearized model of the ΔV penalties for launch delays found just before the third impulse, the major contributors are the time delay (∂t), the magnitude of the V-infinity vector, and the time it takes to go from point of getting on the hyperbola to the point of intercept (T). The linearized equation is

$$\Delta V = \frac{\partial d}{T} = \frac{\partial t \, V_\infty}{T}$$

Using this equation for various encounters, hypothetical time delays, and hyperbolic transfer time, ΔV penalties were calculated. For Earth encounters the time delays were every 20 minutes up to 80 minutes which is slightly less than the period of the LEO spaceport orbit. For the Mars encounters the delays were every hour up to 4 hours which is about half of the period of Phobos' orbit. The hyperbolic transfer times or catch up days were varied from one to ten days. All outside perturbations were ignored in this analysis. Figure 41 show the results of the launch delays.

The ΔV shown in the graphs is the additional ΔV that is needed beyond the normal ΔV of the transfer. The ΔV penalty for leaving late increases as the delay increases. However, as the time the Taxi has to travel for the rendezvous with the CASTLE, the ΔV penalty decreases. The penalty for leaving late from the spaceport near Phobos is greater than at LEO because the V-infinity magnitude is greater. Therefore, the penalties would vary from encounter to encounter depending upon the V-infinity vector.

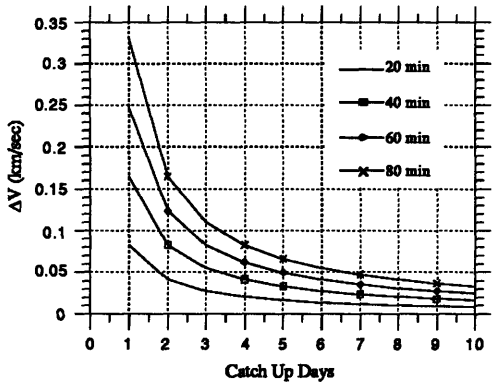

Delay at Earth

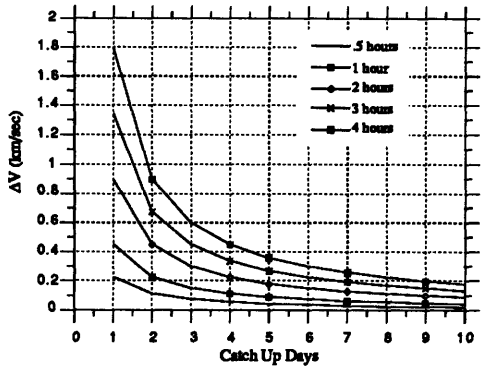

Delay at Mars

Figure 41 ΔV Penalty for Launch Delays for the 1st Encounters of Earth and Mars

If the first impulse is in error and the error is caught before the second impulse, then two options exist. The correction can be made, as discussed before, at the third and fourth impulses if a hyperbola rendezvous is used. Alternately, the correction can be made at the second impulse by changing the length of the apoapse of the intermediate ellipse to achieve the proper transfer time.

The options to correct for a mistake at the third impulse are very limited. For a periapse rendezvous nothing can be done if the Taxi does not get onto the CASTLEs hyperbola at the instant when the CASTLE passes through periapse. If the error at third burn during a hyperbolic rendezvous does not prevent an interception of the two hyperbolas, the fourth burn can accommodate the extra ΔV needed. However, if the intercept occurs after the passage of the CASTLE by the intercept point, then nothing can be done to rendezvous with the CASTLE.

The possibility of launch delays has to be considered when choosing the trajectory for both the manned and unmanned Taxi. In Section 6.1.2, the lengthy transfer time for a hyperbolic rendezvous made the shorter periapse rendezvous option look better for the manned Taxi. However, the likelihood of rendezvousing with the CASTLE at its periapse in the event of a launch delay at the second or third impulse is slim compared with the hyperbolic rendezvous. Depending upon the reliability of the Taxi propulsion system, the manned Taxi may have to endure long transfer times to ensure rendezvousing with the CASTLE.

7.2 BEHAVIOR OF FIRST IMPULSE CONSTRAINED TRAJECTORIES

The most critical optimized variable in the three-impulse program is θ1 (Gerbracht, 1968). θ1, as mentioned before, is the angle between the projection of the V-infinity vector onto the parking orbit plane and the location of the first impulse. Since it is unreasonable to assume that the Taxi will be able to leave at exactly the optimal θ1 value, the behavior of the other variables should be examined for a fixed value for θ1.

The three-impulse program was altered by simply ignoring one of the subroutine calls that optimizes the value for θ1. Then θ1 was used as an input that could be varied along with all the other inputs. For encounters both at the Earth and Mars, θ1 was varied from 0° through 360° by 10° increments.

7.2.1 Earth Encounters

Figure 42 depicts total ΔV vs the position of θ1 for all the encounters of Earth for the Down Cycler orbit. The apoapse radius of the intermediate ellipse was fixed at 50,000 km for all the encounters. Generally as θ1 increases around the optimal value, the ΔV increases. The shape of the curve is sinusoidal with the amplitude proportional to the relative declination of the encounter.

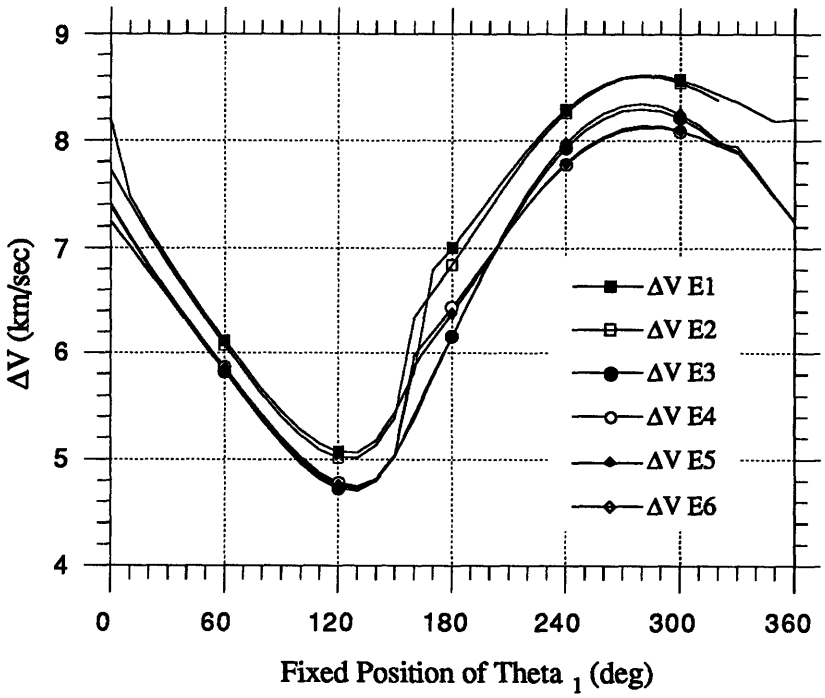

Figure 42 ΔV vs Position of θ1 for All Earth Encounters - Down Cycler Orbit

The next graph seen in Figure 43 shows the same ΔV vs θ1 for different values of the apoapse of the intermediate ellipse. The second Earth encounter by the Up Cycler orbit was used for this graph. The scale of the graph is too large to show the variation of the optimal θ1 value for the various values of the apoapse. The straight portions of the curve near the optimum is caused by the large 10° increments of θ1 used to produce the graph.

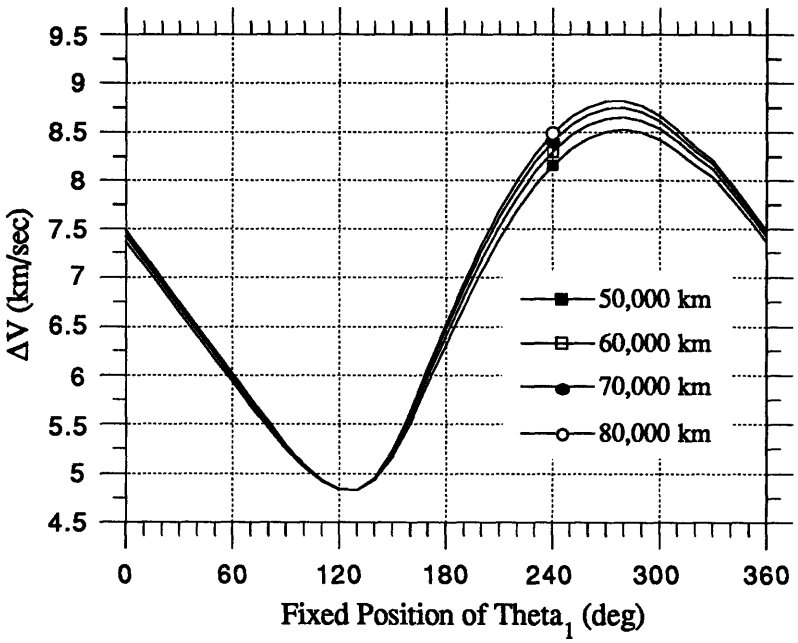

Figure 43 ΔV vs Position of θ1 for the 2nd Earth Encounter - Up Cycler Orbit

The first figure on the next page (Figure 44) shows ΔV vs θ1 for the first two Earth encounters of the Up Cycler orbit for an apoapse value of 50,000 km. The additional comparison here is between the hyperbola rendezvous and the periapse rendezvous. Only a small difference in ΔV separate the periapse and hyperbola rendezvous options at the optimal θ1 position.

7.2.2 Mars Encounters

Figure 45 is a graph of ΔV vs θ1 for the Mars encounters by the CASTLE on the Up Cycler orbit. The shape is similar to the graphs of the Earth encounters, but the amplitude is smaller because of the smaller variations in the relative declination at Mars. Data is also missing from two of the encounters for higher values of θ1 because the three-impulse program fails to converge. As mentioned before, the three-impulse program is not

guaranteed to converge for every situation that is input. Again the values of ΔV increase around the optimal θ1 but not as severely as in the graphs for the Earth encounters.

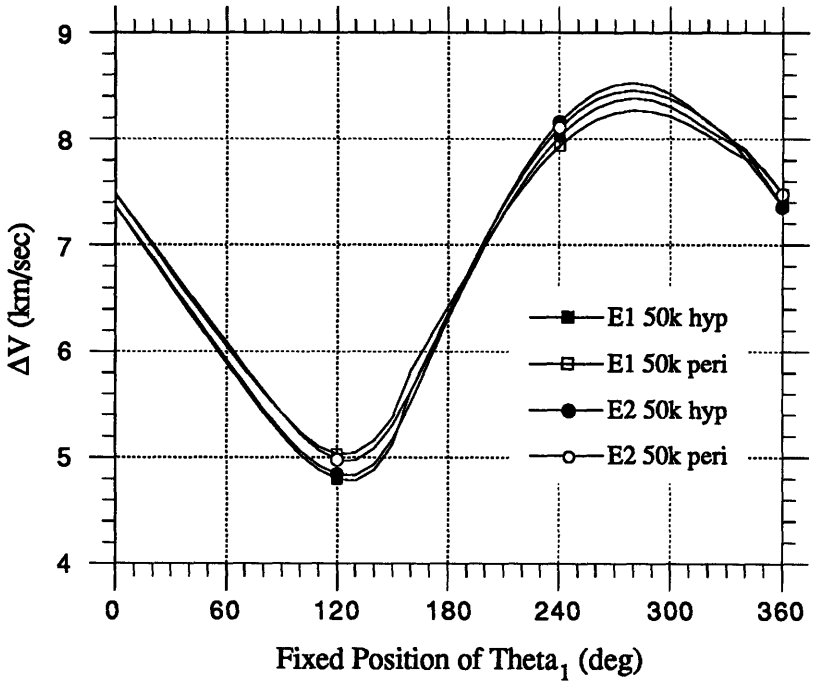

Figure 44 ΔV vs θ1 for Two Rendezvous Options at Earth - Up Cycler Orbit

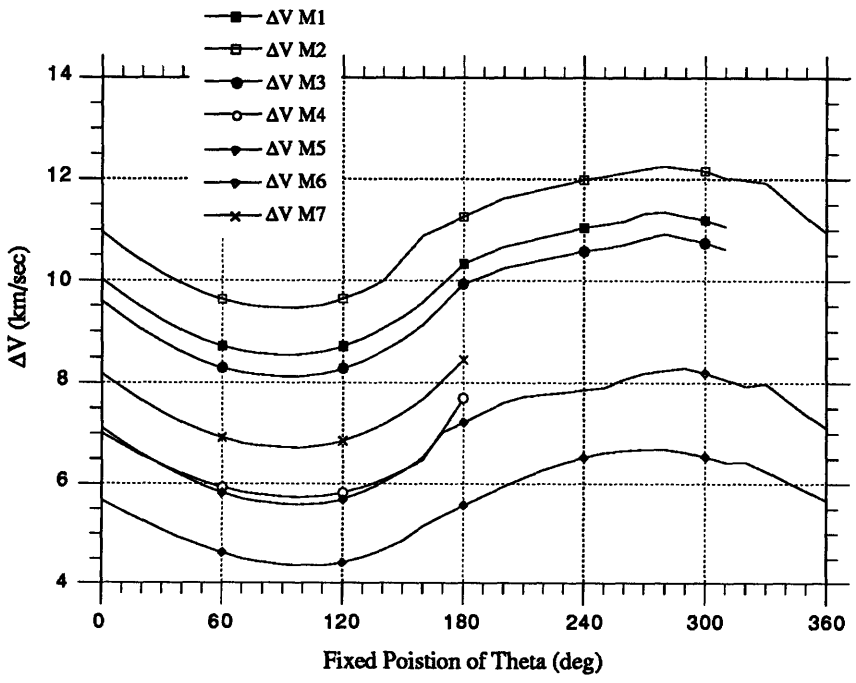

Figure 45 ΔV vs Position of θ1 for All Mars Encounters - Up Cycler Orbit

7.3 PRACTICAL FIXED FIRST IMPULSE TRAJECTORIES

Time phasing is knowing when and where to leave the parking orbit so that the Taxi can rendezvous with the CASTLE most economically. Transfer time has been mentioned but only as a trip length for the Taxi and not as a precise launch time. In order for the position in the orbit and the launch time to be calculated, the parking orbits must be defined in space as well as in time. The spaceport orbit which would have been ideal were L1 and Phobos. Since L1 was not a good location to use with the three-impulse program, a low Earth orbit was arbitrarily defined to use in this section. Phobos remained a good choice because it could be used with the three-impulse program, and the planetary ephemerides could provide its location at any time.

To perform this analysis the three-impulse program was again modified from its original form to search for the possibility of leaving at the optimal $\theta 1$ on every orbit of the parking orbit prior to the approach of the CASTLE. The program would initially calculate the positions of the spaceport for a given range of values for $\theta 1$. A corresponding time before the arrival of the CASTLE at its periapse is also calculated. Those values are compared to the values calculated by the program for a certain value for the apoapse of the intermediate ellipse. If the transfer time differs somewhat from the time when the spaceport is in position, the apoapse is increased or decreased appropriately; and the program recalculates values for ΔV, transfer time, and $\theta 1$. The increase or decrease in the apoapse may produce a change in $\theta 1$, so careful attention must be paid to the initial range of $\theta 1$. The iteration process is continued until the difference between the transfer time and the time at which the spaceport is in the correct position is less than .005 hours. The result of the iteration process will be optimal position ($\theta 1$), apoapse of intermediate ellipse, time (hours before periapse passage of the CASTLE), and ΔV.

7.3.1 Low Earth Orbit

The low Earth orbit defined was a 370 km circular orbit inclined at 28.5° with the ascending node and the argument of periapse defined to be at 0° with respect to the equinox when the CASTLE is at its periapse. The opportunities for the Taxi to launch are found by selecting the number of revolutions of the parking orbit that precede the the CASTLE passing through its periapse. The number of revolutions correspond to a position of the spaceport in its orbit and to a time before the CASTLE passes through its periapse. If the time of periapse passage is considered to be zero, then all the time before the passage should be

negative. However, for convenience sake, all time before passage will be the absolute value of the time.

An initial guess is made for the number of revolutions of the LEO so that the corresponding position of the spaceport will be the optimal θ1 value. An initial apoapse of the intermediate ellipse is also input into the program. The program will output a transfer time needed for the Taxi to complete its transfer. Most of the time, this transfer time and the time before periapse passage will not match. The two times will be resolved by changing the length of the apoapse to change the transfer time.

This process can be repeated for every orbit of the spaceport in LEO. Each opportunity to launch or arrive at the spaceport will be represented by a ΔV, a time before the CASTLE passes its periapse (which is equal to the transfer time of the Taxi), and the position of the spaceport either relative to the planet or to the V-infinity vector. Depending upon the ΔV capability and the maximum allowable transfer time of the Taxi, a large window will open many days (≈10) before periapse passage. It is at this time when Taxi transfers can begin between the CASTLE and the spaceport. A smaller window exists for each orbit of the spaceport defined by the ΔV capability of the Taxi. The larger window will close several hours before periapse passage due to the larger ΔV needed to make short time transfers. Figure 46 shows ΔV vs the true anomaly of the spaceport in the low Earth orbit for the first Earth encounter of the Up Cycler orbit.

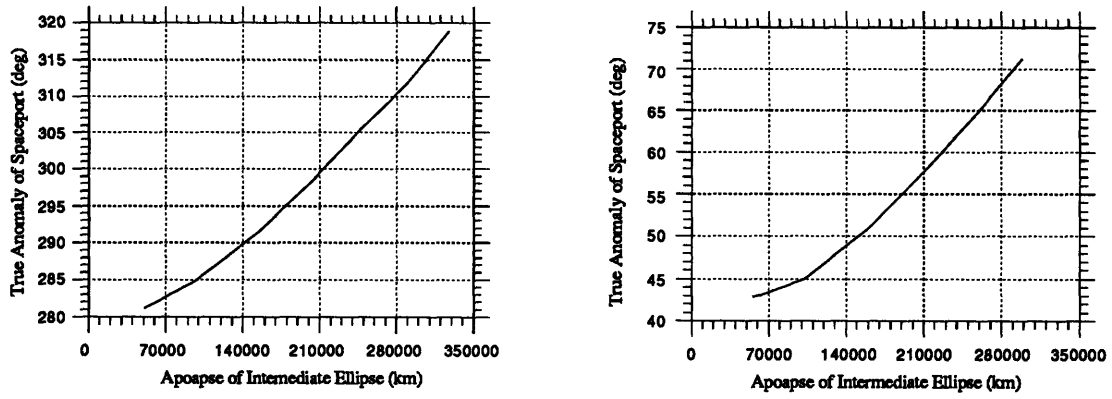

Figure 46 True Anomaly of Spaceport versus the Apoapse for the 1st and 3rd Earth Encounters of the Up Cycler Orbit

The circular parking orbit was given a slight eccentricity of 0.0001 to define the existence of an argument of periapse and to provide consistency between the graphs presented in this subsection.

Now, the positions of the spaceport around the Earth and Mars are both defined by the true anomaly of the respective parking orbits. The increasing curve seen in Figure 46 can be explained by the cancelling effects of the regression of the node and progression of the argument of periapse. The node regresses at a rate of -0.299°/hr while the argument of periapse progresses at 0.487°/hr. The net result is a decreasing true anomaly for the spaceport as the transfer time and apoapse decrease.

7.3.2 Phobos

The same procedure that was used for the LEO spaceport is used for the spaceport in the orbit of Phobos just behind the moon. The position of Phobos was generated by using an analytical ephemeris found in the JPL software libraries. Again the number of revolutions of Phobos in its orbit and the apoapse of the intermediate ellipse are input into the program to get a transfer time, total ΔV, and $\theta 1$. The two times are then matched by changing the length of the apoapse.

The opening for the large window still depends on maximum exposure time (maximum transfer time) and the small window length depends upon the ΔV capability of the Taxi. However, since the period of Phobos' orbit (7.65 hours) is much larger compared with the 1.53 hours of the spaceport in LEO, the number of opportunities that exist for a Taxi transfer at Mars encounters is smaller.

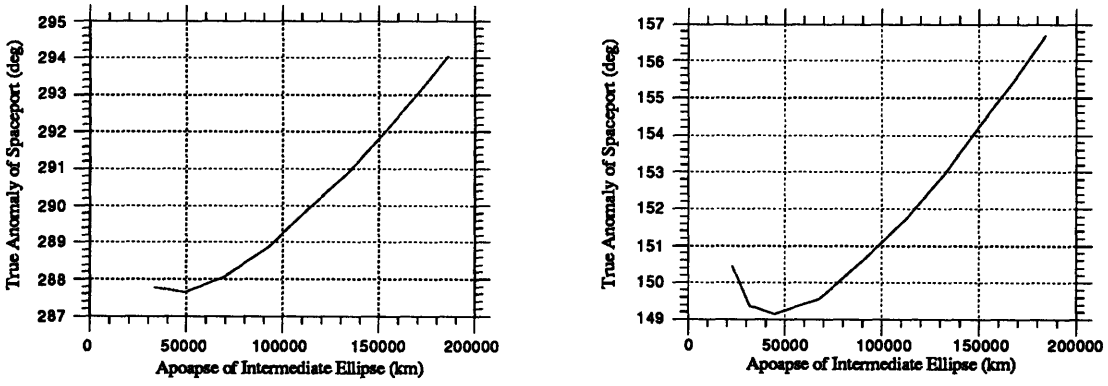

Figure 47 True Anomaly of Spaceport versus the Apoapse for the 1st and 5th Mars Encounters of the Up Cycler Orbit

Figure 47 shows the true anomaly of Phobos in its orbit (with the spaceport just behind the moon) versus the apoapse of the intermediate ellipse of the Taxi trajectory. These two graphs exhibit the same behavior as seen in the graphs for the LEO spaceport. In this case

the regression of the node of Phobos' orbit is only 0.434°/day while the progression of the argument of periapse is 0.871°/day. Again the true anomaly of the spaceport in its parking orbit decreases as the apoapse of the intermediate ellipse decreases. Another way to describe this behavior is as the time to the CASTLEs closest approach gets shorter the parking orbit rotates in such a way that the position of the spaceport at the time of launch changes.

8. PARAMETRIC STUDY

The situations already examined are fairly unique. Several examples do not show the behavior for the whole realm of possibilities. Varying the inputs of the program over a range of values helps to give insight into other scenarios.

As was mentioned previously in Section 5, the inputs to the program which define the initial conditions are the characteristics of the parking orbit and the V-infinity vector. The parking orbit is defined by its apoapse, periapse, inclination, ascending node, latitude, and longitude with respect to the planet's equator and equinox. The V-infinity vector is defined by its speed, radius of periapse, latitude, and longitude with respect to the planet equator and equinox (i.e. declination and right ascension with respect to the planet equator and equinox).

8.1 EARTH ENCOUNTERS

To show the effects of the various inputs, only one was varied while the others where held constant. The inputs were fixed at the following values: V-infinity magnitude = 5.8 km/sec, CASTLE periapse = 16,000 km, right ascension = 250°,declination = 15°, parking orbit radius = 6748 km with inclination of 28.5°. Each run included the two methods by which the Taxi can rendezvous with the CASTLE: an intercept at the periapse of the CASTLE fly-by and an intercept of the CASTLE hyperbola by another hyperbola. Recall Figures 6 and 7 in Section 4. The high, low, and the range are shown in the tables in Appendix A. The other tables in Appendix A show the variation of the other parameters. Graphs of the corresponding tables are also included in the appendix.

Some comments can be made relating the different effects of the inputs. Changing the V-infinity magnitude had the most dramatic variations and will be discussed first. The differences between the highs and lows for this case are greatest for ΔV and $\theta 1$. The magnitude was varied from 3 to 11 km/sec by 1 km/sec increments. A small V-infinity

produces a small ΔV and a large θ1. On the whole as V-infinity increases, ΔV and transfer time increase almost linearly while θ1 decreases.

The periapse of the CASTLE was varied from 8000 to 56,000 km by 4000 km increments. The range did not cover the entire range seen in the actual encounters of the Earth by the circulating orbits, but the range is large enough to show the general behavior. For the hyperbola rendezvous case, all the outputs remained constant because the Taxi gets onto a hyperbola that is independent of the CASTLE hyperbolic fly-by. For the periapse rendezvous case both ΔV and transfer time increased while θ1 decreased for the increasing values of the periapse of the CASTLE.

The right ascension was varied from 0° to 360° by 10° increments. The behavior of the outputs was not very smooth as compared to the other input variations. The behavior the ΔV and transfer time for the variation of the right ascension is shown in the following graph.

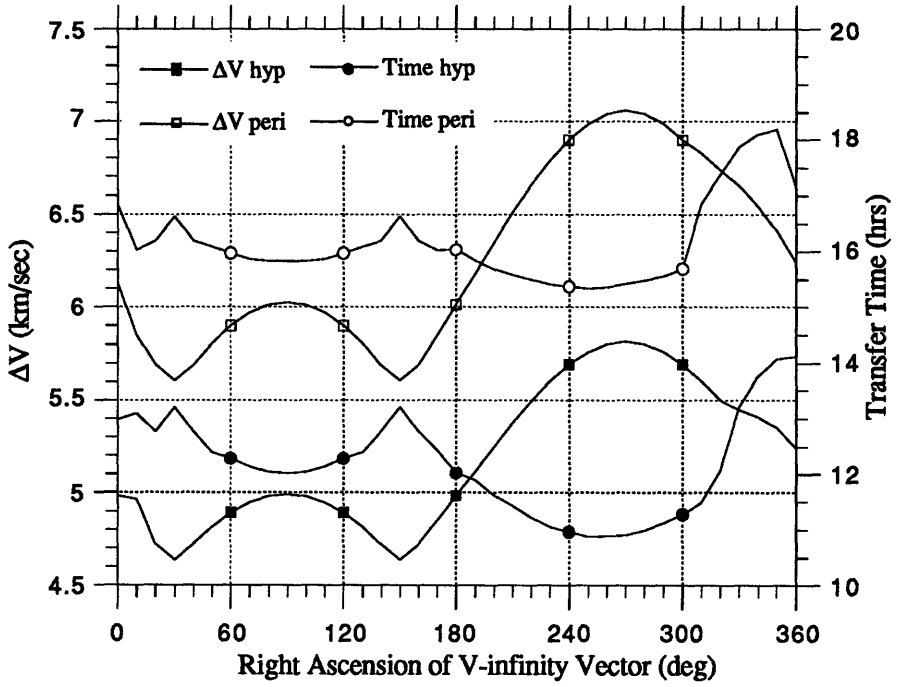

Figure 48 ΔV and Transfer Time vs Right Ascension of the V-infinity Vector

The highs and lows of the ΔV and time correspond to the highs and low of the relative declination. A low ΔV and long transfer time correspond to a low relative declination.

The key to declination variation is the relative declination between the V-infinity vector and the parking orbit. The declination was varied from -80° to 80° in 10° increments and the

corresponding relative declination varied from 0° to 80° but without a one to one correspondence. The smaller the relative declination, the smaller the plane change has to be and consequently smaller ΔV. The transfer time increases as the relative declination decreases. Both intercept cases behave the same way for ΔV and time. The behavior of $\theta 1$ was odd in that its curve had relative maximums at both the high and low values of the relative declination.

When the parking orbit radius was increased from 6678 to 9078 km at 200 km increments, the ΔV decreases for the hyperbolic intercept case while the ΔV decreases with a steeper slope for the periapse intercept. The ΔV for the hyperbolic intercept will be less than the periapse intercept unless the periapse of the CASTLE is the same as the radius of the parking orbit. As the parking orbit increases, $\theta 1$ decreases for the hyperbolic intercept but remains constant for the periapse intercept.

8.2 MARS ENCOUNTERS

The same procedure was used for a Mars encounter. The V-infinity characteristics that were used are as follows: V-infinity magnitude = 10.5 km/sec, CASTLE periapse = 10,000 km, right ascension = 250°, declination = 15°, and parking orbit radius = 3600 km with 0° inclination. The apoapse of the intermediate ellipse was held at 50,000 km. Again each run included the two methods by which the Taxi can rendezvous with the CASTLE: an intercept at the periapse of the CASTLE fly-by and an intercept of the CASTLE hyperbola by another hyperbola. The high, low, and range for Mars encounters are shown in the tables in Appendix A for the variation of the right ascension between 0° and 360°. The rest of the tables in Appendix A show the variation of the other parameters. Graphs of the corresponding tables are also included in the appendix.

The behavior of the outputs does not greatly differ from the Earth case. The only thing that can be seen is the lack of large differences between the maximum and minimum values of ΔV, time, and $\theta 1$ for the right ascension variation. If the inputs were plotted against ΔV, transfer time, and $\theta 1$, many of the graphs would be flat in contrast to the same graphs plotted for the Earth case. The lack of an inclination on the parking orbit around Mars causes little variation in the relative declination and thus not much change in ΔV. Another difference is in the variation of the parking orbit radius. For the hyperbolic rendezvous case the ΔV increases rather than decreases as it does for the parking orbit around the Earth.

Common sense could have produced most of the answers without the data. If a entirely new set of planetary encounters were given to be analyzed a number of generalized statements could be made. Over the set of encounters, the encounter that will have the lowest ΔV and the shortest transfer time will be the one with the smallest relative declination, smallest V-infinity, lowest parking orbit radius, and the lowest CASTLE periapse. The right ascension of the V-infinity vector must also be compared with the parking orbit to find the relative declination.

An attempt was made to qualify the results of the parametric study by looking at the partials created in each parameter variation. The partials may give some clue to the sensitivity of the outputs of ΔV, transfer time, and optimal $\theta 1$ to certain variations in the parking orbit and V-infinity vector. The following tables give the partials in a matrix-like format.

Table 4 Parameter Partials for Earth Hyperbolic Intercept

	ΔV	Transfer Time	Optimal $\theta 1$
V-infinity Magnitude	.16897	.16118	-6.3053
Right Ascension of V-infinity	-.02406	-.0342	.02591
Declination of V-infinity	.027	-.04734	.1432
Radius of Parking Orbit	1.1085 E-4	-6.0595 E-4	.004108
Closest Approach of CASTLE Hyperbola	1 E-8	1 E-6	1 E-7

Table 5 Parameter Partials for Earth Periapse Intercept

	ΔV	Transfer Time	Optimal $\theta 1$
V-infinity Magnitude	.38028	.74574	-5.3020
Right Ascension of V-infinity	-.01596	.01586	.06784
Declination of V-infinity	.03366	-.0269	-.05377
Radius of Parking Orbit	2.818 E-4	-1.296 E-4	0
Closest Approach of CASTLE Hyperbola	-1.478 E-4	-4.889 E-4	.002524

Table 6 Parameter Partials for Mars Hyperbolic Intercept

	ΔV	Transfer Time	Optimal θ1
V-infinity Magnitude	.5728	1.305	-9.310
Right Ascension of V-infinity	≈ 0	≈ 0	≈ 0
Declination of V-infinity	.00484	-.0935	.3590
Radius of Parking Orbit	1.985 E-4	.00118	-.001485
Closest Approach of CASTLE Hyperbola	0	5 E-7	7.5 E-7

Table 7 Parameter Partials for Mars Periapse Intercept

	ΔV	Transfer Time	Optimal θ1
V-infinity Magnitude	.7614	.860	-5.800
Right Ascension of V-infinity	≈ 0	≈ 0	≈ 0
Declination of V-infinity	.0076	-.01222	.0663
Radius of Parking Orbit	-2.135 E-4	3.4 E-4	0
Closest Approach of CASTLE Hyperbola	2.4522 E-4	.001071	-6.2825 E-4

The numbers in the matrices back up the comments already made about the behavior of the parameters. In general, the greater the number, the more sensitive that output is to a change in the input. However, not much can be done with the partials because not all the partials behave in a linear fashion. If they had, then a variation in the outputs could have been calculated from the matrix and the parametric study would have produced a good mathematical tool for predicting the behavior of the three-impulse transfer. With a little more mathematical ingenuity a weighting factor might be devised so that these matrices could produce output variations with an error matrix input.

9. DISCUSSION FOR FURTHER STUDY

This thesis has analyzed Taxi trajectories between planetary spaceports and the CASTLE on a circulating trajectory. The suggestions made by Hoffman et al. have been expanded upon but there is still room for a more detailed analysis in the areas analyzed here and other related areas. In general, the three-impulse routine can be improved by switching it from a patched-conic routine with a numerical integration routine. Other extensions of this study include making a very detailed study of the usefulness of Lagrangian points as a spaceport location, looking at other locations for spaceports, and an overall mass study needs to be made to compare the circulating system with a traditional mass transport system.

9.1 LAGRANGIAN POINTS

Two areas need to be investigated in the future in reference to using Lagrangian points as spaceport locations. The first area is to justify, without a doubt, that having a manned spaceport at these locations is practical and useful in terms of a Earth-Mars Transportation System. The next area to investigate are trajectory studies which include transfers from all Earth-Moon Lagrangian points to a hyperbolic escape V-infinity vector.

The studies made to justify placing a spaceport at the Lagrangian points are not numerous according to the literature search made of the international aerospace papers. A Soviet paper was found whose abstract mentioned that spaceports at Earth-Moon Lagrangian points will be an integral part of any manned exploration of the solar system (Brykov, 1981). Most of the other papers found did not touch on the issue of practicality but rather on the necessary station keeping problem of keeping a large object at stable and unstable libration points (Seward, et. al, 1971). One of the papers mentioned in the introduction said that L1 was chosen as a spaceport location because of the relative low ΔV needed to get mass to L1 from Earth's surface and the Lunar surface (Hoffman, 1986). That was the only reason stated. Future studies in this area will have to incorporate all of the factors, ΔV to get there, ΔV to keep it there, space radiation protection, abort constraints, and other concerns of constructing a space station.

Trajectories to the Earth-Moon Lagrangian points from the Earth or from the Moon have already been defined (Eagle Engineering (a, b), 1988). However, the literature search did not produce any studies of launching spacecraft from a Lagrangian point on an escape trajectory. Concerns for finding these trajectories include using the Moon and/or the Earth for gravity assistance, worrying about all the perturbations at the Lagrangian points

especially at L1 where the point is inside the Lunar sphere of influence, and looking at time phasing.

9.2 OTHER SPACEPORT LOCATIONS

In this study the spaceport for Taxi staging has been located at two locations at each planet. At Earth the spaceport was located at L1, the Lagrangian point between the Earth and the Moon, and in a potential Space Station Freedom orbit. At Mars the spaceport was following just behind Phobos and in a low Mars orbit arbitrarily selected at a 200 km altitude. In the introduction several other locations were mentioned. This section will make additional comments on those potential spaceport location that were not studied in detail.

Suggested locations that were not examined were a low Lunar orbit, an Earth-Sun Lagrangian point, and Earth-Moon cycler orbit. The first to be examined is an Earth-Sun Lagrangian point. That point whether it is mathematically stable or not would most likely be unstable in the real word because of the numerous perturbations felt that far from the Earth. The Trojan asteroids exist at the Jupiter-Sun Lagrangian points but a spaceport at an Earth-Sun Lagrangian point may be more trouble than first anticipated. The unstable colinear Earth-Sun Lagrangian points would experience perturbations from Jupiter and would be subject to solar radiation pressure. Those factors have to be examined even though they may turn out to be insignificant over the lifetime of the spaceport

Next is a low Lunar orbit. Such an orbit would present a doubly difficult phasing problem as compared to the L1 position. Not only must the position of the Moon relative to the Earth be taken into account but also the position of the spaceport in its orbit around the Moon. The spaceport will have to be in the right position to encounter the Earth and the Moon has to be in the right position to allow a transfer to the hyperbolic fly-by. To ease the timing constraints that may occur, phasing orbits around the Earth may be used to wait for the proper moment to start the Taxi's rendezvous with the CASTLE.

The last location is a spaceport located in an Earth-Moon Cycler orbit (see Figure 49). The numbers in the figure show the progression of spaceport in the orbit. A more detailed discussion of the Earth-Moon Cycler can be found in one of the references (Niehoff, 1986). The Earth-Moon Cycler orbit has both advantages and disadvantages. Its main disadvantage is the complexity of getting a spaceport in that repeating trajectory. The level of difficulty would probably be on the same level as putting a CASTLE in a Earth-Mars

circulating orbit. One advantage is found in the ΔV requirements to transport material between the spaceport and the Moon or the Earth. That ΔV is the lowest among all spaceport locations in the Earth-Moon system (Hoffman, et al., 1986). The opportunities to launch a Taxi between the CASTLE and the spaceport may be extremely limited because the geometry of the Earth-Moon Cycler does not allow frequent chances to launch or receive a Taxi during a CASTLE fly-by.

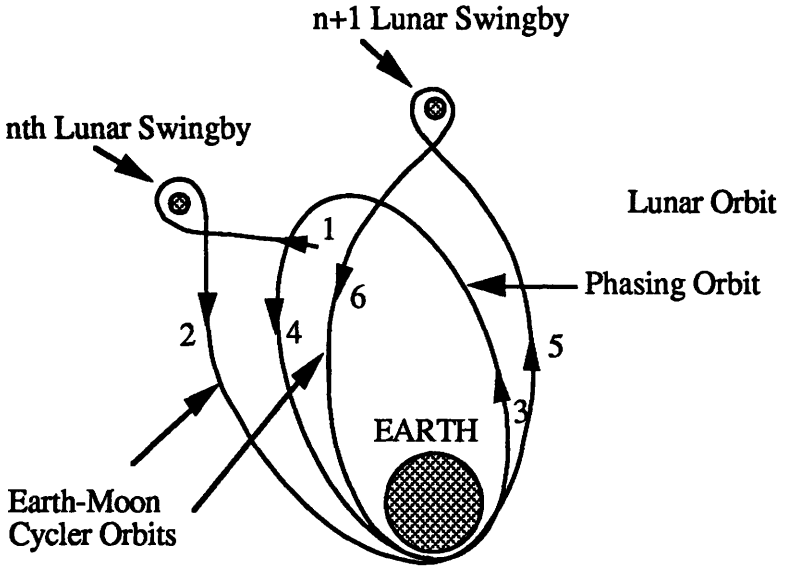

Figure 49 Earth-Moon Cycler Orbit (Niehoff, 1986)

9.3 MASS RATIO STUDY

As was performed for the Cycler and VISIT orbits, a new mass study needs to be performed to include the new data on the Taxi trajectories. The study performed by Hoffman, et al. compared interplanetary transportation systems over 15 to 20 years. In that study over the time period the Cycler and VISIT orbits provide some ΔV savings as compared to normal conjunction and opposition class trajectories over the same time period. The details of the Taxi trajectory study would be included to again verify the savings or lack of savings between the two transportation systems. This future mass study would also take on the added responsibility of looking at a transportation system where no extra-terrestrial propellants are used. Another point that would be addressed in this study is the comparison of an Earth launched Taxi with a spaceport launched Taxi. A Taxi using a direct ascent trajectory from the Earth's surface would enter into the plane containing the CASTLE fly-by and would then later get onto a hyperbola to rendezvous with the CASTLE. From launch-to-orbit theory, two launch windows usually occur every day that

allow the Taxi to launch into the proper plane. The length of the windows are constrained by launch azimuth limits for range safety, lighting restrictions at the launch site, and other constraints (Sergeyevsky, 1983). Once the Taxi has entered the plane containing the V-infinity vector, it will wait for the proper time to enter a phasing orbit which would enable the Taxi to properly time the rendezvous with the CASTLE. A comparison would decide whether a system which transports astronauts from the Earth to a spaceport and transports them to the CASTLE is more economical than a non-stop ride from the Earth's surface to the CASTLE.

This study would also be an appropriate place to discuss in detail the options for aerobraking the Taxi for transfers to the spaceports. The Taxi spacecraft both in its manned and unmanned versions should be capable of aerobraking in both the Martian and Earth atmospheres. The aerobraking should almost eliminate the large first impulse going from a hyperbolic to an elliptical orbit. Drawing from other recent aerobraking studies should provide enough information to determine whether the heat shield would be ablative or completely reusable. Over a long period, the aerobraking Taxis may save enough to make the circulating orbit transportation system to be the more economical one.

10. SUMMARY AND CONCLUSIONS

This section will give an overview of the tasks analyzed and provide some concluding remarks on the Taxi trajectories between planetary spaceports and circulating orbits.

10.1 SUMMARY

This thesis began with an introduction to circulation orbits and their potential for routine travel between the Earth and Mars. Up and Down Cycler orbits along with VISIT orbits provide repeating trajectories between Earth and Mars for a large spacecraft (CASTLE) to follow year after year. The trajectories between Earth and Mars are well defined, but the trajectories for the spacecraft (Taxi) which travels between the circulating trajectories and the orbiting planetary spaceports have not been well defined.

Previously only cursory examinations of the Taxi trajectories have been made to get ball-park ΔV figures for a large mass ratio study. The details of plane changes, time phasing, and launch penalties had not been examined in great detail. This thesis examined the details of the Taxi trajectories. A three-impulse conic trajectory routine was used to optimize the Taxi trajectories between the planetary spaceports and the outgoing V-infinity vector of the circulating interplanetary orbits. Each encounter of Earth and Mars by the circulating orbits

provides a different V-infinity vector for the Taxi to match. Two spaceport orbits were chosen at each planet; one a low planetary orbit and the other a high planetary orbit. Each encounter was examined for a total ΔV value, a total transfer time, and an optimal position from which to leave the spaceport to achieve the optimum ΔV.

A parametric study was also performed to analyze the relationship between the output parameters of ΔV, time, and position to the orientation of the parking orbit and the V-infinity vector. The study helps to give some insight into the behavior for a generalized planetary encounter. Two other tasks were performed to look at the practical side of the Taxi trajectories. The first examined the penalties encountered if the Taxi could not leave the spaceport at the optimal position. The second looked at a parking orbit fixed in time to observe the affects of nodal regression on the number and length of the optimal windows for the Taxi trajectories.

10.2 CONCLUSIONS

First and foremost, Taxi trajectories are available despite the difficulties of plane changes, time phasing, and launch delays. The difficulties just make the Taxi trajectories more complex and more costly. The costs and complexity of the Taxi trajectories are best illustrated through a typical encounter scenario. The encounter used is the second Earth fly-by of the CASTLE on the Up Cycler orbit. As the CASTLE approaches within 7 days of its closest approach of the Earth, a large window opens for a Taxi departing from its spaceport in LEO. This window can open earlier depending upon factors not explicitly discussed here such as maximum time limits for crew exposure in an unprotected Taxi or gravitational perturbations from the Moon or the Sun. The gravitational effects only come into play when the apoapse of the intermediate ellipse is close to the Moon or is larger than the Earth's sphere of influence. The departing Taxi has been given a certain ΔV capability of 6 km/sec to perform its rendezvous with the CASTLE. The Taxi can leave on any orbit of the spaceport until the transfer time to rendezvous is so short that more than the allotted ΔV is needed. At that point in time the large window closes. However, the taxi can not leave at just any time within the large window because a small window opens and closes on each spaceport orbit. For this scenario, the small window stays open a total of 28 minutes, 10 minutes before the optimum time and 18 minutes after. If the Taxi waits for another orbit to launch, the small window will shorten in length but not by much. The window's size is also proportional to the amount of extra ΔV over the minimum value. Sometime during the period when both windows are open the Taxi will depart the spaceport on its three-impulse trajectory. If mechanical problems arise, the Taxi can wait for several

spaceport revolutions to try to launch again. If all is well with the trajectory, the Taxi will transfer onto an intercept hyperbola at the same time the CASTLE passes through its perigee. The Taxi then continues on for 43 hours until a fourth impulse of 7 m/sec matches the two hyperbolas of the Taxi and CASTLE. The fourth impulse increases as the periapse of the CASTLE fly-by increases.

When the CASTLE crosses the Earth's sphere of influence, about 40 hours before closest approach, another Taxi will depart the CASTLE on its trip to the spaceport. Therefore, two Taxis will be in flight around the Earth at the same time. The three-impulse trajectory is performed in reverse order. As the CASTLE passes through its periapse, the arrival Taxi transfers from its hyperbola to the intermediate ellipse. Depending upon the structure of the Taxi, it may use aerobraking or propulsive braking to get onto the intermediate ellipse. More braking at this impulse will result in a shorter transfer time to the spaceport. With a ΔV capability of 6 km/sec, the Taxi can arrive at the spaceport in as few a 55 hours after leaving the CASTLE. If any delays occur at the CASTLE, the Taxi can leave at any time until the CASTLE crosses its periapse. As the delay increases, the ΔV requirement for the trajectory increases.

The case just presented was one of the more expensive Earth encounters. A ΔV capability of 6 km/sec during any other Earth encounter will increase the size of both windows. The encounters by the VISIT circulating orbit will provide the longest windows (up to 7.5 days and 43 minutes for the 2nd Earth encounter) with the stated ΔV capability. However, it the Taxi has the same capability at Mars, it would only be able to transfer from the VISIT orbit and one or two of the seven encounters of Mars by the Up / Down Cycler orbits.

The V-infinity magnitudes are so high for the Cycler orbits that in some cases 10 km/sec is needed to make the rendezvous. An encounter of the third fly-by of Mars by the Up Cycler will need 9 km/sec to provide ample window lengths. At approximately 12 days before the CASTLE reaches the periapse of its Hyperbolic fly-by, the departure Taxi at the spaceport behind Phobos can start its preparations to leave. In other words, the large window opened. The ΔV capability provides a small window of 2.8 hours every spaceport orbit, 1.3 hours before the optimum time and 1.5 hours after. The large window will close about 10 hours prior to the closest approach of the CASTLE.

The arrival Taxi will leave the CASTLE when the orbit crosses Mars' sphere of influence, 15 hours prior to closest approach. Leaving later will use ΔV capability leaving shorter windows for rendezvousing with the spaceport. The Taxi will have to propulsively brake

or aerobrake to slow itself down in the transition from the hyperbolic trajectory to the ellipse.

The other encounters at Mars are both better and worse in terms of ΔV requirements. At the bad end, a ΔV capability of 9 km/sec will not even allow completion of the transfer. At the opposite end, 9 km/sec will allow a transfer at just about any time once the large window opens.

The interplanetary transportation system needed is one that uses little ΔV and takes little time, but this system has not been found yet. A trade off between ΔV and time always appears. In this analysis more ΔV will get the Taxi to the CASTLE faster and more time will allow for delays but at the price of added ΔV. The trade off comes down to a decision between human endurance in space and energy costs. The energy cost in terms of ΔV will be low if long-term human exposure to the space environment is safe. The system with the circulating orbits and Taxis is expensive in terms of ΔV and it does not set any speed records. The VISIT circulating orbit would be the best choice if low ΔV of the Taxi is top priority. However, the time between interplanetary encounters on the VISIT orbit would be several years. One possibility is to find a circulating orbit with low V-infinity magnitudes that has short transfer times between Earth and Mars. Just such a possibility might exist in a Cycler-type orbit that uses a combination of Venus and Earth gravity-assists. Such an orbit would probably have lower V-infinity magnitudes at the Earth and Mars which means lower Taxi ΔV requirements. The orbit also allows fly-bys of Venus which might be of some scientific use.

APPENDIX A DATA AND GRAPHS

Earth and Mars Encounter graphs for ΔV, Transfer Time, and Optimum θ1. The graphs in this appendix include the Earth and Mars encounters by the Up and Down Cycler orbits as well as the VISIT orbit for spaceports in low planetary orbits.

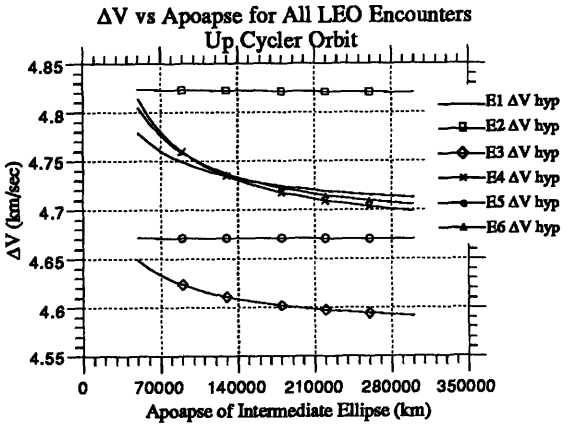

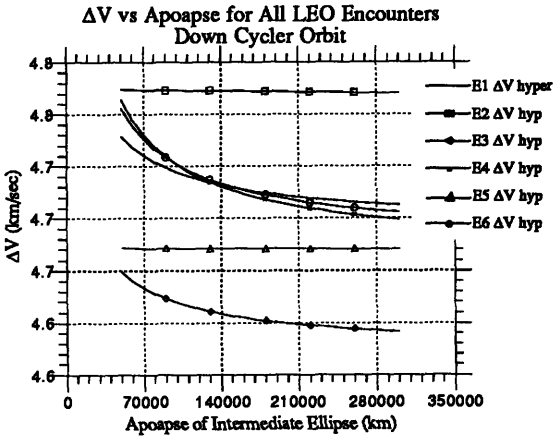

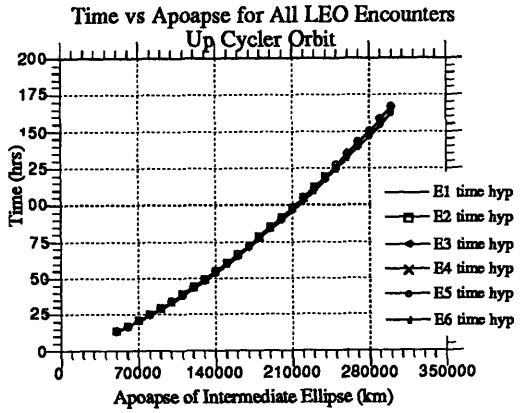

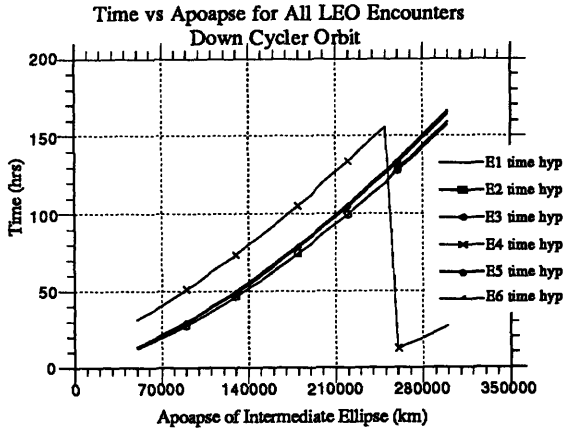

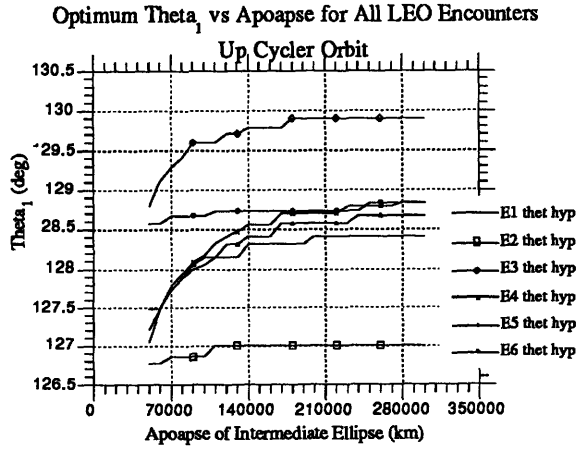

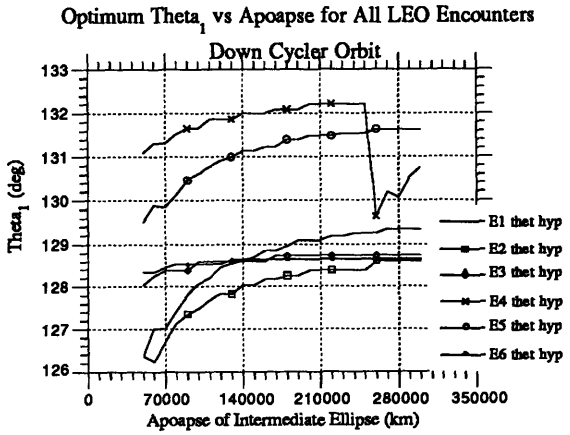

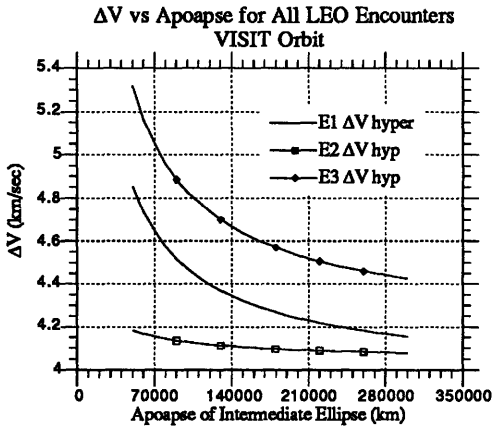
ΔV vs Apoapse for All LEO Encounters
VISIT Orbit
E1 ΔV hyper
E2 ΔV hyp
E3 ΔV hyp
ΔV (km/sec)
Apoapse of Intermediate Ellipse (km)

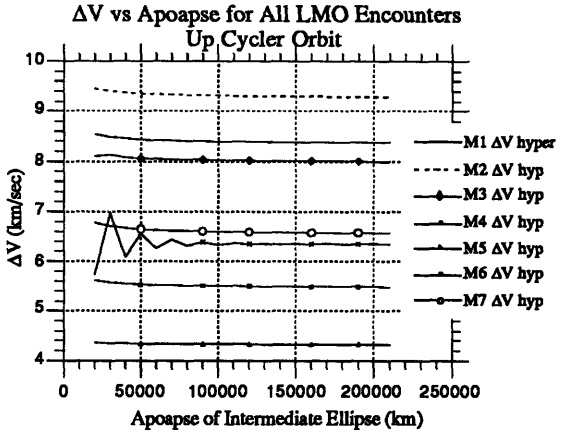
ΔV vs Apoapse for All LMO Encounters
Up Cycler Orbit
M1 ΔV hyper
M2 ΔV hyp
M3 ΔV hyp
M4 ΔV hyp
M5 ΔV hyp
M6 ΔV hyp
M7 ΔV hyp
ΔV (km/sec)
Apoapse of Intermediate Ellipse (km)

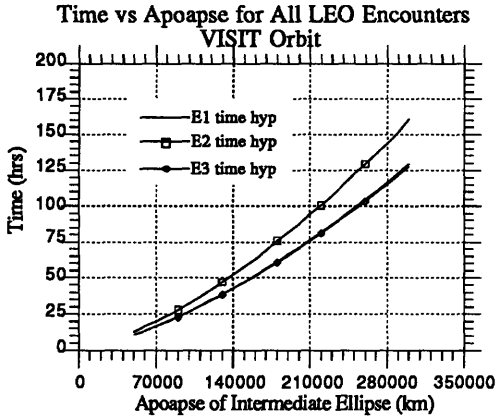
Time vs Apoapse for All LEO Encounters
VISIT Orbit
E1 time hyp
E2 time hyp
E3 time hyp
Time (hrs)
Apoapse of Intermediate Ellipse (km)

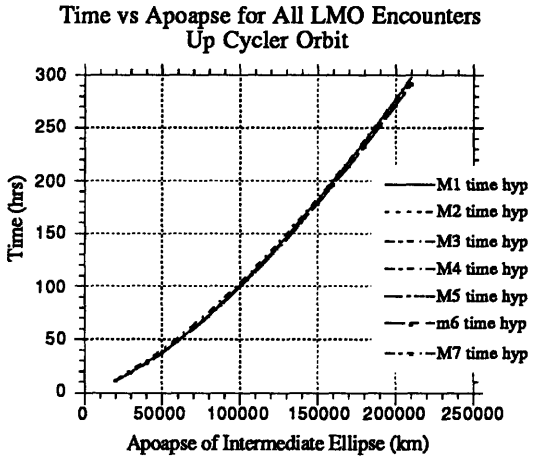
Time vs Apoapse for All LMO Encounters
Up Cycler Orbit
M1 time hyp
M2 time hyp
M3 time hyp
M4 time hyp
M5 time hyp
m6 time hyp
M7 time hyp
Time (hrs)
Apoapse of Intermediate Ellipse (km)

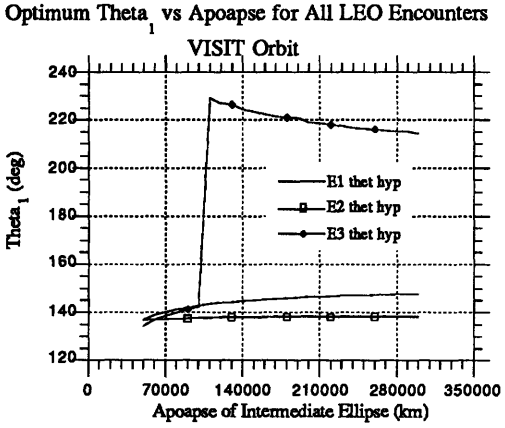
Optimum Theta1 vs Apoapse for All LEO Encounters
VISIT Orbit
E1 thet hyp
E2 thet hyp
E3 thet hyp
Theta1 (deg)
Apoapse of Intermediate Ellipse (km)

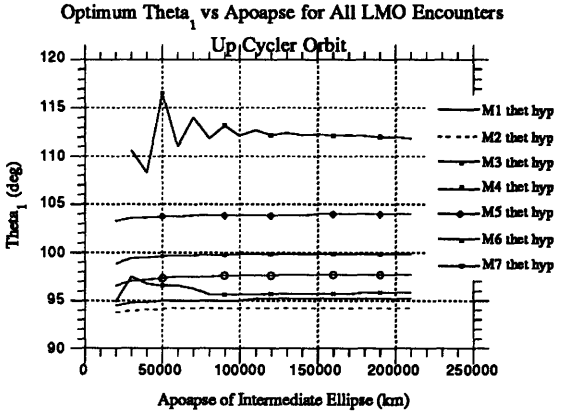
Optimum Theta1 vs Apoapse for All LMO Encounters
Up Cycler Orbit
M1 thet hyp
M2 thet hyp
M3 thet hyp
M4 thet hyp
M5 thet hyp
M6 thet hyp
M7 thet hyp
Theta1 (deg)
Apoapse of Intermediate Ellipse (km)

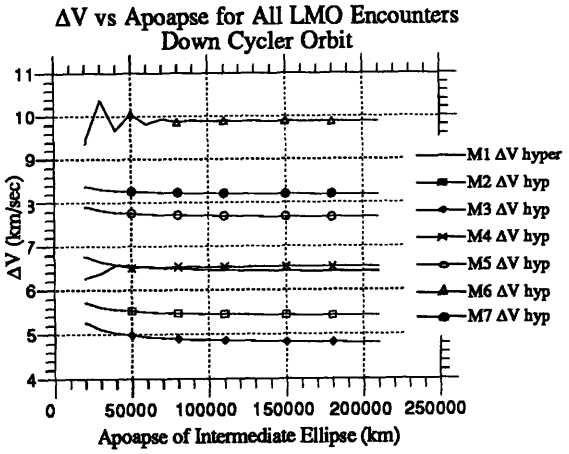
ΔV vs Apoapse for All LMO Encounters
Down Cycler Orbit
ΔV (km/sec)
Apoapse of Intermediate Ellipse (km)
M1 ΔV hyper
M2 ΔV hyp
M3 ΔV hyp
M4 ΔV hyp
M5 ΔV hyp
M6 ΔV hyp
M7 ΔV hyp

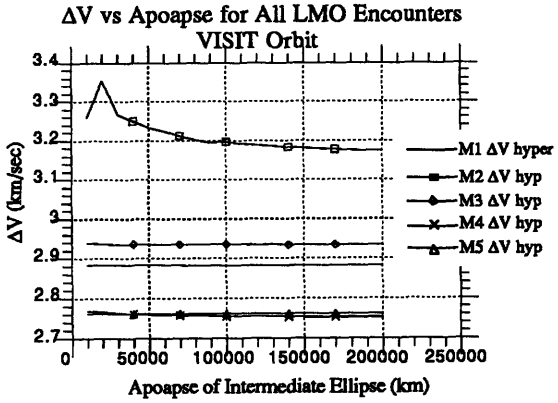
ΔV vs Apoapse for All LMO Encounters
VISIT Orbit
ΔV (km/sec)
Apoapse of Intermediate Ellipse (km)
M1 ΔV hyper
M2 ΔV hyp
M3 ΔV hyp
M4 ΔV hyp
M5 ΔV hyp

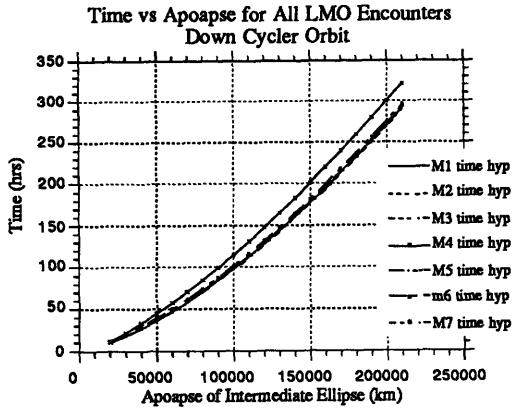
Time vs Apoapse for All LMO Encounters
Down Cycler Orbit
Time (hrs)
Apoapse of Intermediate Ellipse (km)
M1 time hyp
M2 time hyp
M3 time hyp
M4 time hyp
M5 time hyp
m6 time hyp
M7 time hyp

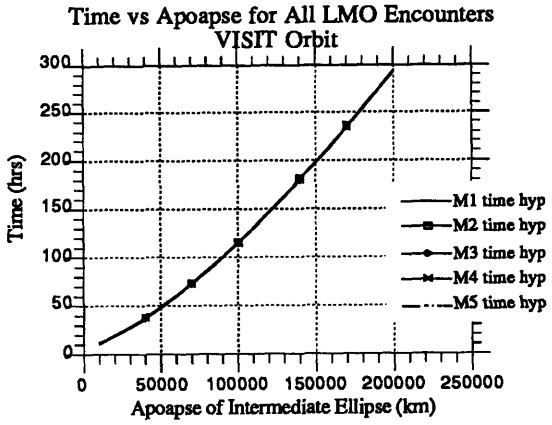
Time vs Apoapse for All LMO Encounters
VISIT Orbit
Time (hrs)
Apoapse of Intermediate Ellipse (km)
M1 time hyp
M2 time hyp
M3 time hyp
M4 time hyp
M5 time hyp

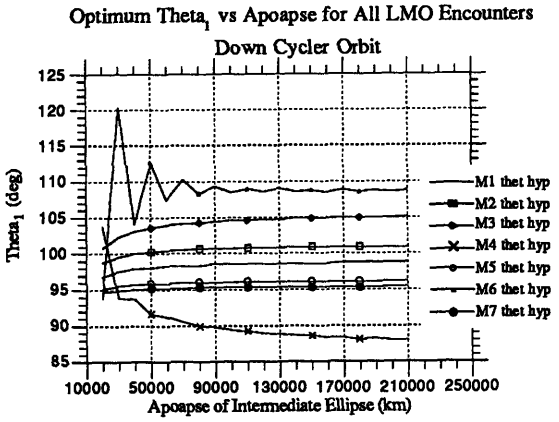
Optimum Theta1 vs Apoapse for All LMO Encounters
Down Cycler Orbit
Theta1 (deg)
Apoapse of Intermediate Ellipse (km)
M1 thet hyp
M2 thet hyp
M3 thet hyp
M4 thet hyp
M5 thet hyp
M6 thet hyp
M7 thet hyp

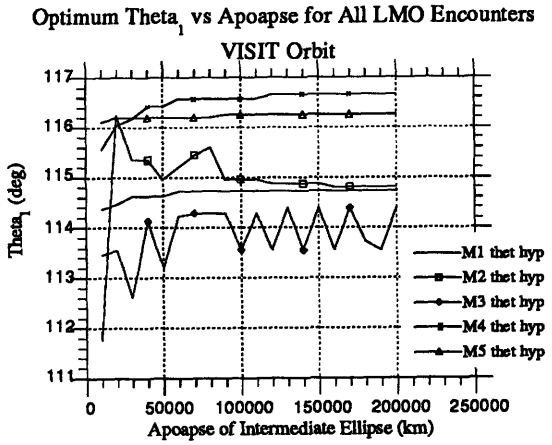
Optimum Theta1 vs Apoapse for All LMO Encounters
VISIT Orbit
Theta1 (deg)
Apoapse of Intermediate Ellipse (km)
M1 thet hyp
M2 thet hyp
M3 thet hyp
M4 thet hyp
M5 thet hyp

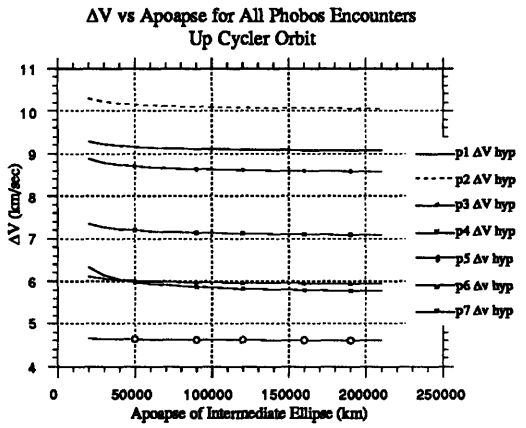
ΔV vs Apoapse for All Phobos Encounters
Up Cycler Orbit
ΔV (km/sec)
Apoapse of Intermediate Ellipse (km)
p1 ΔV hyp
p2 ΔV hyp
p3 ΔV hyp
p4 ΔV hyp
p5 Δv hyp
p6 Δv hyp
p7 Δv hyp

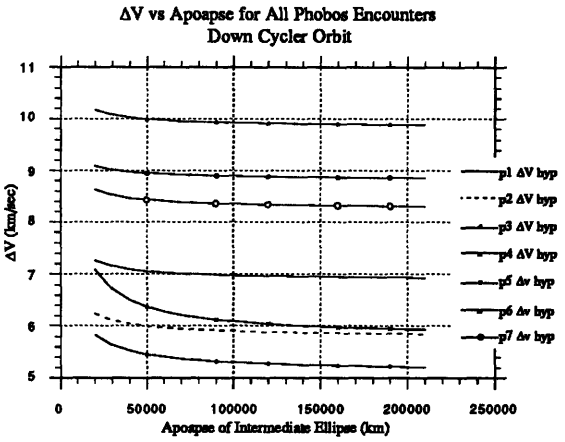
ΔV vs Apoapse for All Phobos Encounters
Down Cycler Orbit
ΔV (km/sec)
Apoapse of Intermediate Ellipse (km)
p1 ΔV hyp
p2 ΔV hyp
p3 ΔV hyp
p4 ΔV hyp
p5 Δv hyp
p6 Δv hyp
p7 Δv hyp

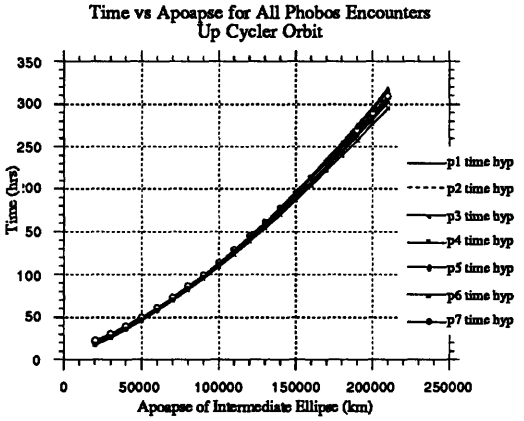
Time vs Apoapse for All Phobos Encounters
Up Cycler Orbit
Time (hrs)
Apoapse of Intermediate Ellipse (km)
p1 time hyp
p2 time hyp
p3 time hyp
p4 time hyp
p5 time hyp
p6 time hyp
p7 time hyp

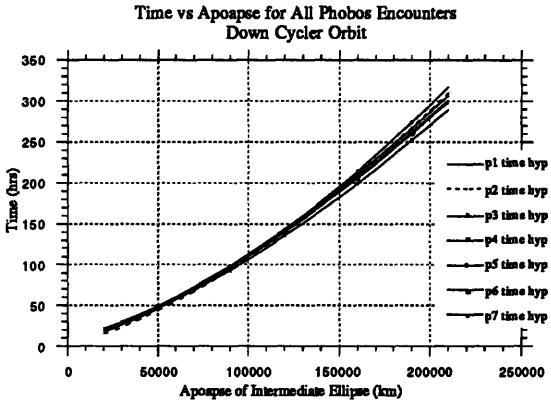
Time vs Apoapse for All Phobos Encounters
Down Cycler Orbit
Time (hrs)
Apoapse of Intermediate Ellipse (km)
p1 time hyp
p2 time hyp
p3 time hyp
p4 time hyp
p5 time hyp
p6 time hyp
p7 time hyp

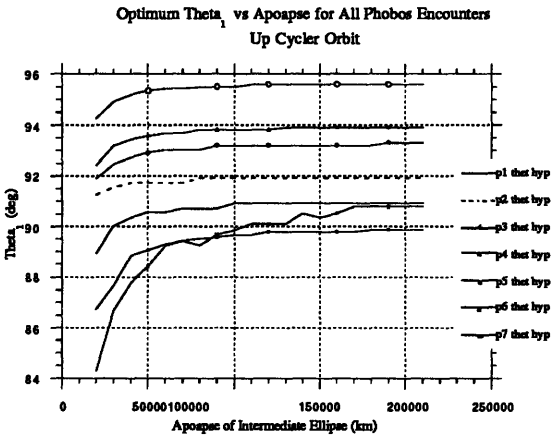
Optimum Theta1 vs Apoapse for All Phobos Encounters
Up Cycler Orbit
Theta1 (deg)
Apoapse of Intermediate Ellipse (km)
p1 that hyp
p2 that hyp
p3 that hyp
p4 that hyp
p5 that hyp
p6 that hyp
p7 that hyp

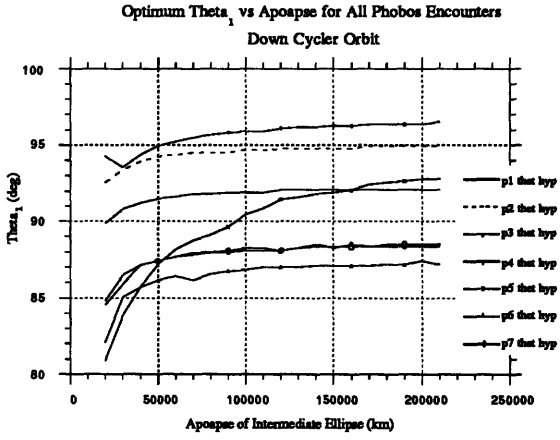
Optimum Theta1 vs Apoapse for All Phobos Encounters
Down Cycler Orbit
Theta1 (deg)
Apoapse of Intermediate Ellipse (km)
p1 that hyp
p2 that hyp
p3 that hyp
p4 that hyp
p5 that hyp
p6 that hyp
p7 that hyp

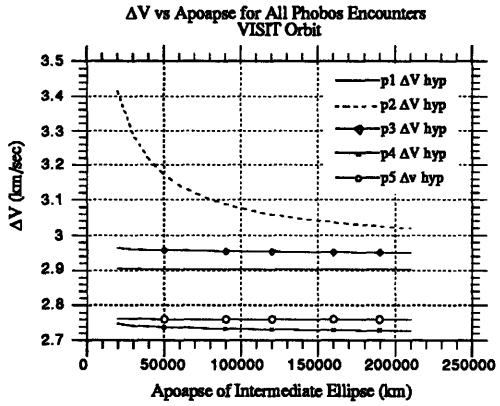

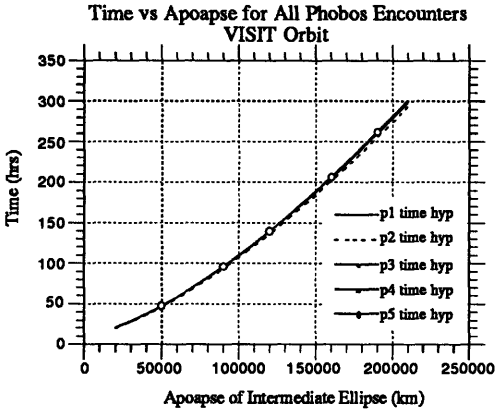

Optimum $Theta_1$ vs Apoapse for All Phobos Encounters

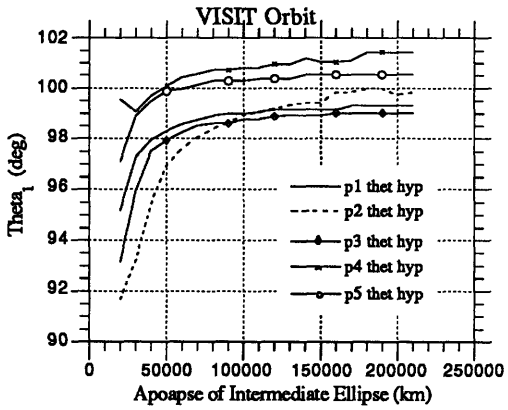

The data produced in the parameter study is shown in the tables that follow. Each table contains the high and low values and the range of the three outputs.

The right ascension was varied from 0° to 360°. The high, low, and range of the ΔV, transfer time, and optimal θ1 are shown in the two tables that follow

Table A1 Right Ascension Variation for Hyperbolic Intercept

	ΔV (km/sec)	Transfer time (hrs)	θ1 (deg)
high	5.817	13.205	129.093
low	4.635	10.893	126.739
Δ	1.182	2.312	2.354

Table A2 Right Ascension Variation for Periapse Intercept

	ΔV (km/sec)	Transfer time (hrs)	θ1 (deg)
high	7.059	16.626	120.533
low	5.606	15.422	108.016
Δ	1.453	1.204	12.517

The declination was varied next from -80° to 80° by increments of 10°. In turn the relative declination varied from 2.93° to 80.15°. The high, low, and the range are shown in the tables.

Table A3 Declination Variation for Hyperbolic Intercept

	ΔV (km/sec)	Transfer time (hrs)	θ1 (deg)
high	6.783	13.308	144.361
low	4.692	9.341	126.724
Δ	2.091	3.967	17.637

Table A4 Declination Variation for Periapse Intercept

	ΔV (km/sec)	Transfer time (hrs)	θ1 (deg)
high	8.180	16.869	113.651
low	5.652	14.408	108.035
Δ	2.528	2.461	5.616

The magnitude of the V-infinity vector was varied from 3 km/sec to 11 km/sec every 1 km/sec. The results are shown in Tables A5 and A6.

Table A5 V-infinity Variation for Hyperbolic Intercept

	ΔV (km/sec)	Transfer time (hrs)	θ1 (deg)
high	8.763	12.609	145.999
low	5.003	10.097	108.728
Δ	3.760	2.512	37.271

Table A6 V-infinity Variation for Periapse Intercept

	ΔV (km/sec)	Transfer time (hrs)	θ1 (deg)
high	10.878	16.656	121.100
low	5.644	13.544	97.704
Δ	5.234	3.112	23.396

Finally the radius of the parking orbit was varied from 6678 km to 9078 km every 200 km. The results are shown in Tables A7 and A8.

Table A7 Parking Orbit Radius Variation for Hyperbolic Intercept

	ΔV (km/sec)	Transfer time (hrs)	θ1 (deg)
high	5.767	12.350	128.914
low	5.587	10.851	120.627
Δ	.18	1.499	8.287

Table A8 Parking Orbit Radius Variation for Periapse Intercept

	ΔV (km/sec)	Transfer time (hrs)	θ1 (deg)
high	7.007	15.685	108.155
low	6.446	15.355	108.155
Δ	.561	.330	0

Finally the closest approach of the CASTLE was varied from 8000 km to 56,000 km by increments of 4000 km. The results are shown in Tables A9 and A10

Table A9 CASTLE Closest Approach Radius Variation for Hyperbolic Intercept

	ΔV (km/sec)	Transfer time (hrs)	θ1 (deg)
high	5.759	10.894	128.618
low	5.759	10.872	128.553
Δ	0	.022	.065

Table A10 CASTLE Closest Approach Radius Variation for Periapse Intercept

	ΔV (km/sec)	Transfer time (hrs)	θ1 (deg)
high	9.069	31.552	124.309
low	5.972	11.514	67.669
Δ	3.097	20.038	56.640

The parameter data for Mars Encounters are found in the following tables. The first two tables are the result of varying the right ascension of the V-infinity vector through 360°.

Table A11 Right Ascension Variation for Hyperbolic Intercept

	ΔV (km/sec)	Transfer time (hrs)	θ1 (deg)
high	8.209	39.041	106.588
low	8.209	36.872	95.162
Δ	0	2.169	11.426

Table A12 Right Ascension Variation for Periapse Intercept

	ΔV (km/sec)	Transfer time (hrs)	θ1 (deg)
high	9.904	47.266	108.299
low	9.636	42.579	91.895
Δ	.268	4.687	16.404

The declination was varied next from -80° to 80° by increments of 10°. In turn the relative declination varied from 0° to 80°. The high, low, and the range are shown in the tables.

Table A13 Declination Variation for Hyperbolic Intercept

	ΔV (km/sec)	Transfer time (hrs)	θ1 (deg)
high	8.562	37.727	105.057
low	8.126	35.661	95.191
Δ	.436	2.066	9.866

Table A14 Declination Variation for Periapse Intercept

	ΔV (km/sec)	Transfer time (hrs)	θ1 (deg)
high	10.190	44.500	93.642
low	9.509	43.942	91.906
Δ	.681	.538	1.736

The magnitude of the V-infinity vector was varied from 3 km/sec to 11 km/sec every 1 km/sec. The results are shown in Tables A15 and A16.

Table A15 V-infinity Variation for Hyperbolic Intercept

	ΔV (km/sec)	Transfer time (hrs)	θ1 (deg)
high	9.584	37.551	123.943
low	2.380	34.499	94.048
Δ	7.204	3.052	29.895

Table A16 V-infinity Variation for Periapse Intercept

	ΔV (km/sec)	Transfer time (hrs)	θ1 (deg)
high	11.087	44.438	106.614
low	2.935	42.431	91.539
Δ	8.152	2.007	15.075

The radius of the parking orbit was varied from 3600 km to 6000 km every 200 km. The results are shown in Tables A17 and A18.

Table A17 Parking Orbit Radius Variation for Hyperbolic Intercept

	ΔV (km/sec)	Transfer time (hrs)	θ1 (deg)
high	8.587	40.923	95.191
low	8.209	37.454	92.976
Δ	.378	3.469	2.215

Table A18 Parking Orbit Radius Variation for Periapse Intercept

	ΔV (km/sec)	Transfer time (hrs)	θ1 (deg)
high	9.636	45.226	91.906
low	9.265	44.307	91.906
Δ	.371	.919	0

Finally the closest approach of the CASTLE was varied from 4000 km to 52,000 km by increments of 4000 km. The results are shown in Tables A19 and A20.

Table A19 CASTLE Closest Approach Radius Variation for Hyperbolic Intercept

	ΔV (km/sec)	Transfer time (hrs)	θ1 (deg)
high	8.209	37.455	95.195
low	8.209	37.442	95.163
Δ	0	.013	.032

Table A20 CASTLE Closest Approach Radius Variation for Periapse Intercept

	ΔV (km/sec)	Transfer time (hrs)	θ1 (deg)
high	11.232	97.534	95.012
low	8.370	37.864	89.987
Δ	2.862	59.67	5.025

The data from the parameter study produced the following graphs. The graphs of the Earth encounters are shown first followed by the graphs for the Mars encounters. Transfer time and ΔV grouped together when an input parameter is varied. The optimal θ1 is not grouped with another output parameter.

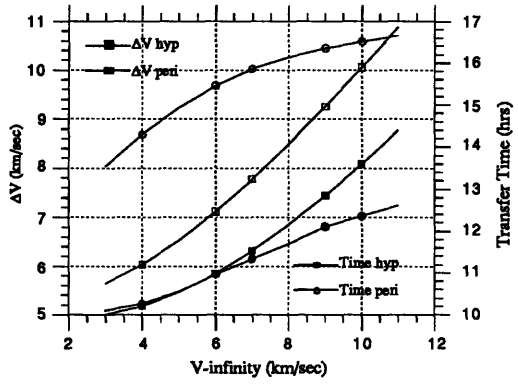

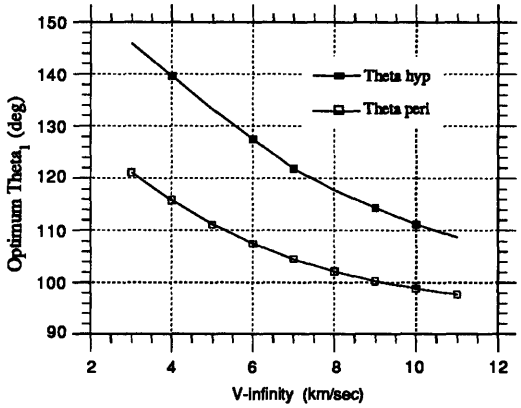

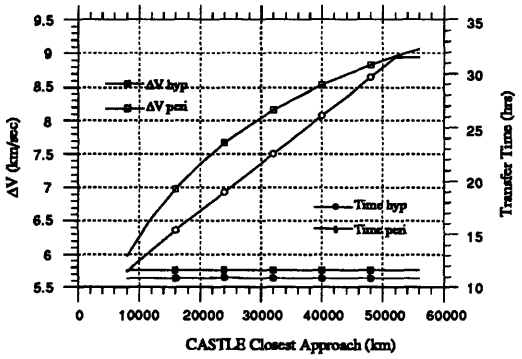

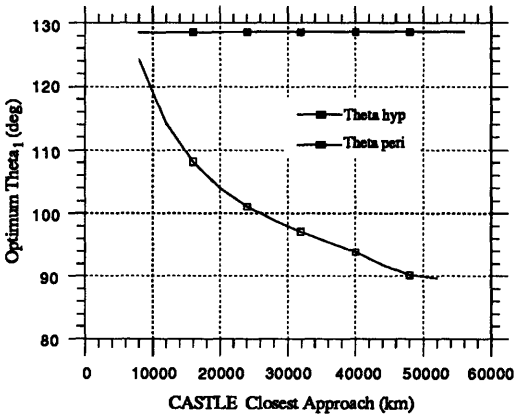

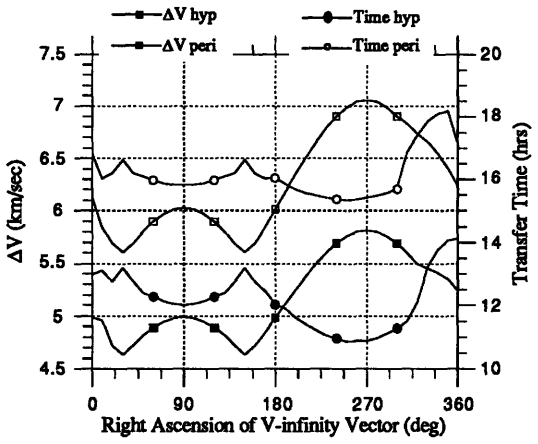
ΔV hyp
Time hyp
ΔV peri
Time peri
ΔV (km/sec)
Transfer Time (hrs)
Right Ascension of V-infinity Vector (deg)

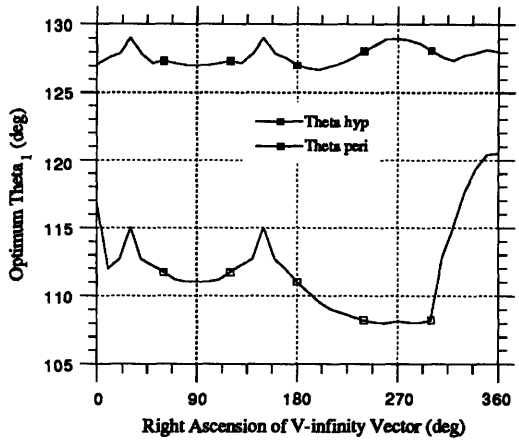
Theta hyp
Theta peri
Optimum Theta$_1$ (deg)
Right Ascension of V-infinity Vector (deg)

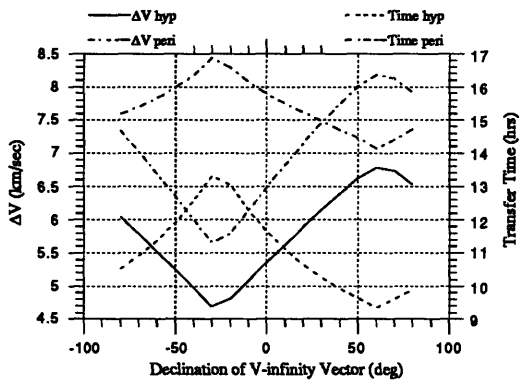
ΔV hyp
Time hyp
ΔV peri
Time peri
ΔV (km/sec)
Transfer Time (hrs)
Declination of V-infinity Vector (deg)

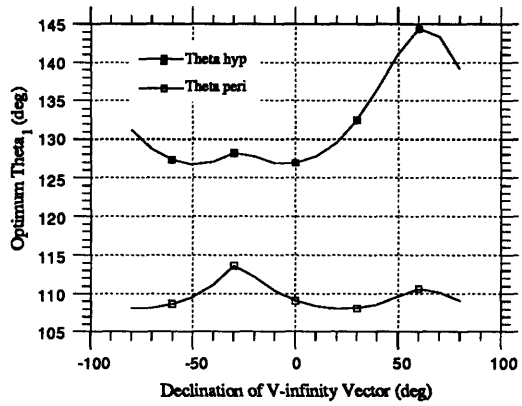
Theta hyp
Theta peri
Optimum Theta$_1$ (deg)
Declination of V-infinity Vector (deg)

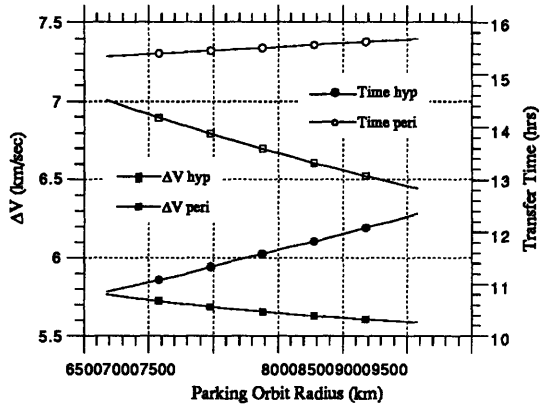
Time hyp
Time peri
ΔV hyp
ΔV peri
ΔV (km/sec)
Transfer Time (hrs)
650070007500
8000850090009500
Parking Orbit Radius (km)

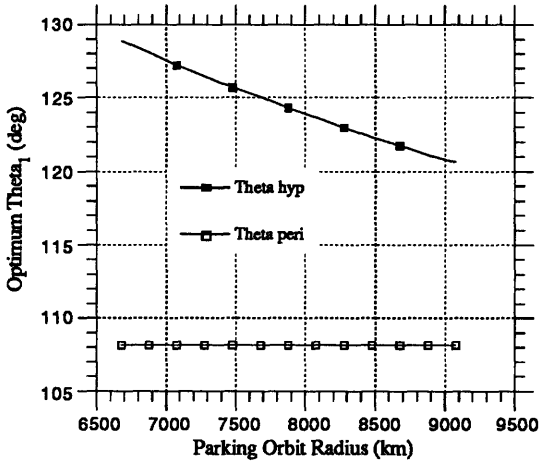
Theta hyp
Theta peri
Optimum Theta$_1$ (deg)
Parking Orbit Radius (km)

Mars parameter graphs.

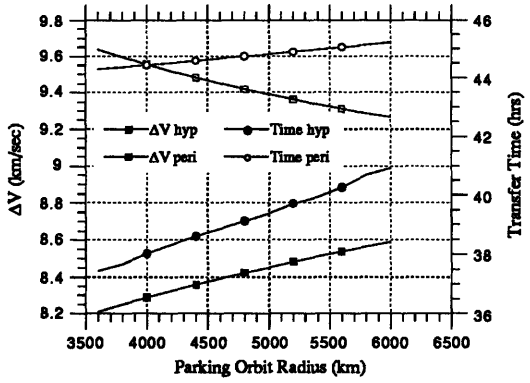

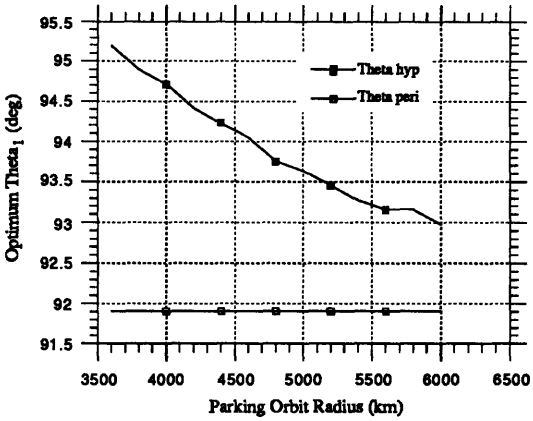

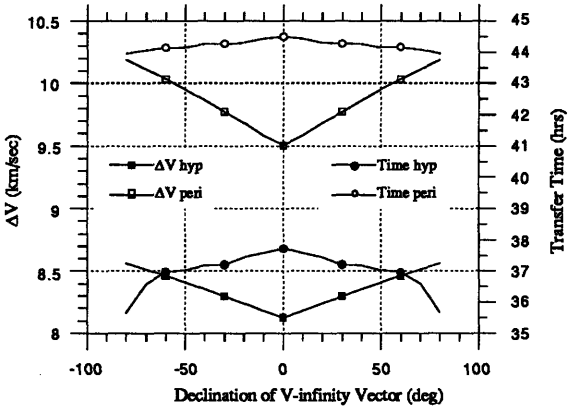

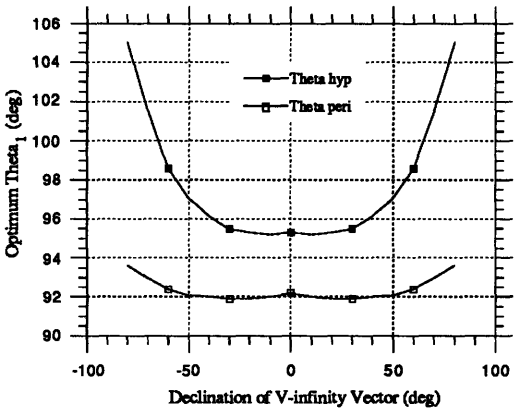

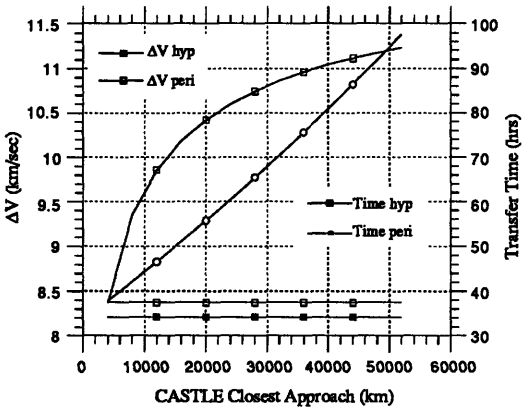

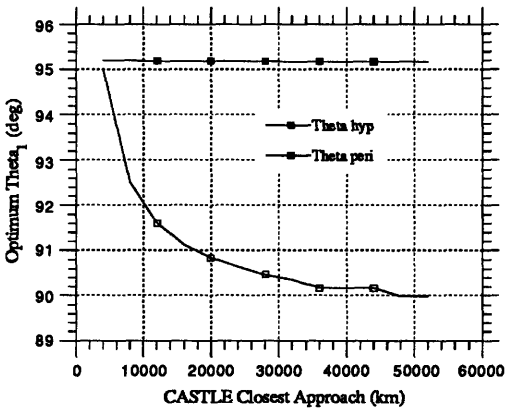

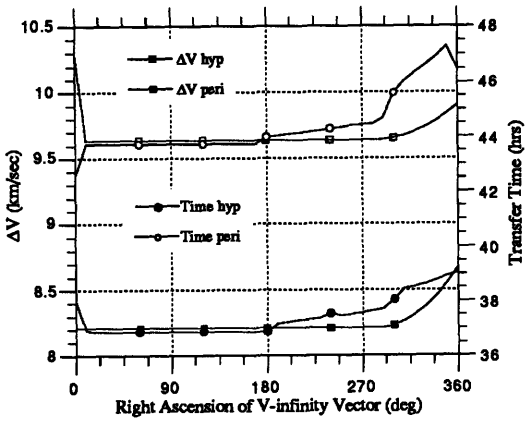
ΔV hyp
ΔV peri
Time hyp
Time peri
ΔV (km/sec)
Transfer Time (hrs)
Right Ascension of V-infinity Vector (deg)

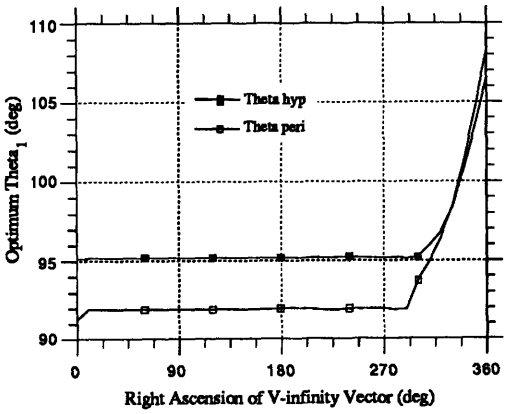
Theta hyp
Theta peri
Optimum Theta$_1$ (deg)
Right Ascension of V-infinity Vector (deg)

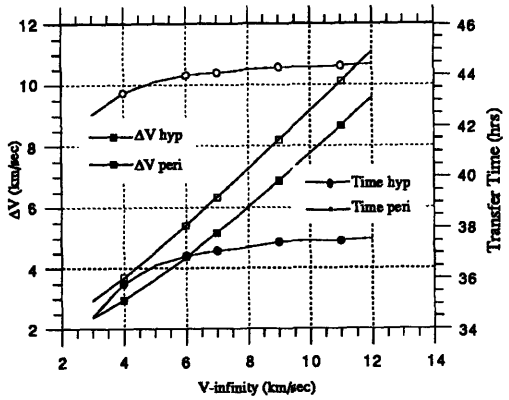
ΔV hyp
ΔV peri
Time hyp
Time peri
ΔV (km/sec)
Transfer Time (hrs)
V-infinity (km/sec)

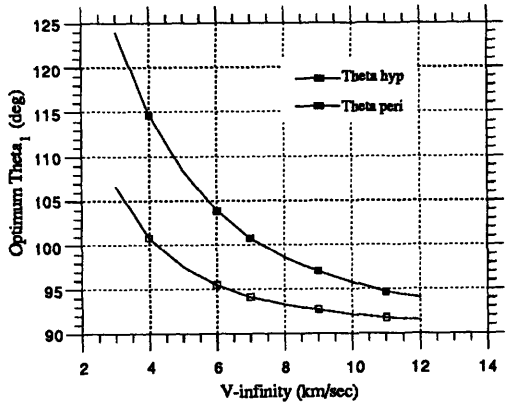
Theta hyp
Theta peri
Optimum Theta$_1$ (deg)
V-infinity (km/sec)

APPENDIX B PROGRAM EQUATIONS

V-infinity characteristics

$\bar{V}_\infty = V_\infty$ magnitude

λ_∞ right ascension

μ_∞ declination

Parking Orbit characteristics

$\bar{r}_p = r_p$ periapse

λ_p longitude

μ_p latitude

i - inclination of parking orbit

Ω - ascending node of parking orbit

r_a - apoapse of the initial ellipse

r_a' - apoapse of the intermediate ellipse

μ - gravitational constant

The relative declination is

$$\delta_\infty = \sin^{-1}\left(\left| \sin \mu_\infty \cos i - \cos \mu_\infty \sin i \sin (\lambda_\infty - \Omega) \right| \right)$$

and the argument of periapse is

$$\omega = \cos^{-1} (\cos \mu_p \cos (\lambda_p - \Omega))$$

$$\gamma = \cos^{-1} \left(\frac{\cos \mu_\infty \cos (\lambda_\infty - \Omega)}{\cos \delta} \right)$$

The angle between the periapse of the parking orbit and the projection of the V-infinity vector onto the parking orbit plane is given by

$$\alpha_\infty = \gamma - \omega$$

The parameters of the parking orbit are as follows

$$e = \frac{r_a - r_p}{r_a + r_p} \qquad a = \frac{r_a + r_p}{2} \qquad p = \frac{2\, r_a\, r_p}{r_a + r_p}$$

The true anomaly at the first impulse is

$$\eta_1 = \alpha_\infty - \theta_1$$

where θ_1 is the angle between $\overline{V}_\infty$ and the 1st impulse.

Then the radius and the velocity at the first impulse can be found by

$$r_1 = \frac{p}{1 + e \cos \eta_1} \qquad V_1^2 = \mu \left(\frac{2}{r_1} - \frac{1}{a}\right)$$

The flight path angle at the impulse can be found using

$$V_1 \sin \beta_1 = \frac{\sqrt{\mu\, p}}{r_1} \qquad \beta_1 = \cos^{-1} \left(\frac{e \sin \eta_1}{\sqrt{1 + e^2 + 2\, e \cos \eta_1}}\right)$$

which enables the radius and flight path angle of the intermediate ellipse to be defined by

$$\beta_1' = \beta_1 + \Delta\beta \qquad r_p' = \frac{r_1 (r_a' - r_1) \sin \beta_1'^2}{r_a' - r_1 \sin \beta_1'^2}$$

Next the characteristics of the intermediate ellipse can be calculated

$$e' = \frac{r_a' - r_p'}{r_a' + r_p'} \qquad a' = \frac{r_a' + r_p'}{2} \qquad p' = \frac{2\, r_a'\, r_p'}{r_a' + r_p'}$$

$$V_1'^2 = \mu \left(\frac{2}{r_1'} - \frac{1}{a'}\right) \qquad \eta_1' = \cos^{-1} \left(\frac{\frac{p'}{r_1} - 1}{e'}\right)$$

The ΔV for the first impulse is found by

$$\Delta v_1 = [V_1^2 + V_1'^2 - 2 V_1 V_1' \cos \Delta\beta + 2(V_1 \sin \beta_1)(V_1' \sin \beta_1')(1 - \cos \Delta A_1)]^{\frac{1}{2}}$$

The next thing to calculate is the plane change angle using two of the degrees of freedom

$$\Delta A_2 = \tan^{-1}\left[\left|\frac{\tan \delta_\infty - \tan \Delta A_1 \sin \theta_1}{\frac{\sin (\eta_2 - \eta_1') \cos \theta_1}{\cos \Delta A_1} - \cos (\eta_2 - \eta_1')(\sin \theta_1 + \tan \delta_\infty \tan \Delta A_1)}\right|\right]$$

The radius and the ΔV of the second impulse are found by

$$r_2 = \frac{p'}{1 + e' \cos \eta_2} \qquad V_2 \sin \beta_2 = \frac{\sqrt{\mu p'}}{r_2} \qquad \Delta V_2 = 2 \frac{\sqrt{\mu p'}}{r_2} \sin \left(\frac{\Delta A_2}{2}\right)$$

Next the angle between the V-infinity vector and the second impulse is calculated using

$$\psi = \cos^{-1} [\sin (\eta_2 - \eta_1') (\cos \delta_\infty \cos \Delta A_1 \sin \theta_1 + \sin \delta_\infty \sin \Delta A_1) + \cos (\eta_2 - \eta_1') \cos \delta_\infty \cos \theta_1]$$

and then the angle between the V-infinity vector and the periapse of the intermediate ellipse is

$$\theta_2 = \eta_2 + \psi$$

The following are calculated for convenience to speed computer calculations

$$\cos \nu = \cos (\theta_2 - \eta_3) \qquad \sin \nu = \sin (\theta_2 - \eta_3)$$

where ν is the angle between $\overline{V}_\infty$ and the 3rd impulse.

Now the radius and velocity at the third impulse can be calculated as follows

$$r_3 = \frac{p'}{1 + e' \cos \eta_3} \qquad V_3^2 = \mu \left(\frac{2}{r_3} - \frac{1}{a'}\right)$$

The flight path angle at the third ellipse is

$$\sin \beta_3 = \frac{\sqrt{\mu p'}}{r_3 V_3} \qquad \cos \beta_3 = \sqrt{1 - (\sin \beta_3)^2}$$

and the velocity of the hyperbola at the third impulse is

$$V_h^2 = V_\infty^2 + \frac{2\mu}{r_3}$$

To calculate the third and final ΔV the following intermediate variables have to be found first.

$$\lambda = \frac{r_3 V_\infty^2}{\mu} \quad \text{and} \quad q \equiv \sqrt{e_h^2} - 1 \quad \text{is given by} \quad q = \frac{\lambda \sin \nu + \sqrt{(\lambda + 2)^2 - (\lambda \cos \nu + 2)^2}}{2}$$

$$\sin \beta_h = \frac{\mu q}{r_3 V_h V_\infty} \qquad \cos \beta_h = \sqrt{1 - (\sin \beta_h)^2}$$

$$\Delta V_3 = \sqrt{V_h^2 + V_3^2 - 2 V_h V_3 (\sin \beta_3 \sin \beta_h + \cos \beta_3 \cos \beta_h)}$$

$$\Delta V_{Total} = \Delta V_1 + \Delta V_2 + \Delta V_3$$

REFERENCES

Aldrin, E. E., "Cyclic Trajectory Concepts," SAIC Presentation to the Interplanetary Rapid Transit Study Meeting, Jet Propulsion Laboratory, October 28, 1985.

Aldrin, E. E., "The Mars Transit System", Air and Space, pp41-47, Oct/Nov 1990.

Bate, R., Mueller, D., and White, J., Fundamentals of Astrodynamics, Dover Publications Inc., New York, 1971.

Battin, R., An Introduction the the Mathematics and Methods of Astrodynamics, AIAA Inc., New York, 1987.

Brykov, A., "Advantages of Space Stations at the Earth-Moon Libration Points", Joint Publications Research Service in its USSR Report: Space No. 14 (JPRS-79711), July 1981.

Byrnes, D. V., Personal Communication, June 15, 1990.

Crocco, G. A. "One Year Exploration Trip Earth-Mars-Venus-Earth", Proceedings of the Seventh International Astronautical Congress, Rome, 1956, pp. 227-52.

a) Eagle Engineering, "Velocity Deltas for LEO to L2, L3, L4, and L5, and LLO to L1 and L2", Eagle Engineering Report No. 88-208, September 30, 1988.

b) Eagle Engineering, "LEO to L1 Trajectory Program", Eagle Engineering Report No. 88-219, October 30, 1988.

Friedlander, A. L., Niehoff, J. C., Byrnes, D. V., and Longuski, J. M., "Circulating Transportation Orbits Between Earth and Mars," AIAA Paper No. 86-2009-CP, AIAA/AAS Astrodynamics Conference, Williamsburg, VA, August 18-20, 1986.

Friedlander, A. L., Telephone Conversation, June 15, 1990.

Gerbracht, R. J., "Three Impulse Transfers Between Elliptic and Hyperbolic Trajectories", TRW Interoffice Correspondence, January 31, 1968.

Gerbracht, R. J., Penzo, P. A., "Optimum Three Impulse Transfer Between Elliptic and Non-Coplanar Escape Asymptote", AAS 68-084, presented at the AAS/AIAA Astrodynamics Specialist Conference, Jackson, WY, September 3-5, 1968.

Henry, P. K., Sergeyevsky, A.B., and Sharma, J., "Planetary Exploration Departures from the Space Station: Trajectory Effects on Station Operations", JPL D-6896-90 (Internal), Jet Propulsion Laboratory, Pasadena, CA, November 1989.

Hoffman, S. J., Friedlander, A. L., and Nock, K. T., "Transportation Mode and Performance Comparison for a Sustained Manned Mars Base," AIAA Paper No. 86-2016-CP, AIAA/AAS Astrodynamics Conference, Williamsburg, VA, August 18-20, 1986.

Hoggatt, V. E. and Meder, A. E. (ed), Fibonacci and Lucas Numbers, Houghton Mifflin, Boston, 1969.

Hollister, W. M., "Castles in Space," Astronautica Acta., January 1967.

Hollister, W. M., "Periodic Orbits for Interplanetary Flight," AAS Paper No.68-102, AAS/AIAA Astrodynamics Specialist Conference, Jackson, WY, September 3-5, 1968.

Hollister, W. M. and Menning, M. D., "Interplanetary Orbits for Multiple Swingby Missions," AIAA Paper No. 69-931, AIAA/AIAA Astrodynamics Conference, Princeton, NJ, August 1969.

Lawden, D. F., Optimal Trajectories for Space Navigation, Butterworths, London, 1963.

Lion, P. M.,"A Primer on the Primer", Aerospace Systems and Mission Analysis Research Program, STAR Memo No. 1, Princeton University, 21 April 1967.

a) Niehoff, J., "Manned Mars Mission Design," Steps to Mars, Joint AIAA/Planetary Society Conference, National Academy of Science, Washington DC, July 1985.

b) Niehoff, J., "Integrated Mars Unmanned Surface Exploration (IMUSE), A New Strategy for the Intensive Science Exploration of Mars," Space Science Board, Woods Hole, MA, July 1985.

Niehoff, J., "Pathways to Mars: New Trajectory Opportunities", The NASA Mars Conference, AAS Science and Technology Series Vol 71, Washington D.C., July 21-23, 1986.

Nock, K. T., and Friedlander, A. L., "Elements of a Mars Transportation System", Acta Astronautica, Vol 15 No 6/7, pp 505-522, 1987

Penzo, P.A., "Orbit/Deorbit Analysis for Mars Rover Sample Return Mission", AIAA Paper No. 88-4231-CP, AIAA/AAS Astrodynamics Conference, Minneapolis, MN, August 15-17, 1988.

Rall, C.S. and Hollister, W.M., "Free-fall periodic orbits connecting Earth and Mars", AIAA Paper No. 71-92, 9th Aerospace Sciences Meeting, New York, N.Y., January 25-27, 1971.

Ross, S., "A Systematic Approach to the Study of Non-stop Interplanetary Round Trips," Interplanetary Missions Conference (9th Annual AAS Meeting), Los Angeles, CA, January 1963.

Roy, A.E., Orbital Motion, Adam Hilger, Philadelphia, 1988.

Sergeyevsky, A. B., Snyder, G. C., and Cunniff, R. A., Interplanetary Mission Design Handbook, Vol 1, Part 2, Jet Propulsion Laboratory, JPL Publication 82-43, 15 September 1983.

Sergeyevsky, A. B., "Planetary Mission Departures from Space Station Orbit", AIAA Paper No. 89-0345, Presented at the 27th AIAA Aerospace Sciences Meeting, Reno, NV, January 9-12, 1989.

Seward, W.D., Steinberg, I.R., and Wolaver, L.E.,"Optimal Control of Libration Point Space Station", Aerospace Research Labs Report No. ARL-71-0016, Wright-Patterson AFB, OH.

Sharma, J., "Asteroid Mission Departure Strategies from a Precessing Space Station Orbit", AIAA Paper No. 90-2913 , AAS/AIAA Astrodynamic Conference, Portland, OR, August 20-22, 1990.

TRW, "Mars Mission Report" under Marshall SFC contract, 1964.

Vajda, S., Fibonacci and Lucas Numbers and the Golden Section, Halsted Press, New York, 1989.

Wilson, S. W., "Analysis of Planetary Hyperbolic Departure Techniques", TRW Note No. 67-FMT-591, December 22, 1967.

Wilson, S. W., Personal Communication, June-December 1990.